Nitrogen fixing trees in the United States: N flux, effect on forest demographics, and nutrient transfer model

Anika Petach Staccone

Submitted in partial fulfillment of the
requirements for the degree of
Doctor of Philosophy
under the Executive Committee
of the Graduate School of Arts and Sciences

COLUMBIA UNIVERSITY

2021

Abstract

Nitrogen fixing trees in the United States: N flux, effect on forest demographics, and nutrient transfer model

Anika Petach Staccone

Patterns and controls of net primary production (NPP) remain a critical question in ecology especially as climate modeling efforts expand. Nutrients, particularly nitrogen (N), can regulate NPP, which couples the N and C cycles. Biological nitrogen fixation (BNF) is the primary natural pathway by which new N enters ecosystems. The magnitude of the natural BNF flux is still not well constrained and the effect of this new N on forest demography and C storage is not well understood. In chapter 1 we use tree census data and two approaches of estimating BNF to make an estimate of the total N fixed by trees across the U.S.: 0.30-0.88 Tg N yr^{-1} (1.4-3.4 kg N ha^{-1} yr^{-1}), smaller than previously expected and on par with N inputs from understory or asymbiotic BNF and less than inputs from N deposition. The tree BNF input is dominated by two tree genera: *Robinia* and *Alnus*. In chapter 2 we use mixed effect models of forest census data to show that N-fixing trees have no net effect on forest biomass accumulate rate, indicating that though they can fertilize forests on long timescales, during the course of their lives the competitive influences they exert on neighbors balance any fertilization effect they may have. However, the net effect of N-fixing trees on forest development and carbon storage depends on

local factors and can be significantly facilitative in contexts where N-fixers are less competitive or when neighbors occupy different forest niches. In chapter 3 we develop a theoretical model which shows lateral leaf litter is a plausible mechanism for observed N-fixer effects, wherein the percent of litter nutrients shared with neighbors can range from almost 0% for small trees to >90% for large isolated trees in low wind, fast decomposition environments. Litter nutrients spread more in windy environments or from trees whose leaf litter falls farther from trees and diffuses more quickly. In sum, N-fixing trees play an important role in temperate forests representing an important N input, however, the flux is smaller than previously expected and the fertilization effect of N-fixing trees is not observed during the census interval.

Table of Contents

List of Charts, Graphs, Illustrations

Acknowledgments

No spark of scientific inquiry can be stoked into a burning curiosity deep enough to start the journey through grad school without a lifetime of support from friends and mentors. Working as a student in Duncan Menge's lab played a huge role in fostering this scientific curiosity, and I am immensely grateful for all he has taught me about science, writing, and good mentorship. Somehow, you taught me to be a scientist while simultaneously creating a supportive lab community, infusing meetings with humor, and cultivating an appreciation of Indian food at the last five years of lab dinners. Our weekly meetings were a lesson in how to ask meaningful scientific questions and how to pivot floundering projects into fascinating and sound scientific study; your unwavering encouragement buoyed me through the tumultuous times of grad school. It has truly been a privilege to be your student.

Thank you to my entire committee who gave me useful feedback and guidance throughout my research journey: Kevin Griffin, Maria Uriarte, Steve Perakis, and Ruth DeFries – your courses, support, and ideas shaped this thesis. Kevin – your compassionate feedback and humility as a scientist were inspirational and taught me to remain curious. Maria – thank you for teaching your statistical modeling, which inspired both my research and future career aspirations, and for teaching thesis development which shaped my research and taught me how to give substantive feedback and speak confidently about ideas. Steve – thank you for helping me through my first chapter and welcoming me into the Powell working group to get to participate

in a collaboration beyond writing a single research paper. Ruth – thank you for welcoming me as a TA in your sustainable development course during my first semester at Columbia which me transition into the department. Also thanks to my collaborators: Sian Kou-Giesbrect, Ben Taylor, Jana Compton, Wenying Liao and Chris Clark. You shaped research questions, discussed findings, proof read endless drafts, and taught me a great deal about forest ecology and biogeochemistry. For financial support, thank you to NSF grant DGE 1644869, the Earth Institute, and the E3B Department.

E3B has been a home to me over the past 5 years and it has been an honor to work with you. Thanks for being such a wonderful and welcoming group of people who effuse friendship and great conversations. In particular, the Menge lab was an amazing place to develop as a scientist. Ben Taylor, Tom Bytnerowicz, and Andrew Quebbeman welcomed me to the lab and taught me so much about the world of nitrogen cycling. I cannot imagine two better lab mates to progress through the program with: Alex Huddell and Sian Kou-Giesbrecht were teachers, collaborators, and companions through the journey. The entire 5th year cohort has been an especially important part of my time here and made living in New York feel like home.

Lastly, thanks to my family. My parents brought me outside as a kid to get a curiosity for nature, taught me to dream big, and supported me over the years of this journey. My brother, Trevor, who paved the way with his endless advice on surviving grad school. My sister, Tanya, who was my first science collaborator and continual companion during grad school as we struggled through together (finally achieved our dream of being in the same grade). The advection-diffusion-reaction model would never have worked without hours on the phone with you. My husband, Anthony, who supported my goals and took the time to listen as my research ideas took shape. And especially, my son Atticus, who reminds me what true curiosity looks like.

Introduction

Patterns and controls of net primary production (NPP) remain a critical question in ecology, especially as climate modeling efforts expand. New NPP can store C in forest biomass that would otherwise reside in the atmosphere. An estimated 25% of anthropogenic C emissions have been stored in forests globally (Pan et al. 2011). Nutrients, particularly nitrogen (N), can regulate NPP, which couples the N and C cycles. With the growing need to accurately characterize NPP (which stores C (Chapin III et al. 2011)), resolving uncertainties in the N cycle as they affect C storage is essential (Peng et al. 2018). In the temperate zone, climate models that include terrestrial processes show that Northern-latitude forests are carbon sinks (Tans 1990, Ciais et al. 1995, Houghton et al. 1999, Pacala et al. 2001) largely due to net reforestation (Houghton et al. 1999). However, the continued growth of these forests and their ability to store carbon is closely tied to N availability (Norby et al. 2010, Coskun et al. 2016).

In climate models NPP is limited by N, especially in temperate forests (Thomas et al. 2015, Wieder et al. 2015). Background N inputs to temperate forests come from N deposition of atmospheric N, rock weathering, or biological N fixation (BNF), where atmospheric N_2 is converted into plant available NH_4^+. However, after decades of research on N limitation there are still knowledge gaps, with the magnitude of the BNF flux remaining a persistent uncertainty. Within the US the estimated BNF flux varies by 25-fold depending on the estimate used (Sobota et al. 2013). This uncertainty is so great that it prevents accurate characterization of N input to estimate NPP, N available for constructing nutrient budgets, and understanding local effects of N-fixing trees on N limitation. Symbiotic BNF in trees (hereafter N-fixing trees), a large natural N input, is uncertain both because the abundance of N-fixing trees is uncertain and the rate of

BNF in those trees is uncertain. Furthermore, the local impact of these N-fixing trees on the N available to neighboring trees to fuel NPP is also unclear.

N inputs from BNF couple the C and N cycles at ecosystem scales by increasing available soil N (Binkley et al. 1992, 1994, Chapin et al. 1994, Perakis et al. 2011) and in young tropical forests almost half of the NPP is fueled by N from N-fixing trees (Batterman et al. 2013). But it is not clear whether contemporary N-fixing trees have the same, fertilizing effect at local scales. In N-limited ecosystems such as Northern-latitude forests, N losses are relatively low, so the key nutrient cycling parameters for local soil effects are plant-mediated inputs and uptake (Brookshire et al. 2012). Since N-fixing trees input their own N (thereby relieving N limitation for themselves), it is often assumed that these N-fixing trees should have a competitive advantage in N-limited ecosystems (Menge et al. 2008), and theoretical models have confirmed that N-fixing plants are strong competitors when N limitation is sufficiently strong (Menge et al. 2017a). On the other hand, N-fixing trees drop N-rich leaf litter which could fertilize neighboring trees, relieving N limitation and allowing neighbors to compete more strongly. Recent empirical work in tropical forests contradicts this hypothesis, suggesting that N-fixing trees either outcompete neighboring trees (Taylor et al. 2017) or are at least neutral in effect (Lai et al. 2018). The hypothesis has not yet been tested in temperate forests where N limitation is more widespread, nor is the mechanism behind the observations confirmed.

There are several mechanisms by which N-fixers might facilitate or reduce nutrient competition on their neighbors: transfer of nutrients via leaf and other sources of litter, transfer of nutrients via direct belowground linkages, or reduced pressure on the soil available nutrient pool (Forrester et al. 2006). One important mechanism by which N-fixing trees might facilitate their neighbors is litter transfer. Litter that decomposes and mineralizes within the rooting radius

of a neighbor can potentially supply available N to that neighbor (Van Kessel et al. 1994, Parrotta et al. 1996). In forests where N-fixing tree leaf litter decomposes within a neighbor's rooting radius, then leaf litter transfer could be an important driver of N-fixers facilitating their neighbors. However, if the N-fixer litter decomposes and mineralizes within its own rooting radius then the N-fixer likely has little facilitative effects on its neighbors and becomes an even stronger competitor itself. The extent to which N-fixing trees retain their leaf litter nutrients from year to year fits into the bigger context of how trees avoid losing nutrients once they have them.

This thesis will be divided into three chapters: Chapter 1, which is published in *Global Biogeochemical Cycles*, discusses the magnitude of the BNF flux across US forests; Chapter 2, which is published in *Journal of Ecology*, outlines the impacts of N-fixing trees on neighboring trees and stand level demographics; and Chapter 3 will examine one mechanism of N-fixing tree interaction with neighbors through leaf litter transfer. Chapter 3 investigates the effects of litter sharing from a theoretical perspective to complement the empirical work in chapter 2 about when N-fixing trees facilitate or outcompete their neighbors. Overall, this work will elucidate the impacts of N-fixing trees on their neighbors, an issue which is still poorly understood though has significant implications for N and C cycling.

Chapter 1: A spatially explicit, empirical estimate of tree-based biological nitrogen fixation in forests of the United States

Authors: Anika Staccone, Wenying Liao, Steven Perakis, Jana Compton, Christopher Clark, Duncan Menge

Staccone, Anika, et al. "A spatially explicit, empirical estimate of tree-based biological nitrogen fixation in forests of the United States." *Global Biogeochemical Cycles* 34.2 (2020): e2019GB006241.

Abstract

Quantifying human impacts on the nitrogen (N) cycle and investigating natural ecosystem N cycling depend on the magnitude of inputs from natural biological nitrogen fixation (BNF). Here, we present two bottom-up approaches to quantify tree-based symbiotic BNF based on forest inventory data across the coterminous USA and SE Alaska. For all major N-fixing tree genera, we quantify BNF inputs using (1) ecosystem N accretion rates (kg N ha^{-1} yr^{-1}) scaled with spatial data on tree abundance and (2) percent of N derived from fixation ($\%N_{dfa}$) scaled with tree N demand (from tree growth rates and stoichiometry). We estimate that trees fix 0.30-0.88 Tg N yr^{-1} across the study area (1.4-3.4 kg N ha^{-1} yr^{-1}). Tree-based N fixation displays distinct spatial variation that is dominated by two genera, *Robinia* (64% of tree-associated BNF) and *Alnus* (24%). The third most important genus, *Prosopis*, accounted for 5%. Compared to published estimates of other N fluxes, tree-associated BNF accounted for 0.59 Tg N yr^{-1}, similar to asymbiotic (0.37 Tg N yr^{-1}) and understory symbiotic BNF (0.48 Tg N yr^{-1}), while N deposition contributed 1.68 Tg N yr^{-1} and rock weathering 0.37 Tg N yr^{-1}. Overall, our results reveal previously uncharacterized spatial patterns in tree BNF that can inform large-scale N

assessments and serve as a model for improving tree-based BNF estimates worldwide. This updated, lower BNF estimate indicates a greater ratio of anthropogenic to natural N inputs, suggesting an even greater human impact on the N cycle.

1 Introduction

Biological nitrogen fixation (BNF), the process by which atmospheric nitrogen $(N)_2$ gas is converted to NH_4^+, is the main natural source of N in most terrestrial ecosystems worldwide (Fowler et al. 2013b) and especially in the USA (Sobota et al. 2013, Sabo et al. 2019). BNF is performed by a variety of prokaryotes, some of which live free in the soil or canopy (Reed et al. 2011), some of which are associative or symbiotic with organisms other than higher plants (e.g., lichens and bryophytes) (Turetsky 2003, Antoine 2004, DeLuca et al. 2007), and some of which live symbiotically in root nodules of certain higher plants (Gyaneshwar et al. 2011, Azani et al. 2017). In forests, symbiotic N-fixing trees often have access to more energy than free-living N fixers, so they can provide much of the N needed to support forest growth and regeneration (Batterman et al., 2013; Binkley, 2003; Binkley et al., 1992; Bormann et al., 1994; Perakis et al., 2012). At local scales tree BNF can be substantial, bringing in over 100 kg N ha^{-1} yr^{-1} (e.g., Binkley et al., 1994; Mitchell & Ruess, 2009), but there is considerable variation across sites. Scaling from local sites to landscape and regional scales is important for understanding the ecological role of N-fixing organisms, quantifying the relative impact of human derived N fluxes compared to natural rates, and parameterizing Earth System models (Hungate et al. 2003, Gruber and Galloway 2008, Wieder et al. 2015, Stocker et al. 2016).

BNF is difficult to estimate accurately at landscape and regional scales because it is spatially heterogeneous and challenging to measure in the field. A variety of approaches have been used to estimate BNF, yielding global estimates ranging from 58 (Vitousek et al., 2013) to

340 Tg N yr^{-1} (Xu-Ri & Prentice, 2017). This six-fold difference demonstrates that after decades of N cycling research there remains a large uncertainty on this flux. The first efforts to quantify regional-scale BNF were bottom-up extrapolations. An early estimate of BNF in USA forests multiplied a single BNF rate (1 kg N ha^{-1} yr^{-1}) by the nonagricultural land area (Jordan and Weller 1996). In 1999 Cleveland *et al.* improved on Jordan and Weller's method by synthesizing literature BNF rates for each biome and for symbiotic and asymbiotic N-fixers separately (Cleveland et al. 1999). To scale up to biome level BNF, Cleveland *et al.* made educated guesses about plant cover for N-fixing trees and understory plants, then multiplied these biome-specific BNF rates by the area of each biome, yielding a global estimate of 195 Tg N yr^{-1}. To get a spatially explicit estimate of BNF, Cleveland *et al.* correlated BNF with evapotranspiration and produced a global BNF map based on this correlation. In 2004 Galloway postulated that N-fixing trees were rarer than assumed in the Cleveland estimate, and the BNF rates were elevated due to bias in literature to study areas where N-fixing trees are important (Galloway et al. 2004). Galloway estimated a global flux of 107 Tg N yr^{-1} based on scaling down the results of Cleveland *et al.* (1999) by assuming that N-fixers were 5% of tree basal area cover.

Following the early efforts to quantify BNF on regional or global scales using bottom up approaches, researchers tried to circumvent the uncertainty in abundance and flux measurements of N-fixing organisms by using top-down modeling approaches. In 2013 Cleveland *et al.* used CASA-CNP, which estimates BNF as the difference between N demand for NPP and N deposition plus N resorption (Cleveland et al. 2013). They also broke the estimate down into contributions from symbiotic N-fixers (105 Tg N yr^{-1}) and asymbiotic N-fixers (22 Tg N yr^{-1}). Ri and Prentice (2017) used DyN-LPJ to estimate demand for total new N inputs, of which BNF is a major part. This produced a single aggregated estimate (340 Tg N yr^{-1}) as well as spatially

explicit maps developed from location-based parameter inputs. Vitousek and collaborators used a ^{15}N isotope modeling approach that assumed a steady state pre-industrial N cycle and calculated BNF as the difference between losses (hydrologic and gaseous, inferred using N isotopes) and inputs aside from BNF (N fixed by lightning and deposition from ocean to land) (Vitousek et al. 2013). This produced a single aggregated BNF estimate (58 Tg N yr^{-1}) for terrestrial ecosystems globally that cannot be mapped or divided into tree, understory, and asymbiotic N-fixers. Sulman and collaborators used LM3-SNAP to estimate plant N acquisition by direct uptake vs. mycorrhizal uptake vs. symbiotic BNF via a return-on-investment framework. They estimated 46 Tg N yr^{-1} of symbiotic BNF globally and provided spatially explicit maps (Sulman et al., 2019). Meyerholt and collaborators used several BNF formulations in the O-CN model to estimate global BNF with a median flux of 128 Tg N yr^{-1} (Meyerholt et al. 2016). Lawrence and collaborators presented CLM5 with a biogeochemical cycle that distributes BNF throughout the year and assigned a C cost for BNF. They estimated 57.9 Tg N yr^{-1} of symbiotic BNF globally (Lawrence et al. 2019).

Despite the long history of work quantifying BNF and the diversity of approaches used, the amount of BNF is still highly uncertain. For example, a review of N inputs in the United States noted that estimates of natural BNF in forests are sufficiently uncertain (0.5 to 12.2 Tg N yr^{-1}) that they hamper development of accurate national N budgets (Sobota et al., 2013). Quantifying natural BNF is essential to contextualize the human perturbation of the N cycle from fertilizer production, cultivated BNF, and fossil fuel combustion (Galloway and Cowling 2002) as well as for understanding N cycling within ecosystems. A well constrained USA national scale BNF estimate would improve predictions of forest response to elevated CO_2 (Hungate et al.

2003), national N budgets (Sabo et al. 2019), water quality (Wise and Johnson 2011), and ecological understanding of N cycling.

Here we present a bottom-up BNF estimate for USA forests based on census estimates of N-fixing tree abundance, which was a key uncertainty in tree BNF estimates such as the Cleveland et al. (1999) estimate. The US Forest Service conducts a systematic survey of forests across the country (FIA), which can be used to document the abundance of N-fixing tree species at scales ranging from local plots to the entire country (e.g., Menge et al. 2010, 2014, 2017; Liao et al. 2016). We combine these abundance and distribution data with updated, ecosystem-scale genus-specific BNF rate data from the literature to estimate tree-based BNF nationally. Additionally, we use a second, independent method that estimates BNF from N demands of N-fixing trees. This second method uses FIA-based growth rates of N-fixing trees to quantify their N demand, along with published data on the percent of N that N-fixing trees derive from fixation. We further explore potential effects of light limitation on BNF rates, which is known to be an important control on rates of BNF (Gutschick, 1981; Heilman & Stettler, 1983, 1985; Myster, 2006; Taylor & Menge, 2018), and evaluate the relative importance of tree-based BNF compared to other forms of BNF and atmospheric N deposition.

2 Materials and Methods

The goals of this research are to produce a national map of N inputs from tree-based BNF, quantify the magnitude of this tree BNF flux at the continental scale, and put this BNF estimate in context by comparing it to other published N input fluxes. We use two complementary methods that take advantage of spatially explicit data on N-fixer abundance to estimate BNF in trees across the US. First we use forest inventory data on the abundance

distribution of N-fixing trees to upscale published genus-specific BNF rates to spatially-explicit values (which we call our "accretion" method). Second, we quantify N demand by N-fixing trees, using forest inventory data for the growth rates of N-fixing trees, published tissue stoichiometry data, and the percent of N derived from fixation ($\%N_{dfa}$) (which we call our "N demand" method). Both methods allow us to estimate genus- and abundance-specific tree-based symbiotic BNF rates at scales ranging from individual plots to the entire US.

Some tree taxa such as pine support endophytic N-fixing bacteria (Moyes et al. 2016, Padda et al. 2019). The extent and rates of BNF in these trees are not widely known, though Wurzburger (2016) extrapolated the rates reported by Moyes et al. (2016) and found that the flux for pines was negligible. Reports also suggest BNF in *Populus trichocarpa*, via endophytes (Doty et al. 2016), and *Pinus contorta*, via bacteria that live within their tuberculate mycorrhizae (Paul et al. 2007, Chapman and Paul 2012). We use the abundance of *Pinus contorta* and *Populus trichocarpa* along with published BNF rates (Paul et al. 2007) to examine their ecosystem level relevance (see Appendix A – section S4).

2.1 Literature Search

In both methods we rely on BNF rate data from a single, systematic literature search. The search terms for genus-specific symbiotic BNF rates include "genus"+"N_2 fixation", "genus"+"BNF rate", "genus"+"nitrogen fix*", and "BNF"+"common name" where the actual genus names (e.g. *Alnus*, *Robinia*) replace "genus" in the search term. In the accretion method, results were screened for fixation rates (units: kg N ha^{-1} yr^{-1}) and stand basal area (m^2 ha^{-1}). Data from Acetylene Reduction Assays (ARA) were excluded because of uncertainties associated with converting the amount of acetylene fixed to N fixed (Giller 2001, Russo 2005), scaling

instantaneous measurements to an annual rates (Shearer et al. 1986, Russo 2005), and sampling nodule biomass (Winbourne et al. 2018). These accretion studies measure BNF rate using a mass balance approach where the change in N of the system is equal to BNF plus N deposition minus denitrification and solution losses (Silvester 1983). Though some accretion studies don't measure N losses, which leads to an underestimate of BNF rates, and others use a space-for-time substitution assuming identical site conditions for all stands, accretion-based BNF rates are relatively robust compared to acetylene reduction extrapolations. Results from accretion studies with other units (e.g., g N m^{-2} yr^{-1}) were converted to kg N ha^{-1} yr^{-1}. In the N demand method literature results of natural abundance and ^{15}N enrichment studies were used to find $\%N_{dfa}$ (the % of N derived from fixation) for each genus. The geographic area screened in the literature review was not constrained to the USA due to the scarcity of studies focusing on measuring BNF in trees.

2.2 Flux Estimate by Scaling BNF Rates from N Accretion Studies (method 1)

We obtained tree census data from version 5.1 of the USFS Forest Inventory and Analysis (FIA) database (Burrill et al. 2017). The FIA is a systematic survey of forest plots with one plot per ~2400 ha of forest, totaling >500,000 unique plots. Most FIA plots are 0.067 ha, comprised of four 7.3 m radius subplots. The FIA defines forest as ≥10% crown cover where the patch is at least 1 acre in area and not part of agricultural or urban system (Burrill et al. 2017). Plot censuses occur every 5-10 years on a subset of plots; we used the most recent census measurement for each plot, which ranged from 1993-2013. In each census, trees ≥ 12.7 cm DBH are recorded, along with their DBH, species identity, and a variety of other data. N-fixing rhizobial species were identified from Sprent (2009) and actinorhizal species from Huss-Danell

(1997). The analysis covered the coterminous United States and SE Alaska. The N-fixing trees we studied belong to five rhizobial genera (*Acacia*, *Albizia*, *Olneya*, *Prosopis*, and *Robinia*), as well as three actinorhizal genera (*Alnus*, *Cercocarpus*, and *Elaeagnus*). The spatial distribution of these genera has a strong geographic pattern (Figure 1a): *Robinia* is most abundant in the eastern US; *Alnus* in Oregon, Washington, southeast AK and the western US; *Cercocarpus* in the Rocky Mountains and Utah; and *Prosopis* in Texas and the southwestern US. These genera vary widely in their BNF rates so have different effects on the natural BNF flux. Other N-fixing genera included in the FIA database (*Casuarina, Sophora, Piscidia,* and *Ebenopsis*) were not included in our analysis because they had fewer than 15 stems across the US (coterminous USA and southeast AK). Overall, >110,000 N-fixing trees from >500,000 unique plots were incorporated in the analysis.

We estimated plot-scale BNF as a function of the basal area of N-fixing trees within the plot. Basal area, the cross-sectional area of all trees in the stand at breast height (1.3 m) divided by the area sampled, is an easily measured predictor for biomass because it accounts for both the size and number of trees. When there were no N-fixing trees in the plot there was also no tree-based BNF. When N-fixing tree basal area in the plot was greater than zero we used genus-specific relationships to estimate plot-scale BNF. Theory suggests that the relationship between N-fixing tree abundance (m^2 ha^{-1}) and BNF (kg N ha^{-1} yr^{-1}) might be linear for the species that have obligate BNF strategies (Menge et al. 2009), but saturating or constant for species that are facultative (Menge & Levin 2017). Therefore, we used the data from our literature review to establish these relationships empirically. When a linear relationship existed in the literature-derived data for BNF rate and N-fixing tree basal area (as was the case for all species other than *Robinia* and *Alnus*), we used it. However, when no positive relationship existed (for *Robinia* and

Alnus) we used a constant value for BNF for any plot with non-zero basal area of that N-fixing genus. At the plot scale fixed N was calculated for each genus (except *Robinia* and *Alnus*) by multiplying stand basal area by the per basal area BNF rate for that genus (equation 1a).

$$F_{plot} = \sum_{g=1}^{\#\ genera}((\sum_{a=1}^{\#\ trees\ of\ genus\ g} BA_{ag} * TPHA_{ag}) * F_g + intercept_g) \qquad \textbf{(1a)}$$

Equation 1a calculates the N fixed per plot, F_{plot}, (kg N). BA_{tg} (m^2) is the basal area of a tree *a* of g. $TPHA_{tg}$ (trees ha^{-1}) is the inverse of the ground area on which tree *a* was sampled. BA_{ag} times $TPHA_{ag}$ gives the stand level basal area represented by tree *a* (m^2 ha^{-1}). The sum of BA_{ag} times $TPHA_{ag}$ for all trees of genus *g* in a plot (m^2 ha^{-1}) is the stand basal area of genus *g* in that plot. F_g (kg N m^{-2} yr^{-1}) is the BNF rate per basal area for genus *g*. Multiplying stand basal area by F_g and adding $intercept_g$ for a given genus gives stand BNF for that genus. F_g and $intercept_g$ were estimated from the literature search using a linear regression between BNF rate (kg N ha^{-1} yr^{-1}) and stand basal area (m^2 ha^{-1}) (see S1 text for details). The regression was bootstrapped at the plot scale to account for the relatively small and variable sample for BNF in each genus from the literature. The plot scale linear regression was bootstrapped 1000 times as a multivariate normal distribution to get the confidence interval on F_g and $intercept_g$ where μ_g is the regression slope mean, σ_g is the standard error of the regression slope, $\mu_{g\text{-}int}$ is the regression intercept mean and $\sigma_{g\text{-}int}$ is the regression intercept standard error (see Table 1 for regression parameters). We aggregated to the genus level because many species had insufficient published BNF data (1 or fewer studies that reported both BNF rate and stand basal area).

To account for the fact that BNF did not appear to scale with stand level BA in *Robinia* and *Alnus* (R^2 = 0.08 and 0.009, Table 1) in the literature search, we assumed a constant BNF rate independent of stand basal area. If a *Robinia* stem was present in a given plot then the BNF rate was bootstrapped based on the mean BNF rate from literature review data for this genus

using a normal distribution with mean 52 kg N ha^{-1} yr^{-1} and standard error 12.3 (Table S2). *Alnus* stems were treated the same way with mean 104 kg N ha^{-1} yr^{-1} and standard error 23.9.

$$Robinia\ Fixed\ N\ per\ plot\ (F_{plot}) = \begin{cases} norm(\mu_{Robinia}, \sigma_{Robinia}), & present \\ 0, & absent \end{cases} \quad \textbf{(1b)}$$

To aggregate the plot level fixed N to the grid cell scale (kg N ha $forest^{-1}$ yr^{-1}) we took the average N fixed across all plots in the grid cell (equation 1c).

$$Fixed\ N\ per\ forest\ area\ across\ grid\ cell\ (F_{cell}) = mean(F_{plot}) \quad \textbf{(1c)}$$

We report BNF rates in two ways: N fixed per forest area and N fixed per ground area. To get the average BNF rate on a per ground area basis (kg N ha $ground^{-1}$ yr^{-1}) we took the average N fixed across all plots in the grid cell and multiplied by the fraction of ground covered by forest (equation 1d). The area of forest within the grid cell was obtained from US FIA land cover maps (USGS 2000) processed in R using the raster (Hijmans 2017) and sp (Pebesma and Bivand 2005) packages.

$$Fixed\ N\ per\ ground\ grid\ cell\ (F_{cell-gr}) = mean(F_{plot}) * frac\ forest \quad \textbf{(1d)}$$

To estimate the total flux of tree-based BNF per year (kg N yr^{-1}) in the coterminous USA we summed the N fixed across each grid cell (equation 1e).

$$Fixed\ N\ across\ coterminous\ US = \sum_{c=1}^{\#grid\ cells} (F_{cell_c} * forest\ area_c) \quad \textbf{(1e)}$$

2.3 Flux Estimates by Scaling N Demands of N-fixing Trees (method 2)

Our second, largely independent approach estimated the N demand by N-fixing trees based on N-fixer growth data, allometric equations, and percent N derived from the atmosphere ($\%N_{dfa}$). The $\%N_{dfa}$ is the fraction of N that was supplied by BNF, as determined by comparing N isotope values of fixing and non-fixing species (Shearer & Kohl, 1986), which we aggregated at the genus level. We used FIA data to estimate incremental growth and calculated the N that

each N-fixing tree required for wood growth, litter turnover, and fine root turnover. We assumed that new N is needed for the increment in wood (not the total wood N) but for the total litter N and total fine root N because those tissues turn over annually. The required N was calculated using allometry and C:N ratios for each tree in each plot and then aggregated to get the total tree N demand across the US. At the plot level,

$$N\ fixed_{plot} = \sum_{g=1}^{\#genera} \sum_{a=1}^{\#trees} \%N_{dfa,i} * (\Delta w_{ga} + f_{ga} + r_{ga}) \quad \textbf{(2a)}$$

Equation 2a calculates plot level N fixed by finding the N demand for each tree ($\Delta w_{ga} + f_{ga} + r_{ga}$), multiplying that demand by the fraction of demand met by BNF ($\%N_{dfa}$), and summing across all trees in the plot. The terms Δw_{ga}, f_{ga}, and r_{ga} represent kg N used for wood growth increment (equation 2b), foliage replacement (equation 2c), and fine root turnover (equation 2e), respectively.

$$\Delta w_{ga} = (\frac{\Delta agb_{ga}}{t})(frac_{wood})(1/C{:}N_{wood})(TPHA_{ga}) \quad \textbf{(b)}$$

$$f_{ga} = (agb_{ga})(frac_{foliage})(1/C{:}N_{foliage})(TPHA_{ga})(1 - res) \quad \textbf{(c)}$$

$$fine\ root_{ga} = 0.072 + 0.354e^{-0.060*1.576agb_{ga}{}^{0.615}} \quad \textbf{(d)}$$

$$r_{ga} = \left(\frac{1}{C{:}N_{fine\ root}}\right) * fine\ root_{ga} * (1 - res_{fine\ root}) \quad \textbf{(e)}$$

The N used for wood growth (Δw_{ga}) is the change in aboveground biomass (kg C) between the two census points divided by the census interval (t in years) multiplied by the fraction of aboveground biomass in the wood (Jenkins et al. 2003) multiplied by the N:C ratio of wood (1/350, (Du and de Vries 2018)) multiplied by the *TPHA* or trees per hectare that tree represents (ha^{-1}). Aboveground biomass (kg C) data are obtained from the FIA database (Jenkins et al. 2003). The fraction of this biomass allocated to different tissues: wood and foliage was also calculated based on Jenkins et al. (2003). For the foliage N calculation (equation 2c), f_{ga} assumed

that deciduous trees lose their entire crown of leaves each year and must replace the N lost during senescence. All genera except *Cercocarpus* are deciduous. Although *Cercocarpus* species span deciduous to evergreen (Abrahamson 2019), most leaves are shed annually in evergreen species so the leaf turnover rate in *Cercocarpus* is about once per year (Ackerly 2004). The foliage N was calculated by multiplying the aboveground biomass (agb_{ga} in kg C) times the fraction of biomass in foliage (from Jenkins et al., 2003) times the N:C ratio in foliage (1/35 kg C kg N^{-1}) (McGroddy et al. 2004) times the inverse of the area on which the tree was sampled $TPHA_{ga}$ (ha^{-1}) times the fraction of nutrients not resorbed before senescence (deciduous fixers: 49.5%; deciduous non-fixers: 59.7%; evergreen fixers: 41.8%; evergreen non-fixers: 54.5% (Vergutz et al. 2012)). The fine root biomass fr_{ga} was calculated based on Li et al., 2003. The fine root N was the fine root biomass (kg C) times the N:C ratio for fine roots (1/43 kg C kg N^{-1}) (Gordon and Jackson 2000). Fine root N resorption of 27% was used (Freschet et al. 2010) for all genera.

Since only 0.9% of FIA plots were measured at a second census time and those time series plots were not evenly distributed geographically, we used the time series plots to build distributions of the relative growth rates of each N-fixing genus based on the DBH of an individual of that genus. These distributions were then used to predict the change in aboveground biomass to calculate N demand for wood growth for all trees in the FIA dataset.

To aggregate to the grid cell scale for method 2, equations 1c and 1d were used (for a per forest area and per ground area basis respectively) where F_{plot} was the N demand in the plot. To aggregate to the continental scale the plot N demand at the grid cell scale was multiplied by the forest area in that grid cell and all grid cells were added (as in equation 1e).

2.4 Upper and Lower Bound of tree BNF (method 2)

To bound the N demand method (method 2) we considered the most relaxed assumptions about the $\%N_{dfa}$ itself. To get the maximum N required to support N-fixing trees we assumed that all N required for annual wood growth, foliar turnover, and fine root turnover is derived from BNF ($\%N_{dfa}$ = 100%) and that no N was resorbed from leaves before senescence (resorption = 0%). To get the (trivial) minimum N requirement to support N-fixing trees (lower bound) we assumed that $\%N_{dfa}$ = 0%.

2.5 Light Limitation to tree BNF

BNF is an energetically expensive process (Gutschick 1981) and light availability can constrain BNF (McHargue 1999, Myster 2006, Taylor and Menge 2018). We considered light limitation in an additional analysis by assuming that trees classified as open grown, dominant, or co-dominant in the FIA dataset fixed at the rate in Table 1, but that those in the understory (intermediate and overtopped) did not fix (F = 0).

2.6 Sensitivity Analysis for tree BNF (methods 1 and 2)

We considered the effect of varying all parameter values that are potential sources of error in the estimate. This allowed us to systematically examine uncertainty in the calculation. For the accretion method (method 1) these factors included fixation rates per basal area, N-fixing tree abundance, and controls on the rates (light availability). To vary fixation rate per basal area we allowed the BNF rate to vary between the upper and lower bounds of the 95% confidence interval for one genus at a time while holding others constant. We tested N-fixing tree abundance at 150% and 50% of its original value in each grid cell. For the fixation rates per basal area and

N-fixing tree abundance we varied these parameters at the plot level. For the N demand method (method 2) these factors included the C:N ratio of each tissue type, N-fixing tree biomass (abundance and growth rate), and resorption rates. We also examined the effect of varying the $\%N_{dfa}$ and fraction of aboveground biomass in the foliage. We examined these factors at 150% and 50% of their original value.

2.7 Understory (Symbiotic Shrubs and Herbs)

We included an existing understory BNF value to contextualize our estimates of tree BNF. We used the symbiotic percent cover from Cleveland et al. (1999), assuming 3% cover by N-fixing understory plants, since no data set exists for understory plants to improve this assumption. To aggregate up to the continent scale we used the understory rate in per hectare of forest from Cleveland et al. (1999; 2.2 kg N ha^{-1} yr^{-1}) and multiplied by the area of forest area obtained from the USGS forest cover map. Though soils, leaves, litter, and lichens can also host symbiotic N-fixers on land, these groups were not included in the understory.

2.8 Asymbiotic Fixation

We also included existing BNF estimates from asymbiotic microbes in litter, soil, and woody debris (Reed et al. 2011). Though individual studies have documented substantial variation across space and time from asymbiotic BNF (Pérez et al. 2010, Reed et al. 2010), we did not have a spatially-explicit dataset of asymbiotic BNF, so we assumed that N fixed by asymbiotic soil microbes was a constant 1.7 kg N ha^{-1} yr^{-1} across forest area based on the temperate forest estimate in the review by Reed et al. (2011). Total N fixed by asymbiotic N

fixers across the country was calculated by multiplying the per ground area BNF rate (1.7 kg N ha^{-1} yr^{-1}) by the area of forest calculated above.

$$Fixed\ N_{asymbiotic} = asymbiotic\ N\ fixation\ rate * forest\ area \quad \textbf{(4)}$$

This method uniformly scales the measured asymbiotic rate based on forest area.

2.9 Nitrogen Deposition and Rock Weathering

N deposition and rock weathering were included to contextualize the magnitudes of BNF. Total N deposition (TDEP) was obtained from Schwede & Lear (2014). Rock N data were obtained from Houlton & Dahlgren (2018). Since these data had 12 km and 0.5° grid resolution, respectively, they were resampled to 1° grid squares using the sp package in R (Pebesma and Bivand 2005).

3 Results

3.1 Literature Review and Genus-level Tree BNF

In total, 17 unique reports of BNF rates in trees met the above criteria for the N accretion method (method 1; Tables 1, Appendix A – S1, S3). Three of the reports were for *Acacia*, ten for *Alnus*, one for *Robinia*, and the other three were for *Prosopis*. The screening criteria that had the greatest impact on narrowing the dataset were only using accretion methods and eliminating papers without stand level basal area of N-fixers reported (or necessary information to calculate stand level BA). For the N demand method (method 2), 37 papers fit the screening criteria. Of those, 14 of the papers were for *Acacia*, 7 for *Alnus*, 6 for *Prosopis*, and 5 for *Robinia* (Appendix A – Tables S1, S2).

a)

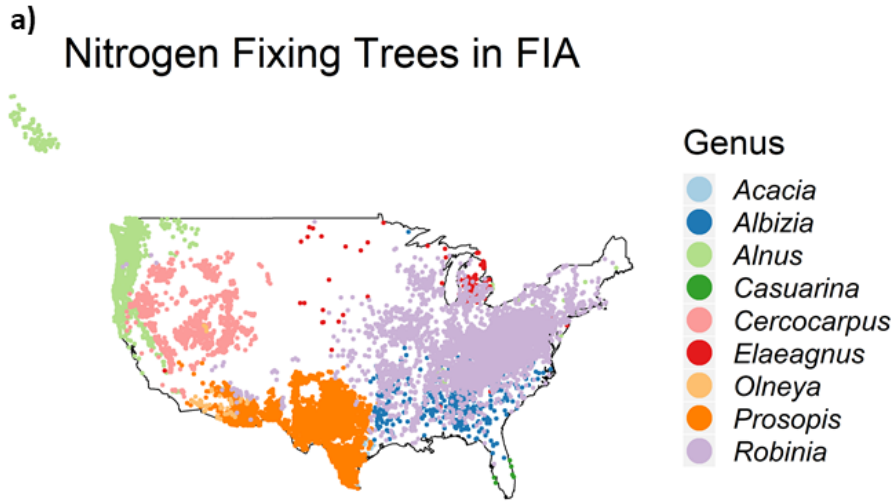
Nitrogen Fixing Trees in FIA
Genus
Acacia
Albizia
Alnus
Casuarina
Cercocarpus
Elaeagnus
Olneya
Prosopis
Robinia

b)

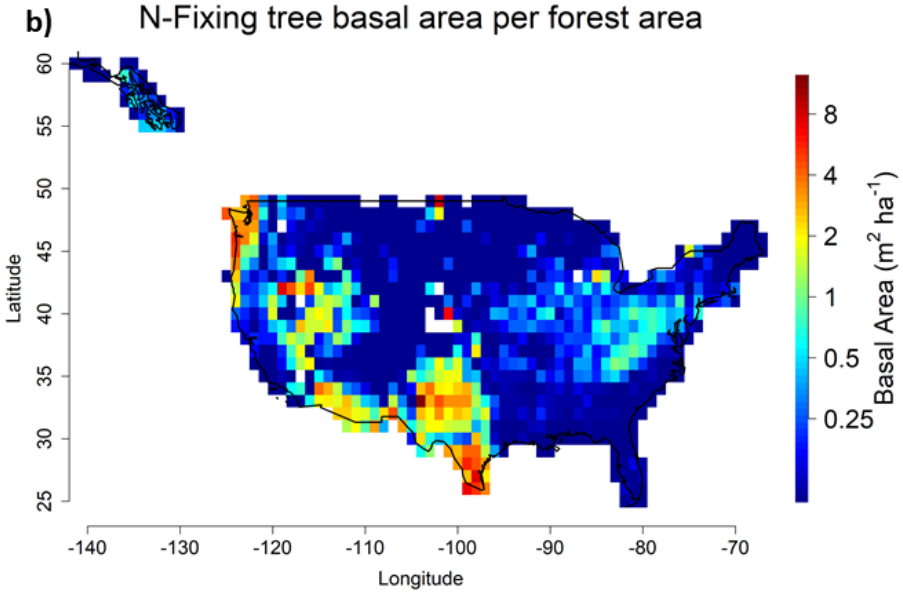
N-Fixing tree basal area per forest area
Latitude
Longitude
Basal Area (m2 ha-1)
25
30
35
40
45
50
55
60
-140
-130
-120
-110
-100
-90
-80
-70
0.25
0.5
1
2
4
8

c)

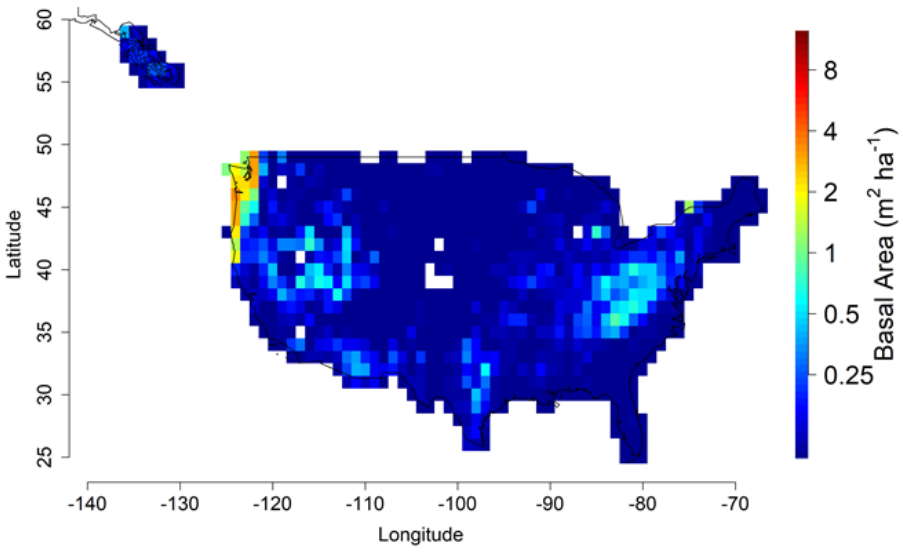
N-Fixing tree basal area per ground area
Latitude
Longitude
Basal Area (m2 ha-1)
25
30
35
40
45
50
55
60
-140
-130
-120
-110
-100
-90
-80
-70
0.25
0.5
1
2
4
8

Figure 1. Symbiotic N-fixing tree abundance across the coterminous USA and SE Alaska **a)** Each point represents one mature tree in the FIA dataset. The color corresponds to genus. N-fixing tree genera are regionally constrained: *Robinia* in the east, *Alnus* in the Pacific Northwest, *Prosopis* in the southwest, and *Cercocarpus* in the southwest and UT. The basal area of symbiotic N-fixing trees is shown **b)** per forest area and **c)** per ground area for each 1° latitude x 1° longitude grid cell. White grid cells in **b)** and **c)** contain fewer than 2 FIA plots. Colors are on a logarithmic scale, but with numbers less than 0.1 m^2 ha^{-1} (including 0) set to the darkest blue for plotting purposes.

Table 1. Genus-specific N fixation rates & $\%N_{dfa}$ from literature search

Genus	Type	Accretion Method				N Demand Method	
		N fixation rate per stand basal area	Intercept			$\%N_{dfa}$	
		[kg N yr^{-1} m^{-2} basal area]	[kg N ha^{-1} yr^{-1}]				
		Mean (SE)	Mean (SE)	R^2	n	Mean (SE)	n
Acacia	Rhizobial	6.28 (3.19)	2.47 (39.83)	0.49	6	50.5 (0.5)	45
Albizia	Rhizobial	2.25 (3.22)	40.37 (48.14)	--	*	78.5 (3.2)	2
Olneya	Rhizobial	2.25 (3.22)	40.37 (48.14)	--	*	53.1 (0.2)	**
Prosopis	Rhizobial	2.73 (0.49)	3.21 (2.69)	0.94	4	40.7 (0.9)	25
Robinia	Rhizobial	*** (--)	52 (12.29)	--	3	66.0 (1.5)	16
Alnus	Actinorhizal	*** (--)	103.8 (23.92)	--	17	75.7 (1.9)	8
Cercocarpus	Actinorhizal	2.25 (3.22)	40.37 (48.14)	--	*	53.1 (0.2)	**
Elaeagnus	Actinorhizal	2.25 (3.22)	40.37 (48.14)	--	*	73.5 (3.9)	2

*Fixation rate obtained from mean of *Acacia*, *Prosopis*, *Robinia*, and *Alnus*.
**$\%N_{dfa}$ obtained from mean of other genera that had data available.
***The regression with *Robinia* has an R^2 of 0.08 and *Alnus* 0.009 indicating no relationship between fixation rate and basal area. If one or more *Robinia* or *Alnus* were present the average rate (kg N ha^{-1} yr^{-1}) from the literature search was used (see text).
Note: sources are listed in the supplementary information (Table S1, Text S2). Some papers looked at several species under different conditions so n is greater than the number of studies

3.2 Tree BNF Across the USA

Accretion studies are conducted across a range of stand ages and likely capture some variety in the degree of downregulation in forests. The average N-fixer tree basal area (m^2 ha^{-1}) within a one degree grid cell ranged from 0 to 12.3 m^2 ha^{-1} per forest area (Fig. 1b) and 0 to 3.1

m^2 ha^{-1} per ground area (Fig. 1c). Although the FIA contains some plots comprised entirely of N-fixers (100% of total stand basal area), on average FIA plots are composed of 1.36% basal area from N-fixing trees. When aggregated at the one degree scale, basal area of N-fixers was highest in the Pacific Northwest with *Alnus* and Texas where *Prosopis* dominates. There is a distinct lack of N-fixing trees across the northern USA and the Rocky Mountain region.

Symbiotic N-fixing trees account for 0.304 ± 0.005 Tg N yr^{-1} (by the N demand method) to 0.878 ± 0.002 Tg N yr^{-1} (by the accretion method) across the coterminous US and southeast Alaska. This is equivalent to 18% or 52% of the N deposition flux by the N demand method and accretion method respectively. On a per forest area basis at the grid cell scale, tree BNF ranged from 0-69 kg N ha^{-1} yr^{-1} (median = 0.4 kg N ha^{-1} yr^{-1}). Tree BNF hotspots occurred in the Pacific Northwest, southwest, Texas, and the mid-Atlantic (Figure 2a). The location of tree BNF hotspots was similar between the two methods (Figure 2a, 2c), although the hotspot intensity was lower in the N demand method for all regions except the Pacific Northwest. Per ground area, trees account for a low BNF rate in the southwest and Texas (Figure 2b, 2d) because a low fraction of the land area in the southwest and Texas is forest.

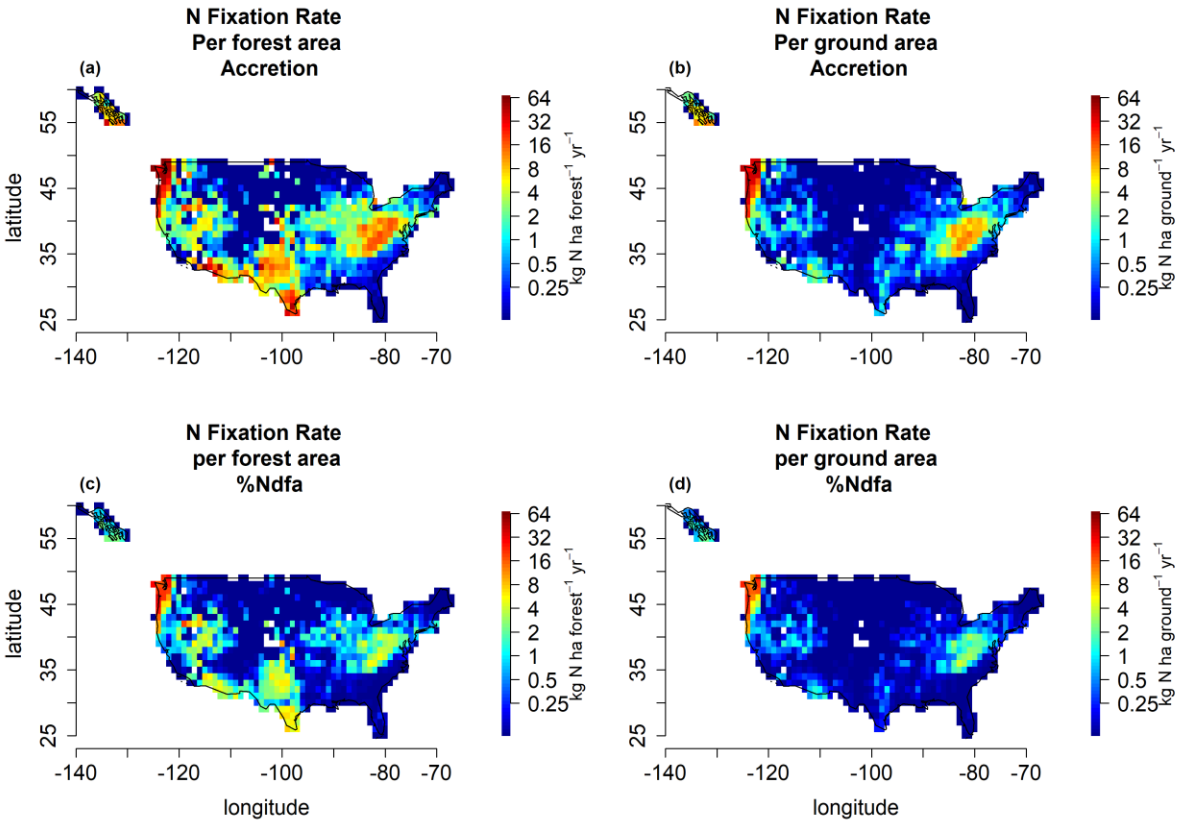

Figure 2. Tree N fixation rate across the United States at the one degree scale
Tree N fixation rate across the United States at the one degree scale. Tree N fixation rate calculated from **a**), **b**) our accretion method and **c**), **d**) our N demand method, **a**), **c**) per forest area and **b**), **d**) per ground area. White cells have fewer than 2 FIA plots. Colors are on a logarithmic scale, but with numbers less than 0.1 kg N ha^{-1} yr^{-1} (including 0) set to the darkest blue for plotting purposes.

The tree BNF hotspots coincide with areas of high N-fixing tree abundance. Tree BNF in the Pacific Northwest is dominated by *Alnus* which fixes 24-32% of total tree BNF across the USA (Figure S3). Tree BNF in the intermountain west is dominated by *Cercocarpus*, which fixes 3-7% of N fixed by trees across the USA. Texas has a high density of *Prosopis* in forested areas, which account for 5-14% of tree BNF across the USA. *Robinia* is the primary N-fixing tree in the mid-Atlantic region, accounting for 46-65% of tree BNF.

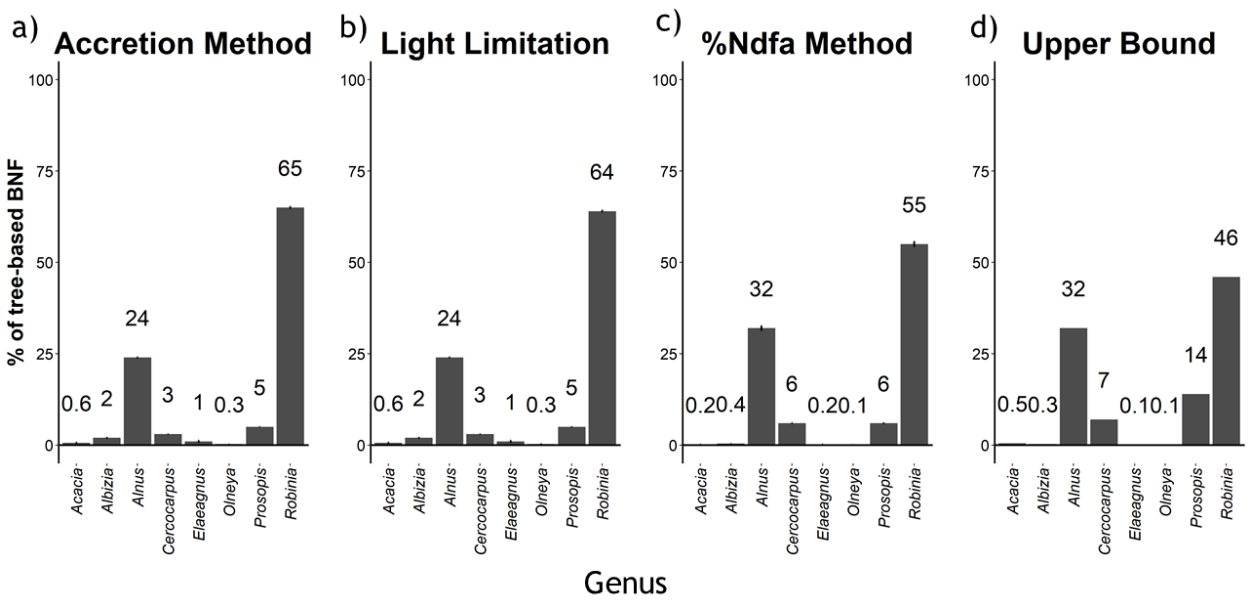

Figure 3. Percent of tree BNF by genus across the coterminous USA and southeast AK Error bars, which are so small on some bars that they are invisible, represent the standard deviation from bootstrapping fixation rates or $\%N_{dfa}$ at the continent scale 1000 times. Fractions are shown for **a)** our standard accretion method, **b)** a light limitation version of the accretion method where we assume that non-canopy trees do not fix N, **c)** our standard N demand method, and **d)** the upper bound of the N demand method ($\%N_{dfa}$=100).

3.3 Tree BNF Sensitivity Analysis

In the accretion method the parameter that had the largest effect on the national BNF estimate is BNF rate per basal area of *Alnus* and *Robinia* (30% and 18% respectively; Figure 4a). The results of the $\%N_{dfa}$ sensitivity analysis indicate that the most sensitive factor was the C:N ratio of wood, which could change the estimate by up to 82% if the value were 150% of the C:N ratio for wood originally used (Figure 4b).

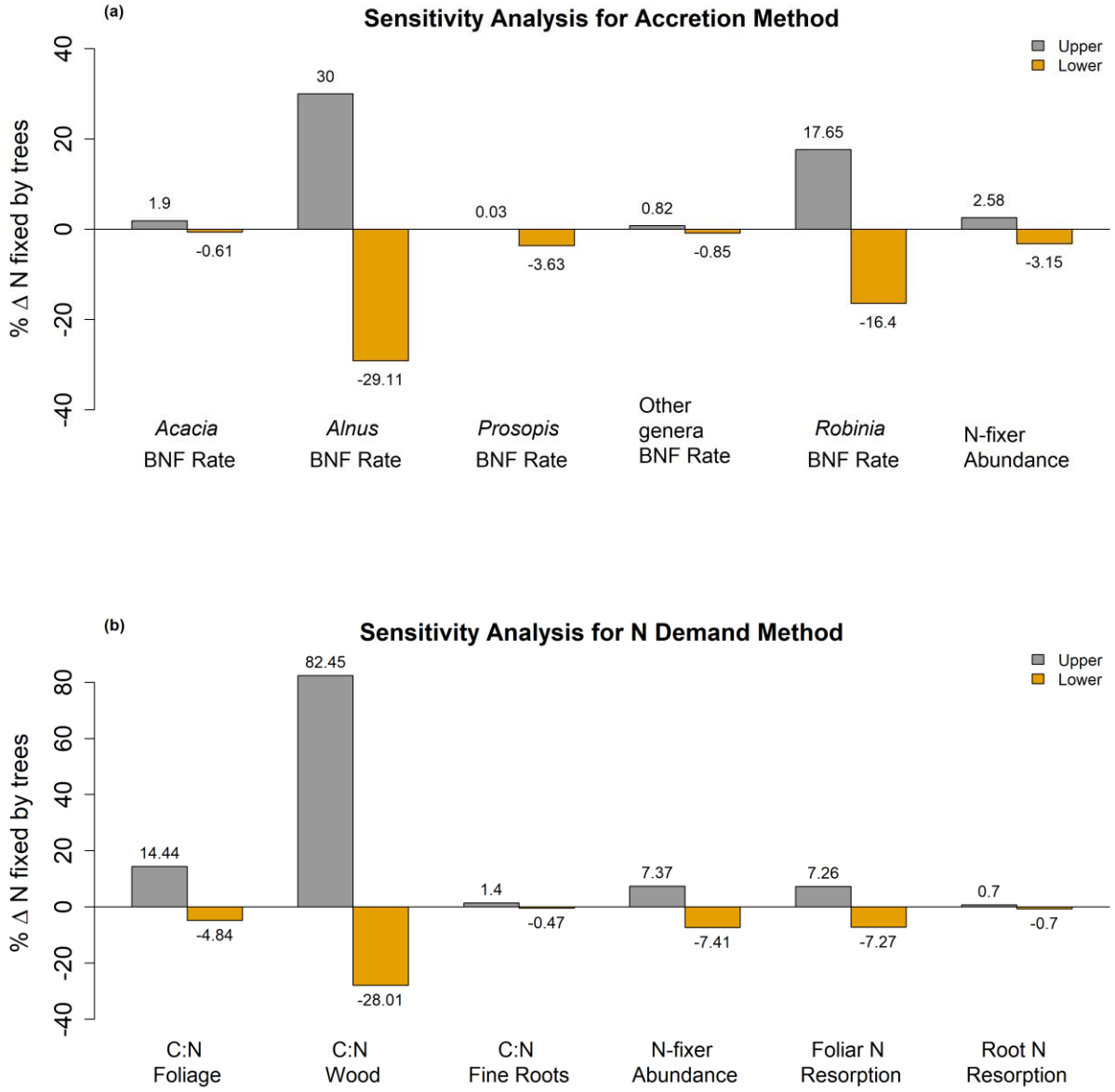

Figure 4. Sensitivity analysis.
These plots show the percent change in tree-based N fixation across the coterminous USA and southeast AK as the sensitivity to different factors for **a)** the accretion method and **b)** the N demand method. **a)** Each genus' N fixation rate was varied from the upper to lower bounds of the 95% confidence interval in one genus at a time while all other genera were held constant at the mean value. In the N-fixer abundance analysis we increased and decreased plot level basal area by 50%. **b)** The C:N ratio of foliage, wood, and fine roots; N-fixer abundance (by aboveground biomass); and the foliar and fine root N resorption were increased and decreased by 50% to examine the effect of these factors on the overall BNF estimate.

If the N-fixer abundance or foliar N resorption were increased by 50% the estimate would increase by about 7%.

3.4 Symbiotic Understory BNF, Asymbiotic BNF, and N Deposition

To compare among different N-input pathways, we re-scaled previously published BNF rates for symbiotic understory plants and asymbiotic fixation in soil to the spatial extent of the FIA data used in our tree analysis. The national scale BNF flux from symbiotic understory fixers was 0.48 Tg N yr^{-1}, which is between the tree BNF estimates for our two methods, and is highly sensitive to the assumption of 3% cover (Table 2). Asymbiotic BNF was lower (0.37 Tg N yr^{-1}) but on the same order of magnitude as understory BNF (Table 2).

Table 2. Summary of Nitrogen Inputs

N Input to forested land	BNF flux per forest area (avg. per grid cell)	US-wide BNF flux estimate	Data source
	[kg N ha^{-1} yr^{-1}]	[Tg N yr^{-1}]	
Symbiotic Tree BNF (accretion; method 1)	3.40	0.88	FIA & accretion lit search (This paper)
Symbiotic Tree BNF ($\%N_{dfa}$; method 2)	1.43	0.30	FIA & $\%N_{dfa}$ lit search (This paper)
Tree BNF with light limitation (accretion)	3.25	0.81	FIA & accretion lit search (This paper)
Tree BNF upper bound ($\%N_{dfa}$)	2.03	0.53	FIA ($\%N_{dfa}$=100) (This paper)
Symbiotic Understory BNF			Cleveland *et al.* (1999)
3%	2.20	0.48	scaled by forest area
10%	7.32	1.53	
17%	12.44	2.60	
Asymbiotic BNF	1.70	0.37	Reed *et al.* (2011) scaled by forest area
Total N Deposition	7.72	1.68	Schwede & Lear (2014) TDEP Total N deposition

Rock Weathering	1.75	0.37	Houlton *et al.* (2018) scaled by forest area
Total N influx to forested land (accretion)		**3.78**	Trees (accretion) + understory (3%) + asymbiotic + deposition + rock
Total N influx to forested land ($\%N_{dfa}$)		**3.20**	Trees ($\%N_{dfa}$) + understory (3%) + asymbiotic + deposition + rock

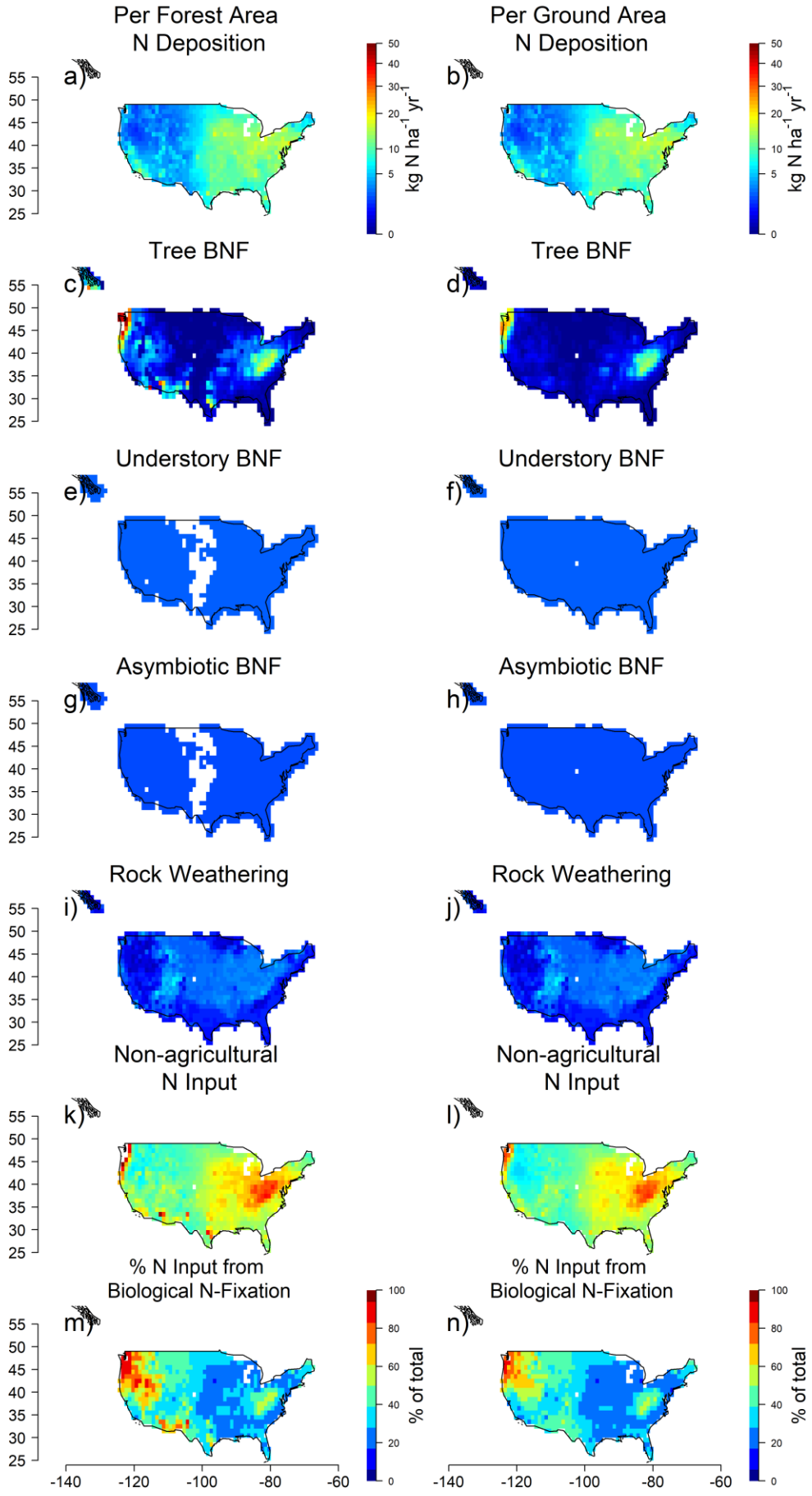
Per Forest Area
N Deposition
a)
Per Ground Area
N Deposition
b)
kg N ha^{-1} yr^{-1}
Tree BNF
c)
Tree BNF
d)
Understory BNF
e)
Understory BNF
f)
Asymbiotic BNF
g)
Asymbiotic BNF
h)
Rock Weathering
i)
Rock Weathering
j)
Non-agricultural
N Input
k)
Non-agricultural
N Input
l)
% N Input from
Biological N-Fixation
m)
% N Input from
Biological N-Fixation
n)
% of total
55
50
45
40
35
30
25
-140
-120
-100
-80
-60
0
5
10
20
30
40
50
60
80
100

Figure 5. Comparison of N inputs to forested land across the coterminous USA and southeast AK.
The average N input rate (kg N ha^{-1} yr^{-1}) per forest (a, c, e, g, i, k, m) and per ground (b, d, f, h, j, l, n) across 1° x 1° grid cells is shown for total N deposition (a, b), N-fixing trees, accretion method (c, d), N-fixing understory plants assuming 2.20 kg N ha $forest^{-1}$ yr^{-1} (e, f), asymbiotic N fixers assuming 1.70 kg N ha $forest^{-1}$ yr^{-1} (g, h), and rock weathering (i, j). Also shown are the total non-agricultural N input rate per forest area and per ground area (N-fixing trees + N-fixing understory + N-fixing asymbiotic + N deposition + rock weathering) (k, l), and the percent of the total non-agricultural N input from BNF: (N-fixing trees + N-fixing understory + N-fixing asymbiotic)/total non-agricultural N inputs (m, n) across 1° x 1° grid cells per forest and per ground. Colors in all panels except f and l are on a square root scale, but with numbers less than 0.1 kg N ha^{-1} yr^{-1} (including 0) set to the darkest blue for plotting purposes.

Understory (Figure 5e, f) and asymbiotic (Figure 5g, h) BNF rates per forest area are shown as constant across the USA because we do not have abundance data to make these spatially explicit. N deposition (Figure 5a, b) is higher in the eastern USA. Total non-agricultural N input (Figure 5k, l) is the sum of BNF from trees, understory, asymbiotic fixers, N deposition, and rock derived N. Total non-agricultural N input is high in the Pacific Northwest where tree BNF is high and the eastern USA where both tree BNF and N deposition are high. The percent of total non-agricultural N input from BNF (Figure 5c, d) and tree-based BNF (Figure 6a, b) show two hotspots where BNF is especially important: The southwest and the Pacific Northwest.

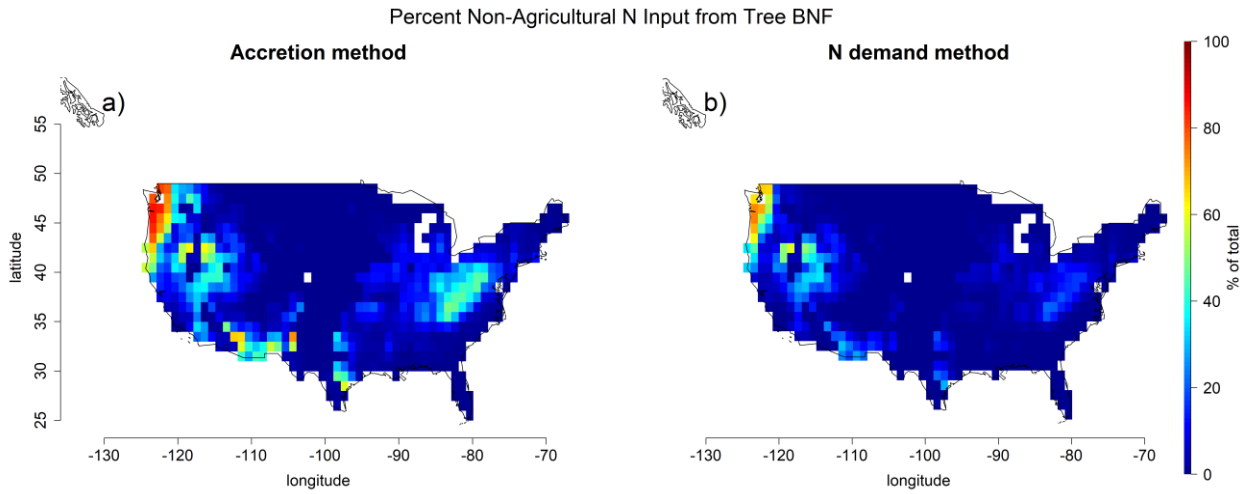

Figure 6. Percent non-agricultural N Input from tree N fixation in forests.
This map shows the percent of N inputs in forested areas that comes from N-fixing trees as opposed to biological N fixation in the understory, asymbiotic biological N fixation, N deposition, and rock weathering. a) accretion method, b) N demand method.

Percent N input from N-fixing trees is highest in the western USA where N-fixing tree basal area is high (*Alnus* stands with plot level BA > 50 m^2 ha^{-1}) and N deposition rates are low.

4 Discussion

Our analyses used tree census data to quantify the abundance of N-fixing trees to better estimate the tree-based BNF flux. These analyses suggest that tree-based BNF in the United States accounts for 0.30-0.88 Tg N yr^{-1}, which averages to 1.4-3.4 kg N ha $forest^{-1}$ yr^{-1}. At a continental scale, N inputs from trees, shrubs and symbiotic herbs, asymbiotic fixers, rock weathering and atmospheric deposition all contribute roughly similar amounts of N. In certain locations, such as the Pacific Northwest and the intermountain west, tree-based BNF accounts for the majority of N inputs, whereas in many parts of the country tree-based BNF is negligible.

Past work has noted that human activity has dramatically altered the amount of reactive N entering terrestrial ecosystems. At the global scale, initial reports suggested that human activity

doubled global N inputs (Vitousek et al. 1997). Recent reports that natural BNF might be lower than initially thought at the scale of the globe (Vitousek et al. 2013, Sulman et al. 2019) and in tropical rainforests (Sullivan et al. 2014) suggest that human impacts have more than doubled—perhaps quadrupled—background terrestrial N inputs. Our estimate of relatively low BNF in the USA agrees with these recent reports that human perturbation of N inputs is even higher than previously thought.

4.1 Interpretation of Our Methods and Numbers

Our accretion and N demand methods suggest fluxes of 0.88 and 0.30 Tg N yr^{-1}, respectively, which differ by a factor of more than two. Which method do we trust more? For a variety of reasons discussed below, we expect that the accretion method provides an overestimate and the N demand method provides an underestimate, so our best estimate is in between these methods.

The accretion method likely overestimates BNF for two reasons. First, field estimates of BNF are somewhat biased toward younger stands, whereas we are applying rates equally to all forests regardless of age. Most *Alnus* and *Robinia* in the FIA dataset are in forests aged 0-150 years (Menge et al. 2010), so the mismatch between the age range of the accretion data (usually 0-65 years) and the FIA data likely results in a moderate overestimate of BNF. Second, the accretion rates from the literature review did not account for N inputs from rock weathering or lichens and few included N deposition or asymbiotic BNF. These biases in the accretion method are probably not dramatic, as BNF rates from trees far exceed other inputs where N-fixing trees are active (Binkley and Giardina 1997), and there are likely fluxes out of the system that are also unaccounted for: N losses via leaching and gaseous emissions are often not considered. Our

sensitivity analysis indicates that a decrease in the accretion method-derived BNF rate for *Alnus* and *Robinia* to the lower 95% confidence interval would reduce the overall estimate by 46% (0.48 Tg N yr^{-1}).

Conversely, our N demand method likely underestimates BNF, for two reasons. First, N-fixing trees tend to have N-rich tissues, so the values we used for the C:N ratios of wood and foliage (which were not specific to N fixers) were likely too high. Our sensitivity analysis indicated that the $\%N_{dfa}$ estimate depended strongly on the C:N ratios of wood and foliage: Increasing the C:N ratio by 50% resulted in a 82% (for the C:N of wood) or 14% (for the C:N of foliage) increase in tree BNF. Second, our method omitted a number of sources of N demand. Trees need significant amounts of N for bark (Toselli et al. 2000), flowers (Toselli et al. 2000), and fruiting bodies (Rufat and DeJong 2001, Carranca et al. 2018), and trees lose additional N to herbivory (Mattson 1980, Lovett et al. 2002), none of which were in our estimate. Between these additional N demands and C:N ratio, the $\%N_{dfa}$ estimate was likely too low. Overall, we consider that the best estimate is between our accretion and N demand-based estimates. Taking the mean of the two, we suggest 0.59 Tg N yr^{-1} as our best estimate. On a per forest area metric this is 2.42 kg N ha $forest^{-1}$ yr^{-1} though spatially explicit estimates are locally higher or lower.

BNF from the combination of shrubs and herbaceous plants was of similar magnitude in forests as BNF from trees, suggesting that we need better abundance data and BNF rate measurements for these understory plants to constrain their contributions to overall BNF.

4.2 Comparison of This Estimate to Previous Work

Our estimate of tree-based BNF in United States forests, 0.59 Tg N yr^{-1}, is about a quarter of 2.09 Tg N yr^{-1}, the total when the central estimate for temperate forest tree BNF from

Cleveland *et al.* (1999) is scaled to the USA (Table 3). Both studies upscale plot-scale field estimates of BNF to the biome or regional scale. The primary difference between the two methods is that Cleveland *et al*. (1999) arbitrarily chose three possible values for N-fixing tree abundance, whereas we constrained N-fixing tree abundance with millions of data points from tree censuses. The FIA dataset has an excellent sampling design for quantifying continent-scale abundance of tree species, so we believe that our estimate is a marked improvement. Some modeling studies have also suggested higher rates (1.2-1.4 Tg N yr^{-1}; Galloway et al. 2004; Cleveland et al. 2013). Our result does agree well with a recent modeling study (0.77 Tg N yr^{-1} for all symbiotic BNF; Sulman et al. 2019), as well as a downscaled version of a global estimate from Vitousek *et al*. (2013) (0.47 Tg N yr^{-1} for all BNF; Table 3). Downscaling a non-spatially explicit global estimate to the USA requires a number of assumptions that are undoubtedly inaccurate, but nonetheless, the congruence of these estimates is encouraging.

Few BNF studies explicitly state whether their estimates represent pre vs. post-industrial rates. We consider that our values reflect contemporary post-industrial BNF estimates, which could partly explain the difference between this estimate and the pre-industrial value of Vitousek *et al* (2013). Though there is no clear evidence that human activities disfavor BNF, changes in N deposition, atmospheric CO_2 concentration, and land use could enhance or limit BNF. Recent work (Horn et al. 2018) did not find evidence that the growth or mortality of N-fixers is more sensitive to N deposition than non-fixers so it is unlikely that N deposition drove down abundance of N-fixing trees. N-fixing trees perform well in elevated CO_2 environments (Terrer et al. 2017). Land use is likely the most important difference between pre- and post-industrial BNF which affects the abundance of N-fixing trees. The pre-industrial tree distribution and extent of N-fixing trees is not known; however, most temperate N fixers are early successional

(Menge et al. 2010) and extensive land use disturbance, especially from logging, converts forests to younger successional states which tend to increase the cover of symbiotic N fixers. Conversely, in semi-arid western areas, widespread 20th century fire suppression may have reduced disturbance N inputs from BNF (Yelenik et al. 2013, Perakis et al. 2015). Overall, there is no evidence for consistent pre- versus post-industrial differences in the abundance or activity of tree N-fixers.

Combining BNF from symbiotic trees, symbiotic understory plants, and asymbiotic bacteria, our estimate of 1.44 Tg N yr^{-1} is at the low end of the range (0.5-12.7 Tg N yr^{-1}) reported in a previous national synthesis (Sobota et al., 2013). Shrubs and asymbiotic N fixers can also be patchy. Shrubs are a particularly significant N input in many regions, rivaling tree BNF (Cleveland et al. 1999), and similar to trees, shrubs can create local-to-regional BNF hotspots that depend strongly on patterns of landscape-level abundance (Yelenik et al. 2013). Herbaceous plants and lichens can be similarly patchy (Reed et al. 2011) and improving the spatially-explicit abundance of these organisms would improve the comparison. Additionally, given our focus on trees, we have not evaluated BNF in grasslands and other non-forest ecosystems, which a comprehensive assessment of BNF would incorporate.

Table 3. Comparison of Large-Scale BNF Estimates Scaled to the coterminous USA and southeast AK.

Study	Type of BNF included	Global estimate	US estimate	Fixation rate per forest area (avg)
		[Tg N yr^{-1}]	[Tg N yr^{-1}]	[kg N ha^{-1} yr^{-1}]
Cleveland (1999)	Symbiotic tree BNF	195	2.09	9.99
Vitousek (2013)	All BNF	58	0.47	2.23[a]
Cleveland (2013)	Symbiotic tree BNF	105	1.37	6.56
Galloway (2004)	All symbiotic BNF	107	1.15	5.48

Sulman (2019)	All symbiotic BNF	46	0.77	3.7
This estimate (accretion)	Symbiotic tree BNF	--	0.88	3.40
This estimate ($\%N_{dfa}$)	Symbiotic tree BNF	--	0.30	1.43
This estimate (mean)	Symbiotic tree BNF	--	0.59	2.81

Note: Details of USA Estimate and Average Fixation Rate per Forest Area calculations are provided in supplementary materials S3.
[a] assumes similar BNF rates across all forests globally

One major difference between our estimate and previous bottom-up estimates is the spatial distribution of BNF. The evapotranspiration-based map in Cleveland et al. (1999) suggested that the southeast was the main hotspot in the USA, whereas our map suggests hotspots in the Pacific Northwest, the Appalachians, and the southwest due primarily to the abundance pattern of N-fixing trees. The southeast, as well as areas such as the central USA and Southern California, have a distinct lack of symbiotic N-fixing trees, and therefore large tree-based fluxes in these regions seem unlikely. Shrubs, herbaceous plants, and asymbiotic BNF still occur in those regions, so the overall N flux into those ecosystems can still be substantial. This finding is consistent with the conclusions of Reed *et al.* (2011) that asymbiotic N fixers make substantial contributions to the reactive N flux. Further analysis is needed to incorporate lichens and bryophytes, which are thought to be important in many regions (DeLuca et al. 2002, Matzek & Vitousek 2003, Antoine 2004, Menge & Hedin 2009, Elbert et al. 2012).

4.3 Methodological Limitations

One of the persistent limitations to bottom up estimates is the lack of data in the literature for tree-based BNF rates of some genera. There is a bias toward genera such as *Robinia* and

Alnus (which are two of the most abundant genera, with 42% and 16% of N fixer stems respectively), while others (e.g. *Albizia* and *Cercocarpus*, 0.4% and 16% of stems respectively) had no studies satisfying our filtering criteria (reporting both BNF rate using the accretion method and basal area of the stand where it was measured). Based on our sensitivity analysis, the lack of information on these unreported genera is a relatively minor source of uncertainty. It does not change the order of magnitude of the result and is negligible compared to the effects of changing the fixation rate data for *Alnus* or *Robinia*. The greatest change in our estimate comes from the BNF rate used for *Robinia* which could change the estimate by 18%. Even though *Robinia* is one of the best studied temperate N-fixers, the high abundance and unclear relationship between BNF rate and stand basal area mean more data on this genus are particularly important for improving the estimate certainty. It is important to note, though, that the lack of accretion studies does not affect our N demand method. One of the reasons we used two methods was to address the relatively sparse number of robust studies of BNF fluxes, and the fact that the two methods give answers within the same range is encouraging. The N demand method requires data on $\%N_{dfa}$, which are also relatively sparse, but the fact that our highest N demand estimate (assuming N-fixing trees fix 100% of their N), still yields a similar total flux suggests that the methods are robust. Our sensitivity analysis for the N demand method shows that the most important area of uncertainty is the stoichiometry of wood, which is among the least-reported stoichiometric value for all plant tissue types.

4.4 Conclusion

This study helps resolve a long-standing short-coming of prior BNF flux estimates: A lack of information on the spatial distribution of important symbiotic N-fixing plants (Galloway

et al. 2008, Sobota et al. 2013). The abundance of symbiotic N-fixing trees is spatially uneven. Further work is still needed to measure BNF rates, particularly in common N-fixing tree genera such as *Robinia* and *Cercocarpus*. It would be helpful to resolve BNF variation with age (Menge and Hedin 2009), N-fixing tree density (Bormann and Gordon 1984, Vitousek and Howarth 1991, Mitchell and Ruess 2009), facultative versus obligate habit (Menge et al. 2009a), and environmental drivers such as climate and soils (Binkley & Giardina, 1997; Uliassi & Ruess, 2002) to estimate site-specific BNF. Since most of the total tree BNF flux is attributed to relatively few species, it increases the likelihood of effectively constraining total tree BNF, and raises the possibility that our spatially-explicit approach could be successful elsewhere. Further work should be conducted in other biomes using forest inventory data to refine BNF estimates globally, especially the tropics where N-fixing tree diversity and abundance are higher (ter Steege et al. 2006, Menge et al., 2017, Gei et al. 2018). Given the importance of tree-based BNF for quantifying human impacts on the N cycle, parameterizing Earth System Models, and understanding the ecological role of N-fixing organisms, a spatially-explicit quantification of BNF is essential.

Acknowledgements

We thank Jeremy Lichstein for pre-processing the FIA data, the Menge lab for valuable feedback on preliminary analysis and drafts, especially Ben Taylor. Data supporting this analysis is available from the USFS FIA, Cleveland et al (1999), Schwede & Lear (2014), Reed et al (2011), Houlton & Dahlgren (2018) and the sources listed in the supplementary information. Funding for AS was from NSF Grant DGE 16-44869. There are no conflicts of interest for any author that are not apparent from their affiliations or funding. Any use of trade names does not imply endorsement by the US Government. The views expressed in this article are those of the authors and do not necessarily represent the views or policies of the U.S. Environmental Protection Agency.

Chapter 2: Nitrogen-fixing trees have no net effect on forest growth in the coterminous United States

Authors: Anika P. Staccone, Sian Kou-Giesbrecht, Benton N. Taylor, Duncan N. L. Menge

Staccone, Anika P., et al. "Nitrogen-fixing trees have no net effect on forest growth in the coterminous United States." *Journal of Ecology* 109.2 (2021): 877-887.

Abstract

1. Nitrogen (N)-fixing trees fulfill a unique and important biogeochemical role in forests through their ability to convert atmospheric N_2 gas to plant-available N. Due to their high N fixation rates, it is often assumed that N-fixing trees facilitate neighboring trees and enhance forest growth. This assumption is supported by some local studies but contradicted by others, leaving the overall effect of N-fixing trees on forest growth unresolved.

2. Here we use the U.S. Forest Service's Forest Inventory and Analysis database to evaluate the effects of N-fixing trees on plot-scale basal area change and individual-scale neighboring tree demography across the coterminous U.S.

3. First we discuss the average trends. At the plot and individual scales, N-fixing trees do not affect the relative growth rates of neighboring trees, but they facilitate recruitment and inhibit survival rates, suggesting that they are drivers of tree turnover in the coterminous U.S. At the plot scale, N-fixing trees facilitate the basal area change of non-fixing neighbors.

4. In addition to the average trends, there is wide variation in the effect of N-fixing trees on forest growth, ranging from strong facilitation to strong inhibition. This variation does not show a clear geographic pattern, though it does vary with certain local factors. N-fixing trees facilitate forest growth when they are likely to be less competitive: under high N deposition and high soil moisture or when neighboring trees occupy different niches (e.g. high foliar C:N trees and non-fixing trees).

Synthesis. N-fixing trees have highly variable effects on forest growth and neighbor demographics across the coterminous U.S. This suggests that the effect of N-fixing trees on forest development and carbon storage depends on local factors, which may help reconcile the conflicting results found in previous localized studies on the effect of N-fixing trees on forest growth.

1 Introduction

Decades of work have demonstrated the importance of forests as a substantial carbon (C) sink (Pacala et al. 2001, Goodale et al. 2002, Pan et al. 2011). However, the size and persistence of the forest C sink are thought to be constrained by the availability of soil nitrogen (N) (Hungate *et al.*, 2003; Wieder, Cleveland, Smith, & Todd-Brown, 2015), which limits primary production in many terrestrial ecosystems (Elser et al. 2007, LeBauer and Treseder 2008). Biological N fixation, which is the conversion of plant-unavailable atmospheric N_2 gas to plant-available N by bacteria, is the dominant natural N flux into terrestrial ecosystems, exceeding natural atmospheric N deposition and rock N weathering (Fowler et al. 2013a, Vitousek et al. 2013, Houlton et al. 2018). N-fixing trees, which are symbioses between trees and N-fixing bacteria that live in root nodules, can exhibit high N fixation rates (> 100 kg N ha^{-1} yr^{-1}) in boreal,

temperate and tropical forests (Binkley et al. 1994, Binkley and Giardina 1997, Ruess et al. 2009), emphasizing the key role of N-fixing trees in forest N cycling.

Forest N budgets have suggested that the N input from N-fixing trees, which fertilizes the soil N pool through turnover and decomposition of N-fixers' N-rich tissues (Binkley and Giardina 1997, Ehrenfeld et al. 2005), is critical to satisfying the N demand of forest growth. For example, N-fixing trees satisfy the majority of the N demand of forest growth in early successional forests in Panama (Batterman *et al.*, 2013) and mature forests in Trinidad (Brookshire et al. 2019). These studies, along with the clear fertilization mechanism, have led to the prevalent view that N-fixing trees relieve N limitation and facilitate neighboring trees, enhancing overall forest growth.

However, the direct evidence for N-fixing trees facilitating their neighbors is mixed. Many studies support the prevailing view (e.g., Binkley *et al*. 1992; Piotto, 2008; Hulvey *et al*., 2013; Minucci *et al*., 2019). Counter to the prevailing view, though, N-fixing trees have similar effects on neighboring trees as non-fixing trees in some circumstances: Lai *et al.*, 2018 (in Panama) and Xu *et al.*, 2020 (pan-tropical) both found that N-fixing trees did not influence basal area change. N-fixing trees can even inhibit neighboring trees: Chapin *et al.* 2016 found that N-fixing trees decreased the growth of non-fixing trees in mature forests in Alaska and Taylor *et al.*, 2017 found that N-fixing trees decreased forest growth in Costa Rica. Because the net effect of N-fixers on their neighbors differs markedly between different studies, the overall effect of N-fixing trees on forest growth remains unresolved.

From a mechanistic perspective, the net effect of N-fixers on their neighbors depends on the balance of facilitative and inhibitory effects. Facilitative effects include increased soil N, as described above, and potentially other factors such as increased soil phosphorus through

increased rock weathering (Perakis & Pett-Ridge, 2019). On the other hand, N-fixers could inhibit neighbors by competing for resources such as light (Taylor & Menge, 2018), water (Adams *et al.*, 2016; Cramer, Van Cauter, & Bond, 2010), or nutrients (Nasto *et al.*, 2014; Perakis & Pett-Ridge, 2019; Rastetter, Vitousek, Field, Shaver, & Herbert, 2001; Vitousek & Field, 1999). The net effect of these potential facilitative and inhibitory effects could be net facilitation (N-fixers promote growth of neighbors), weak inhibition (competition from N-fixers inhibits neighbor growth but less than competition from non-fixers), or strong inhibition (N-fixers inhibit neighbor growth more than non-fixers; Taylor *et al.*, 2017). (Here we do not distinguish between facilitation and weak inhibition, referring to both as facilitation.)

Different net N-fixer effects on forest growth—facilitation vs. inhibition vs. neither—might stem from differences in the competitive dynamics between N-fixing and non-fixing trees in these sites. Many factors have been linked to N-fixer versus non-fixer competition, from climatic factors such as temperature and precipitation to local factors such as the relative supply of nitrogen, water, or light, or the traits of individual trees (e.g., Houlton *et al*., 2008; Adams *et al*., 2016; Cramer, Van Cauter, & Bond, 2010; Vitousek & Field 1999; Rastetter *et al*., 2001; Fisher *et al*., 2010).

To determine the effect of N-fixing trees on forest growth across the coterminous U.S., we used the U.S. Forest Service's Forest Inventory and Analysis (FIA) database to evaluate how N-fixing trees impact plot-scale basal area change and individual-scale neighboring tree demography. Specifically, we ask five questions. The first two questions address the overall magnitude and direction of N-fixing tree effects: (1) How do N-fixing trees affect basal area change at the plot scale? (2) How do N-fixing trees affect demographic rates of neighboring trees at the individual scale? The third, fourth, and fifth questions address drivers of the N-fixing tree

effects: How do N-fixing tree effects vary with (3) geography and climate, (4) plot-scale abiotic factors (stand age, N deposition, and soil moisture), and (5) individual-scale tree traits (mycorrhizal association, foliar C:N, N fixation status, and canopy position)? We focused on these particular drivers because they are associated with plausible mechanisms and we could reliably quantify them at the proper scale.

2 Methods

2.1 FIA Database Description

We used Version 5.1 of the U.S. Forest Service's Forest Inventory and Analysis (FIA) database (Burrill *et al.*, 2018), which contains 57,264 plots that have been censused at least twice. Census intervals were usually 5-10 years. Plot size varies, but the most common plot size is 670 m^2. We classified tree species as rhizobial N-fixers (from Sprent 2009), actinorhizal N-fixers (Huss-Danell 1997), or non-fixers. Hereafter, we refer to rhizobial and actinorhizal species as N-fixing trees, although N fixation activity for any individual N-fixing tree was not possible to assess at this scale. The N-fixing tree genera in the dataset that were sufficiently abundant for analysis (> 10 stems) were *Acacia, Albizia, Alnus, Cercocarpus, Elaeagnus, Olneya, Prosopis,* and *Robinia* (Appendix B - SI Table 1). There were 7,050 *Robinia* out of 8,292 total N-fixers.

We give an overview of our analyses here. The details of the analyses are in SI Text 1 and 2. All analyses were implemented in R (R Core Team, 2017) using lme4 (Bates, Mächler, Bolker, & Walker, 2015).

2.2a How do N-fixing trees affect basal area change at the plot scale? (Q1)

We assessed the effects of N-fixing trees on plot-scale basal area change (Q1) using linear mixed-effect models. At the plot scale, we studied four response variables, each of which measured basal area change from one census to the next. The variables were total basal area increment (BAI), basal area increment of non-fixing trees (BAI_n), and two of the components of BAI: recruitment rate and survival rate (henceforth referred to as recruitment and survival). Because our questions concerned the effects of N-fixing trees, the primary predictor variable of interest was the relative prevalence of N-fixing trees. At the plot scale, we quantified the relative prevalence of N-fixing trees as the percent of basal area comprised of N-fixing trees, following Taylor *et al.* (2017). This is a continuous variable that ranges from 0% (all individuals in the plot are non-fixing trees) to 100% (all individuals in the plot are N-fixing trees) and is defined mathematically in Appendix B - SI Text 1.

The plot-scale models also included a control covariate and a random effect (Appendix B - SI Text 2, SI Table 2). In general, control covariates control for measured factors that are important but are not of specific interest for the study. The control covariate we used was total basal area in the plot. We also included a state-level random effect to account for unmeasured factors that cluster geographically, such as climate.

The result of interest for each statistical model is the effect of N-fixing trees on each response variable, i.e. the model coefficient for the percent of basal area comprised of N-fixing trees. The interpretation of this model coefficient is not particularly intuitive (Appendix B - SI Table 3), so to facilitate understanding, we translated the coefficient into a more intuitive number: The expected percent change in a response variable (*e.g.*, basal area increment) from when a plot is comprised entirely of non-fixing trees to when a plot is comprised entirely of N-fixing trees. We call this number the "N-fixer effect," and abbreviate it for each response

variable with the subscript "NFE". A positive NFE indicates net facilitation (or weak inhibition) by N-fixing trees on the response variable, and a negative NFE indicates net inhibition by N-fixing trees on the response variable. For example, the N-fixer effect on BAI is:

$$BAI_{NFE} = 100 * \left(\frac{BAI_{100\%\,BA_{pct}} - BAI_{0\%\,BA_{pct}}}{BAI_{0\%\,BA_{pct}}}\right) \quad (1)$$

where $BAI_{100\%\,BA_{pct}}$ and $BAI_{0\%\,BA_{pct}}$ are the BAI values predicted by the linear mixed-effect model when the percent of basal area comprised of N-fixing trees are 100% and 0%, respectively (see Appendix B - SI Text 2 for more details). A BAI_{NFE} of 10% would mean that the expected BAI of a plot with an average basal area is 10% higher when a plot is comprised entirely of N-fixing trees than when a plot is comprised entirely of non-fixing trees.

We calculated confidence intervals on the NFE with a parametric bootstrap analysis to simulate data at 0% basal area comprised of N-fixing trees and 100% basal area comprised of N-fixing trees separately. Coefficient values were bootstrapped 1000 times using the coefficient estimates and standard errors, and using mean values for the control covariates.

2.2b How do N-fixing trees affect neighboring tree demography at the individual scale? *(Q2)*

Similar to our plot-scale analysis, we used linear mixed-effect models to assess the individual-scale effects of N-fixing trees. Instead of plot-scale rates, though, our response variables were individual-scale demographic rates (Q2). Specifically, our individual scale response variables were the relative growth rate, the recruitment rate, and the survival rate of individual trees (henceforth referred to as growth, recruitment, or survival). Similar to the plot-scale analysis, the primary predictor variable of interest was the relative prevalence of N-fixing trees. At the individual scale, though, we quantified the relative prevalence of N-fixing trees as

the percent of the neighbor crowding index (NCI) comprised of N-fixing trees, following Taylor *et al.* (2017). NCI is a metric that factors in the number of neighboring trees within a given radius of a focal tree (here, 7.3 m), their size, and their proximity to the focal tree (Canham, LePage, & Coates, 2004). As makes intuitive sense, more trees, larger trees, and trees closer to the focal tree increase NCI (crowding). Similar to BA_{pct}, the percent of the NCI comprised of N-fixing trees is a continuous variable that ranges from 0% (all crowding is from non-fixing trees) to 100% (all crowding is from N-fixing trees) and is defined mathematically in Appendix B - SI Text 2.

The individual-scale models also included control covariates and a random effect, as in the plot-scale models (Appendix B - SI Text 2, SI Table 2). The control covariates we used were the focal tree's total crowding (NCI) and diameter at breast height (DBH). We also included a plot-level random effect to account for unmeasured factors that cluster geographically, such as climate.

As in the plot-scale analysis, we calculated the N-fixer effect (NFE) at the individual scale as the expected percent change in the response variable (*e.g.*, relative growth rate) from when all crowding is from non-fixing trees to when all crowding is from N-fixing trees. For example, the N-fixer effect on relative growth rate is:

$$RGR_{NFE} = 100 * \left(\frac{RGR_{100\%\ NCI_{prop}} - RGR_{0\%\ NCI_{prop}}}{RGR_{0\%\ NCI_{prop}}}\right) \quad (2)$$

where $RGR_{100\%\ NCI_{prop}}$ and $RGR_{0\%\ NCI_{prop}}$ are the relative growth rates predicted by the linear mixed-effect model when the percent of NCI comprised of N-fixing trees is 100% and 0%, respectively. A RGR_{NFE} of 10% would indicate that the expected relative growth rate of an average-sized tree with average total crowding in an average plot is 10% higher when all crowding is from N-fixing trees vs. when all crowding is from non-fixing trees.

2.3a How do N-fixing tree effects vary with geography and climate? (Q3)

To assess the geographic patterns in the NFE for each response variable, we used a Moran's I test from the ape package (Paradis, 2020), which evaluates spatial autocorrelation. If there is a geographic pattern to the NFE then plots physically closer together would have more similar NFEs (e.g. one region of the U.S. might have negative NFE while other regions do not). We used the inverse Euclidean distance for the weight matrix so that physical proximity of plots weighted the Moran's I test statistic. To further assess the geographic patterns in NFE we examined the Pearson's correlations between the plot-scale NFE and latitude and longitude, which were obtained from the FIA database. To assess how the NFE varied with climate we examined the Pearson's correlation between the plot-scale NFE and mean annual temperature (MAT) and precipitation (MAP), which were obtained from WorldClim (Fick & Hijmans, 2017).

2.3b How do N-fixing tree effects vary with plot-scale abiotic factors? (Q4)

We obtained abiotic plot-scale data from several sources: the FIA (stand age), the National Atmospheric Deposition Program (total N deposition) (National Atmospheric Deposition Program, 2018), and the Soil Moisture Active and Passive dataset (soil moisture) (Reichle *et al.*, 2018). To assess the effect of different abiotic factors on the NFE, we designated plots as "high" or "low" for each abiotic factor where "high" was above the mean value and "low" was below the mean value.

Each abiotic factor was considered in the model separately by using an interaction between the abiotic factor status of the plot ("high" or "low" for the given abiotic factor) and prevalence of N-fixing trees (percent of basal area comprised of N-fixing trees). We determined

whether the NFE was different between high and low levels of each abiotic factor by assessing whether the 95% confidence intervals from the parametric bootstrap analysis overlapped each other.

2.3c How do N-fixing tree effects vary with individual-scale traits of trees? (Q5)

We obtained species traits from several sources: mycorrhizal association from Jo *et al.* (2019), foliar C:N from the USDA Plants database (USDA, 2019) (designated "high", "moderate", or "low"), deciduousness from a database synthesis (SI Text 3), and canopy position from the FIA. We re-categorized foliar C:N as "high" and "low" (where "low" included both the USDA levels "medium" and "low"). We re-categorized the FIA crown classes into canopy positions where "open grown," "dominant," and "co-dominant" trees are canopy trees and "intermediate" and "overtopped" trees are non-canopy trees.

As in section 2.3b, each trait was considered in the model separately by using an interaction between the trait status of the focal tree (AM or EM, high C:N or low C:N, deciduous or evergreen, canopy or non-canopy, and N-fixer or non-fixer) and prevalence of N-fixing trees (percent of NCI from N-fixing trees) in the model. We used a t-test to determine whether the NFE was different between the levels of each trait of the focal tree.

3 Results

3.1a How do N-fixing trees affect basal area change at the plot scale? (Q1)

Aggregating across the entire coterminous U.S., N-fixing trees have no systematic effect on plot-scale total BAI (the confidence intervals are distributed across 0), but did facilitate the

plot-scale BAI of non-fixing trees (Table 4). N-fixing trees facilitated plot-scale recruitment but inhibited plot-scale survival (Fig. 7, Table 4).

Table 4. Average N-fixer effects on plot-scale metrics in the coterminous U.S.
The metrics are the total basal area increment (BAI), basal area increment of non-fixing trees (BAI_n), and two of the components of BAI, plot-scale recruitment rate (R) and plot-scale survival rate (S). The N-fixer effect (NFE) for each metric is the expected percent change in the metric between plots comprised of N-fixing trees and plots comprised of non-fixing trees (see Methods for more details). Numbers shown are means (95% CI).

N-fixer effect on plot-scale basal area increment (BAI_{NFE})	N-fixer effect on plot-scale basal area increment of non-fixing trees ($BAI_{n,NFE}$)	N-fixer effect on plot-scale recruitment rate (R_{NFE})	N-fixer effect on plot-scale survival rate (S_{NFE})
1% (-35%, 35%)	34% (0.6%, 72%)	60% (32%, 87%)	-7% (-12%, -1%)

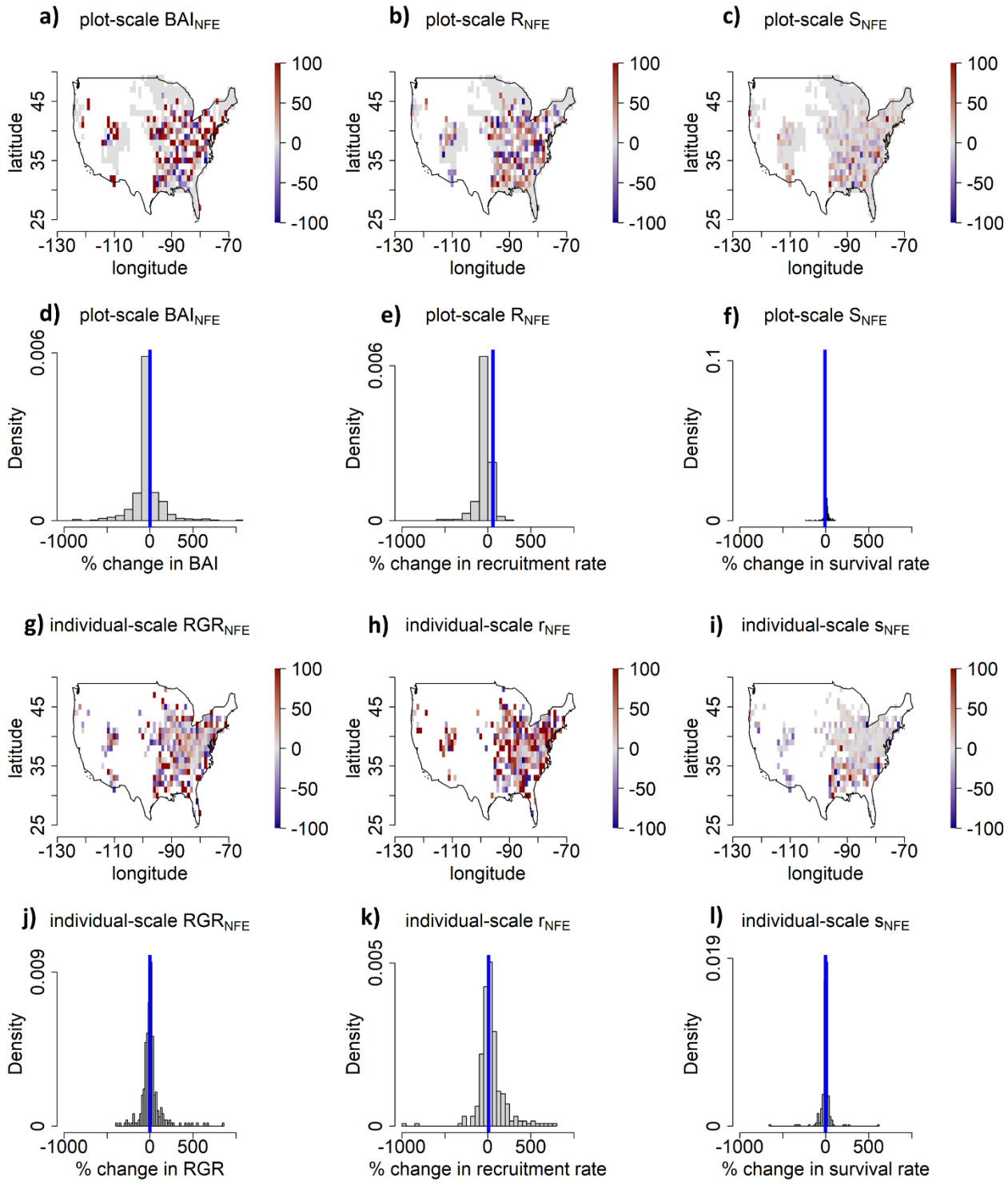

Figure 7. N-fixer effects

N-fixer effects (as defined in Table 1 and the Methods) on plot-scale metrics and individual-scale demographic rates across the coterminous U.S. Maps are shown for analyses at the plot-scale (a-c) and individual-scale (g-i). Grid cells are 1° x 1°; white cells had fewer than 5 plots with N-

fixing trees (excluded from spatial analyses (Q3)). Red, blue, and gray cells indicate that N-fixing trees had positive, negative, and neutral effects, respectively, compared to non-fixing trees. The ends of the color scale include outliers with values 100% and above or -100% and below for clarity. Histograms are also shown for the plot-scale metrics (d-f) and individual-scale demographic rates (j-l). Blue lines on histograms represent the average NFE evaluated across the coterminous U.S. BAI: basal area increment, R: recruitment (plot-scale), S: survival (plot-scale), RGR: relative growth rate, r: recruitment (individual-scale), and s: survival (individual-scale).

3.1b How do N-fixing trees affect neighboring tree demography at the individual scale? (Q2)

At the individual scale, N-fixing trees did not affect the growth of their neighbors, but they had a positive effect on the recruitment of their neighbors and a negative effect on the survival of their neighbors (Fig. 7g-l, Table 2).

Table 5. Average N-fixer effects (as defined in Table 7 and the Methods) on individual-scale demographic rates in the coterminous U.S.
The demographic rates are the relative growth rate (RGR), individual-scale recruitment rate (r), and individual-scale survival rate (s).

N-fixer effect on relative growth rate (RGR_{NFE})	N-fixer effect on individual-scale recruitment rate (r_{NFE})	N-fixer effect on individual-scale survival rate (s_{NFE})
-1.5% (-3.6%, 2.1%)	7.5% (5.3%, 11.2%)	-0.9% (-1.6%, -0.1%)

3.2a How do N-fixing tree effects vary with geography and climate? (Q3)

The plot-scale (Fig. 7a-f) and individual-scale (Fig. 7g-l) NFEs were variable across plots (Fig. 7d-f,j-l) and grid cells (Fig. 7a-c,g-i), leading us to ask whether NFEs varied geographically or with large-scale climatic variables. However, Moran's I test found no spatial autocorrelation for either the plot-scale or individual-scale NFEs (Appendix B - SI Table 4). Furthermore, there was no significant Pearson's correlation between plot-scale or individual-scale NFE and latitude, longitude, MAT, or MAP (Appendix B - SI Figure 2) using the same models described above to calculate NFE.

3.2b How do N-fixing tree effects vary with plot-scale abiotic factors? (Q4)

Given the lack of geographic and climatic explanations for the large variation in N-fixer effects, we asked whether N-fixer effects could be explained by local abiotic factors. For the abiotic factors, we looked at stand age, N deposition rate, and soil moisture.

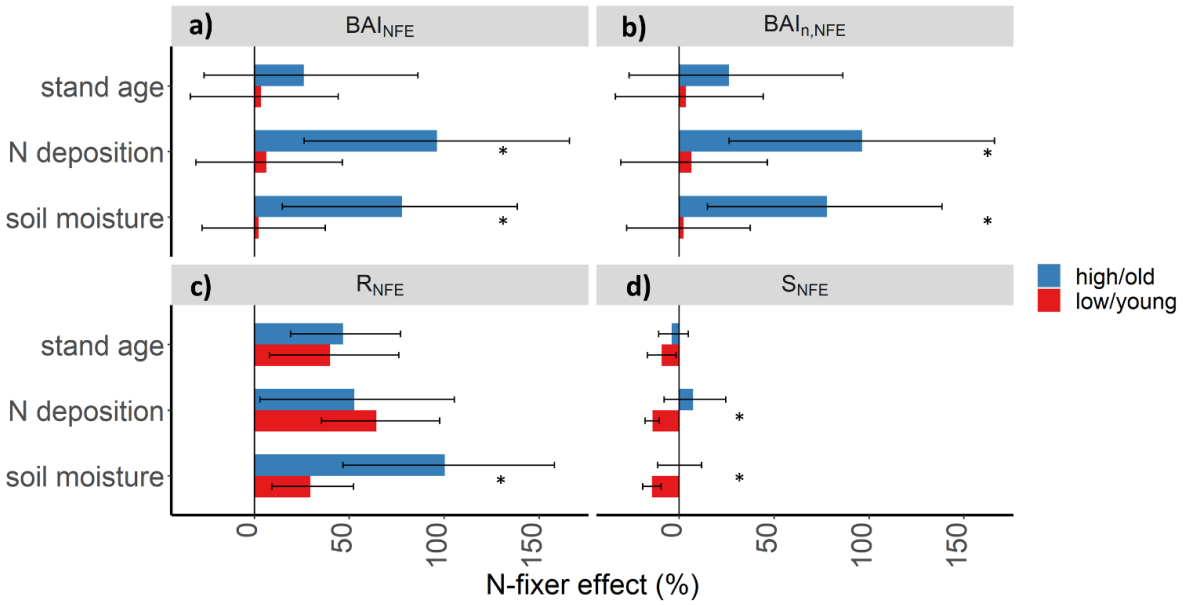

Figure 8. N-fixer effects on plot-scale metrics for high and low values of plot-scale abiotic factors
Panels show the N-fixer effects on a) total basal area increment (BAI_{NFE}), b) basal area increment of non-fixing trees ($BAI_{n,NFE}$), c) recruitment (R_{NFE}), and d) survival (S_{NFE}). Cutoffs between red and blue bars are: 60 years (stand age), 3.64 kg N ha^{-1} yr^{-1} (N deposition), and 0.27 g g^{-1} (soil moisture). For example, the bottom-most red bar in c) shows the NFE in low soil moisture plots (<0.27 g g^{-1}), whereas the bottom-most blue bar in c) shows the NFE in high soil moisture plots (>0.27 g g^{-1}). Error bars show the 95% confidence interval of a parametric bootstrap analysis with 1000 bootstraps. Stars indicate significant differences between levels at $p < 0.05$ (*), $p < 0.01$ (**), and $p < 0.001$ (***). Values reported in SI Table 5.

Some of the plot-level NFEs (on BAI, BAI_n, recruitment, and survival) differed significantly at different levels of abiotic factors (t-test with $p < 0.05$, Fig. 8, Appendix B - SI Table 5). N-fixer effects on BAI_n were nearly 15 times more positive in high (> 3.64 kg N ha^{-1} yr^{-1}) compared to low N deposition plots, and N-fixer effects on BAI, BAI_n, and R were three to 35 times more

positive in wetter (> 0.27 g g^{-1}) than in drier plots. Stand age was not a significant mediator of the N-fixer effect on any of the plot-scale metrics (Appendix B - SI Table 5).

3.2c How do N-fixing tree effects vary with individual-scale traits of trees? (Q5)

We also asked whether N-fixer effects could be explained by traits of trees. To assess how tree traits mediated the N-fixer effect on individual-scale demographic rates (Q5), we looked at five individual-scale tree traits: mycorrhizal association (AM/EM), foliar C:N (high/low), deciduousness (deciduous/evergreen), canopy position (canopy/non-canopy), and N fixation status (N-fixer/non-fixer).

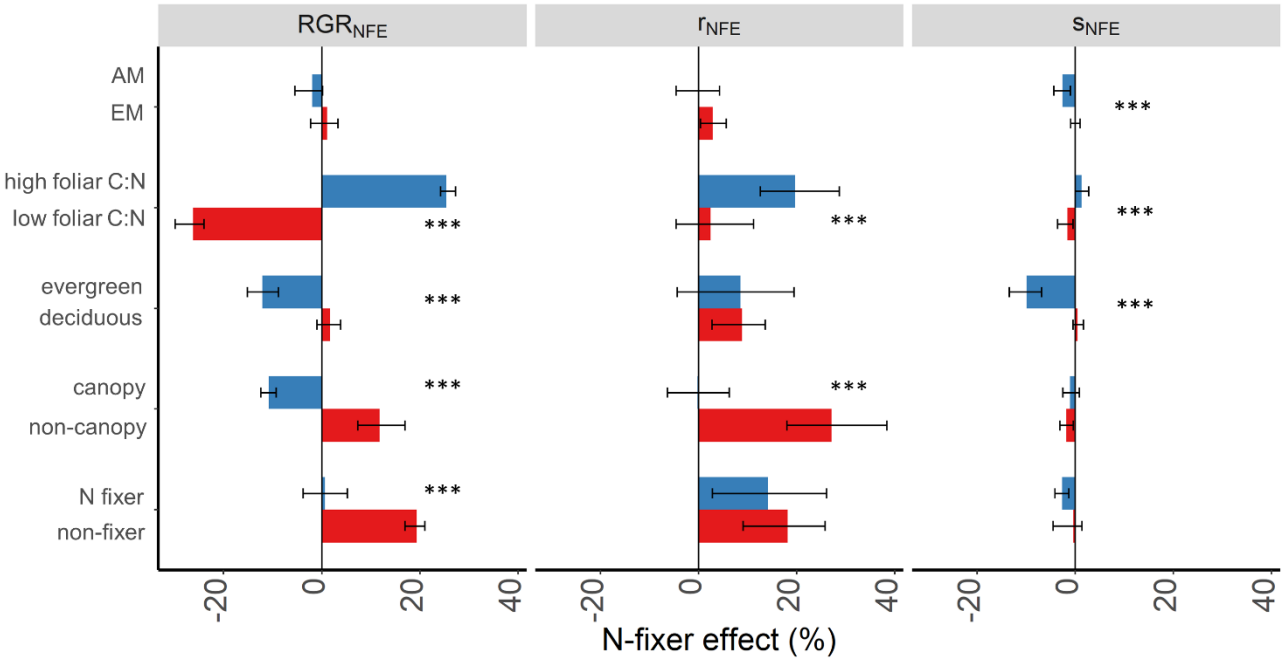

Figure 9. N-fixer effects on individual-scale demographic rates as mediated by individual-scale tree traits.
Panels show the N-fixer effects on a) growth (RGR_{NFE}), b) recruitment (r_{NFE}), and c) survival (s_{NFE}). Error bars show the 95% confidence interval of a parametric bootstrap analysis with 1000 bootstraps. Stars indicate significant difference between levels at $p < 0.05$ (*), $p < 0.01$ (**), and $p < 0.001$ (***). Values reported in SI Table 5.

Mycorrhizal association was a significant mediator of the effect of N-fixers on survival. The N-fixer effect on the survival of AM trees was negative (-2.5%), but there was no effect of N-fixers on the survival of EM trees.

Foliar C:N was a significant mediator of the N-fixer effect on all three demographic rates. N-fixers had a negative effect on the growth of low foliar C:N trees (-26.2%) but had a positive effect on the growth of high foliar C:N trees (25.3%). N-fixers had no effect on the recruitment of low foliar C:N trees but had a positive effect on the recruitment of high foliar C:N trees (19.6%). The survival of low foliar C:N trees was negatively affected by N-fixers (-1.6%) while the survival of high foliar C:N trees was not affected by N-fixers.

Deciduous and evergreen trees were affected differently by N-fixers. N-fixers did not significantly affect the growth or survival of deciduous trees but significantly negatively affected the growth (-12.1%) and survival (-9.9%) of evergreen trees.

Canopy and non-canopy trees were affected differently by N-fixers. The growth of non-canopy trees was positively affected by N-fixers (11.8%) while the growth of canopy trees was negatively affected by N-fixers (-10.8%). N-fixers had a positive effect on the recruitment of non-canopy trees (27.0%), while N-fixers had no effect on the recruitment of canopy trees. However, recruitment of canopy trees was rare since the tree, which was less than 12 cm DBH or nonexistent to not be included in the first census, would have to recruit and grow into the canopy by the second census.

Finally, N fixation status was a significant driver of the N-fixer effect on growth. N-fixers positively affected the growth of non-fixers (19.3%) but did not significantly affect the growth of N-fixers.

4 Discussion

On average, N-fixing trees had no effect on basal area change (net 0 NFE on basal area increment) in the forests of the coterminous U.S (Table 4). However, N-fixing trees did increase plot-scale non-fixer BAI by an average of 34% (0.66-72% 95% CI; Table 1). N-fixing trees facilitated recruitment more than they inhibited survival, suggesting that N-fixing trees are drivers of tree turnover in these forests. The effect of N-fixing trees on forest growth did not show a clear geographic pattern (associated with latitude or longitude) or climatic pattern (associated with MAT or MAP) within the coterminous U.S., but it did vary with abiotic factors and tree traits. Below, we put our results in the context of related work, provide a competition framework for understanding the wide variation we observed across plots and individuals, and point to key areas for future studies to address.

4.1 Comparison of this Study with Previous Studies of N-Fixer Effects

Past work on the N-fixer effect was conducted at a smaller scale than our analysis. In total, our study included over 2.5 million trees, 57,264 plots, and 3,837 ha of forest, which is over >10 times more trees and area than other studies: Taylor *et al.* (2017) sampled 20,586 trees on 8 plots totaling 8 ha, Lai *et al.* (2016) sampled 36,518 trees on 87 plots totaling 8.7 ha, Chapin *et al.* (2016) sampled 7,812 trees on 12 plots, and Xu *et al*. (2020) sampled 11 plots totaling 381 ha. The geographic extent of our study was also large: it covered 276 1° latitude x 1° longitude grid cells, which included wide variation in community composition and environmental characteristics. The studies of Taylor *et al.* (2017), Lai *et al.* (2018) and Chapin *et al*. (2016) all spanned a spatial extent equivalent to less than one of our grid cells, and Xu *et al*. (2020)

included 11 plots, each in a different grid cell. It is also worth noting that the small size of the individual FIA plots in our analysis (0.07 ha, much smaller than the 16-60 ha plots in Xu *et al*. 2020 and the 1 ha plots in Taylor *et al.* 2017, and slightly smaller than the 0.1 ha plots in Lai *et al*. 2018) contributes to the wide variation in the N-fixer effects in our study, since each plot sampled relatively few trees. Given the large scale and the breadth of environmental characteristics in our analysis, the distribution of N-fixer effects we observed (e.g., Fig. 7d-f, j-l) is at least as informative as the average trend.

Although past studies have come to differing conclusions about the N-fixer effect, all of their findings fit within the distribution of N-fixer effects we observed. Positive N-fixer effects in boreal (Chapin *et al.*, 2016) and temperate (Minucci *et al.*, 2019) forests, null N-fixer effects in temperate (Binkley *et al.*, 1992) and tropical (Lai *et al.*, 2018; Xu *et al*., 2020) forests, and negative N-fixer effects in boreal (Chapin *et al.* 2016) and tropical (Taylor *et al.*, 2017) forests all fit well within the distribution of the N-fixer effects we observed across temperate forests in the coterminous U.S. It is therefore of great interest to understand its variation. For both the variation within our study and across previous studies, why is the N-fixer effect positive in some circumstances but null or negative in others?

4.2 What Mediates the N-Fixer Effect?

Abiotic factors that were major drivers of the N-fixer effect were N deposition and soil moisture, while tree traits that drove the N-fixer effect were foliar C:N, canopy position, evergreen/deciduous and N fixation status. The unifying theme of these results was that N-fixing trees facilitated forest growth when they were expected to be less competitive, such as in plots with high N deposition and soil moisture or when neighboring trees occupied different niches

(i.e. high foliar C:N, understory, and non-fixing trees). In the following sections we explain our results within the context of this competitive framework.

We had initially expected that N-fixing trees would facilitate forest growth under N-limited conditions, following the prevailing view of the role of N-fixing trees in forest N cycling and forest growth. This has also been suggested by previous studies of N-fixer effects: a study in Washington, U.S. demonstrated that N-fixing trees increased total biomass in a low N site but not in a high N site (Binkley *et al.*, 1992), and N-fixing trees inhibited forest growth in generally N-rich forests in Costa Rica (Taylor *et al*., 2017). Because the data to quantify N limitation at the scale of our analysis do not exist, we examined N deposition, which is well quantified at the proper scale. N deposition does not necessarily indicate N limitation, which depends on all sources of N supply and their relationship to N demand. All else equal, though, we expected plots with higher N deposition to be less N limited, as suggested by a positive relationship between N deposition and forest growth (Thomas *et al.* 2010). Against our expectations, we found that N-fixing trees facilitated BAI_n more in high N deposition plots than in low N deposition plots. This is likely because N-fixers were stronger competitors in low N deposition plots than in high N deposition plots. In N-limited conditions, even though non-fixers could benefit from the N input of N-fixers, N-fixers themselves benefit first and most from their ability to fix N, and N-fixers' success allows them to outcompete non-fixers. Non-fixers can access fixed N only after the turnover and decomposition of N-fixer tissues, which causes a time lag in non-fixer access to fixed N. Therefore, N-fixers are most competitive in N-limited conditions, as predicted by theory (Vitousek & Field 1999; Rastetter *et al*., 2001; Menge *et al*. 2017; Bytnerowicz & Menge, in review). Under less N-limited conditions, N-fixers are less competitive because their ability to fix N gives them less of a competitive advantage over non-

fixers. Therefore, somewhat counterintuitively, the competition framework predicts that net facilitation by N-fixers should increase as N limitation decreases. Although N limitation can be correlated with stand age, latitude, and temperature, none of those mediated the effect of N-fixing trees on forest growth in our analyses, potentially due to confounding factors.

N-fixers are more water efficient than non-fixers (Adams *et al.*, 2016), so they compete strongly with non-fixers in dry environments (Gei *et al.*, 2018; Liao, Menge, Lichstein, & Ángeles-Pérez, 2017; Minucci, Miniat, Teskey, & Wurzburger, 2017; Pellegrini, Staver, Hedin, Charles-Dominique, & Tourgee, 2016; Wurzburger & Miniat, 2014). Consistent with the competitive framework, N-fixing trees facilitated basal area change (BAI, BAI_n, and recruitment) more in wetter plots than in drier plots. Curiously, mean annual precipitation had no relationship to N-fixer effects in our analyses, suggesting that the more localized soil moisture index is a stronger mediator of the interactions between N-fixers and non-fixers. Furthermore, there was no geographic (latitude or longitude) driver of the NFE, which further supports that local, site-specific conditions were more important in determining competitive and facilitative dynamics than were broad gradients of temperature and precipitation.

N-fixing trees facilitated neighboring trees that occupied different niches, consistent with coexistence theory (Morin, 2011). N-fixing trees competed less with these individuals and thus they were less inhibited by N-fixing trees (i.e. higher net facilitation by N-fixing trees). The clearest example of this distinction is the N-fixer vs. non-fixer dichotomy itself: N-fixing trees promoted basal area change of non-fixing trees (BAI_n) more than total basal area change (BAI). This was also consistent with Liao & Menge (2016), who showed that N-fixing trees tend to grow slower, recruit slower, and die faster than non-fixing tree counterparts in the coterminous U.S. The lower growth, recruitment, and survival rates of N-fixers (Liao and Menge 2016)

decreased total basal area growth relative to basal area growth of non-fixing trees. Additionally, at the individual scale, N-fixing trees facilitated the growth of neighboring non-fixing trees more than the growth of neighboring N-fixing trees.

Notably, N-fixing trees facilitated neighboring trees with high foliar C:N more than neighboring trees with low foliar C:N. N-fixers generally have low C:N because they have higher foliar percent N relative to non-fixers (Reed et al. 2007, Fyllas et al. 2009, Nasto et al. 2014, Adams et al. 2016). N-fixing trees may compete less with neighboring trees with high C:N than with neighboring trees with low C:N because they have different nutrient requirements. Another possible explanation for this foliar stoichiometry finding is that a given N increment transferred from an N-fixing tree to a neighboring tree makes a greater impact on overall photosynthetic capacity for a species with high C:N than a species with low C:N because it enables a greater relative change in foliar percent N and new leaf production (Lambers, Chapin, & Pons, 1998). N-fixing trees can associate with both AM (e.g. *Robinia pseudoacacia*) and EM (e.g. *Alnus rubra*) which could explain why symbiotic association did not mediate the effect of N-fixing trees on neighboring tree demographic rates.

Generally we found N-fixers facilitate neighboring trees that occupy different niches, but inhibit neighbors that share the same niche. Evergreen trees were inhibited by N-fixers. Evergreen trees, which conserve nutrients by turning over tissue slower (Franklin et al. 2009) so are more tolerant of low soil N conditions and colonize early successional habitats, occupy a similar ecological niche to N-fixers. However, N-fixers and evergreens occupy different physiological niches (e.g. evergreens are shade tolerant and have high foliar C:N; Hallik, Niinemets, & Wright, 2009). Further research is needed to reconcile the evergreen results with other traits that mediated the NFE. Canopy position followed the competition framework. Most

N-fixing trees were canopy trees (81%). N-fixing trees may have facilitated neighboring trees in the understory more than neighboring trees in the canopy because there was less light competition between N-fixing trees and neighboring understory trees than between N-fixing trees and neighboring canopy trees.

4.3 Caveats and Extensions

The presence of N-fixing trees does not mean that they are actively fixing N (Barron, Purves, & Hedin, 2011), and in this study we could not distinguish between N-fixers that were actively fixing N from those that were not. When N fixation is down-regulated, N-fixers consistently still maintain high foliar N (Wolf, Funk, & Menge, 2017), and could take up large quantities of N from the soil N pool. These N-fixers would have been strong competitors for light and other resources while also competing with neighboring non-fixers for N. More field studies on N fixation rates of our common genera (*Robinia*, *Alnus*, *Prosopis*, and *Cercocarpus*), would help clarify our results.

Although the spatial scale of this study was large, the time span was limited to a single census interval (range 1-16 years, mean 5.2 years). A time-lagged nurse effect of N-fixers was reported by Schuster & Hutnik (1987) who found that *Robinia pseudoacacia* inhibited interplanted neighbors but facilitated growth of trees planted after the *Robinia pseudoacacia* died. Our study may have missed impacts of N-fixing trees that only manifested as changes in forest demography years or decades later by only considering trees that were present at the census points. Further work should be conducted on time lags and legacy effects of N-fixers (Perakis and Sinkhorn 2011) in census data.

The vast majority of N-fixers in our dataset were *Robinia pseudoacacia*, so our results are skewed toward *Robinia pseudoacacia* interactions, which tended to occur with evergreens such as pines, junipers, or fir trees. Different N-fixing tree species may have affected their neighbors differently but the sample size of other taxa was not large enough to make clear conclusions.

5 Conclusion

Some reforestation strategies target planting N-fixing plants to relieve N limitation and promote forest growth (Chazdon, 2008, Rosenstock, Tully, Neufeldt, *et al.*, 2014, Jensen *et al.* 2012, Cunningham *et al.* 2015). Whether N-fixing trees should be recommended for reforestation depends on a complex set of factors that determine facilitation of and competition with neighboring trees, and, if the goal of reforestation includes climate mitigation, the net effect of N-fixers on soil N_2O emissions (Bühlmann, Caprez, Hiltbrunner, Körner, & Niklaus, 2017; Kou-Giesbrecht & Menge, 2019; Rosenstock, Tully, Arias-Navarro, *et al.*, 2014).

Here, we demonstrated that, on average, N-fixing trees in the coterminous U.S. do not affect forest growth, though they do facilitate growth of non-fixing trees. N-fixers can also be important drivers of demographic processes, though their interactions with neighbors vary based on abiotic factors such as soil moisture and N deposition and the traits of neighboring trees such as foliar C:N, canopy position, and N fixation status. The large spatial extent of the FIA data provides a uniquely robust assessment of the N-fixer effect on forest growth and its ecological drivers. Overall, our results suggest that planting N-fixing trees may be a viable reforestation strategy in temperate forests in specific contexts such as wet, high N deposition sites dominated by non-fixing trees that are ecologically dissimilar to the N-fixing trees planted.

Chapter 3: Individual trees could access a large or small fraction of their leaf litter depending on tree traits and environmental conditions

Authors: Anika Petach Staccone, Duncan N. L. Menge

Abstract

The degree to which individual trees can recapture nutrients from their leaf litter could have major implications for plant-soil feedbacks. To explore this question we used a theoretical advection-diffusion-reaction model that considered litter movement and decomposition as functions of species traits (e.g., root distributions and leaf properties) and environmental conditions (e.g., wind, hillslope, and precipitation). Rooting extent, the rate of decomposition, and the advection velocity of litter were the strongest drivers of litter nutrient recapture by a focal tree, which suggests both species-traits and environmental conditions drive litter nutrient return. We observed a feedback loop where trees that drop nutrient rich leaf litter had a greater opportunity to recapture nutrients because the litter decomposed before moving outside the rooting zone.

1 Introduction

How much of the nitrogen (N) in an individual tree's litterfall can it recover? This fundamental question has implications for a wide range of topics, but it has received little attention. At the ecosystem scale, litterfall is an important nutrient supply process (Sayer and

Tanner 2010, Neumann et al. 2018) as most N is recycled internally in ecosystems (Cleveland et al. 2013). Although much is known about recycling at the ecosystem scale (Cleveland et al. 2013), much less is known about recycling at the individual scale, which is more relevant for questions about plant-soil feedbacks, stand dynamics, and fertilization of the forest by specific species. Nutrient recycling at the individual scale is altered by species composition driven litter quality and mobility, slope, and weather conditions, which could, in turn affect dynamics among trees.

The nutrient return from a tree's leaf litter could have major implications for plant-soil feedbacks (PSF) and resource competition with neighbors. Trees influence the soil around them through leaf and root litter inputs (Hobbie 2015, Bennett and Klironomos 2018) which influence soil temperature, chemistry, and pathogens which in turn influence tree growth, recruitment, and survival either positively or negatively (van der Putten et al. 2013) creating a plant-soil feedback. Through the plant-soil feedback, plants can engineer conditions around themselves to promote conspecific individuals and suppress competitors. Leaf litter can enhance soil physical and chemical fertility to enact a positive PSF (Veen et al. 2019) by altering soil chemistry to promote offspring with similar nutrient use strategies (i.e. species with fast strategies make conditions better for offspring with fast strategies and those with slow nutrient strategies make conditions better for other slow strategy offspring). Direction and strength of plant-soil feedbacks can be unpredictable suggesting that different plant traits may affect whether they are detected (van der Putten et al. 2013, Kardol et al. 2015, De Long et al. 2019). Leaf litter input is a crucial mechanism for trees to affect local soil conditions causing Zinke effects and plant-soil feedbacks. The percent of leaf litter that decomposes in the rooting zone of a tree based on the tree's traits

and environmental conditions is an unresolved question but potentially critical to explaining observed tree effects.

If most focal tree litter stays within their own rooting zone, their litter nutrients could enhance their own growth making them strong competitors. The percent of nutrients recovered by a tree affects both its own and its neighbors' soil environment (Veen et al. 2019). PSF theory suggests that positive PSF occur when an individual's leaf litter remains close to influence soil chemistry and increase the individual's fitness (Wedin and Tilman 1990, Binkley and Giardina 1998, Miki and Kondoh 2002, Chapman et al. 2006, Cross and Perakis 2011, Uriarte and Menge 2018). Other literature, such as on N fixer facilitation (Boyden et al. 2005, Siddique et al. 2008), implicitly assumes that litter moves to neighbors, but the rate at which it does so is unclear. Batterman et al. (2013) found that almost half of ecosystem N was supplied by N-fixation in early succession even though N-fixers accounted for only 5% of basal area, implying rapid nutrient transfer from N-fixers to neighbors.

Species influence each other by drawing down resources and the species that can draw down a resource most is the most competitive (Tilman 1977, 2003). Tree species influence soil N both by competing for access to the standing soil N pool and by replenishing soil N through turnover. Stronger competitors capture the largest fraction of nutrient supply which prevents others from accessing those nutrients (Craine et al. 2005). Trees prevent their neighbors from accessing soil nutrients by extending their roots and pre-emptively capturing soil nutrients (Craine and Dybzinski 2013). Since trees vary both in the nutrient content of their leaf litter due to different green leaf nutrient content (Wright et al., 2004) and different resorption efficiencies (Aerts 1996), in traits that affect how far leaf litter moves before decomposition (Ferrari and

Sugita 1996), and in root length (Kalliokoski et al. 2008, Roumet et al. 2016) different traits could have important implications for competitive nutrient dynamics and plant soil feedbacks.

Individual and population scale resource strategies can affect ecosystem scale patterns (Menge et al. 2009b, 2015, Boudsocq et al. 2011, 2012). Ecosystem models incorporate individual-scale litter nutrient recycling in different ways. Classic resource competition models assume a fixed nutrient supply where a plant does not have access to nutrients from mineralized leaf litter and they assume that nutrient access is independent of plant litter (Tilman 1980, 1982, Klausmeier et al. 2004). Models that do incorporate ecosystem recycling use two paradigms: (1) an individual and all of its neighbors access nutrients mineralized from all leaf litter since the model assumes global nutrient access (Miki and Kondoh 2002, Ballantyne et al. 2008, Menge et al. 2009b, 2012, Miki et al. 2010, Kou-Giesbrecht and Menge 2019), or (2) trees do not share litter with neighbors. Though there are exceptions to these assumptions (Marleau et al. 2015, Barot et al. 2016, Menge and Levin 2017), the majority of ecosystem and plant-soil feedback theory is based on either all or none access. Reality is likely between these extremes (100% and 0% litter access). Updating model assumptions with a realistic litter nutrient return and sharing could have major implications on our understanding of ecosystem dynamics. A recent litter dispersal model found that the distance litter moves from a focal tree depends on the size and species though for average sized trees most litter remains within 20-50 m of the focal tree (Nickmans et al. 2019).

The nutrients that a focal tree can recapture is based on the interplay among the leaf litterfall distribution, subsequent movement of leaves across the ground (random diffusion and non-random advection), leaf physical immobilization rate (getting physically stopped, then decomposition and mineralization), and tree rooting distribution. Together these properties

describe how far leaf litter moves from the focal tree before it decomposes and mineralizes, as well as how far from its base a focal tree can potentially access the decomposed and mineralized nutrients. Though microbial dynamics can also be important, they were not explicitly considered here.

To explore how litterfall may supply nutrients to focal source trees versus neighborhood competitors, we used a theoretical advection-diffusion-reaction model that considers spatial patterns of litterfall deposition, movement, nutrient release, and subsequent nutrient uptake by plants. We ask three questions: (1) What proportion of nutrients return to a focal tree from its own litterfall? (2) How do tree properties such as height, rooting distribution, specific leaf area (SLA), and leaf decomposability affect the percent of nutrients recovered by a focal tree? (3) How do environmental characteristics such as slope and precipitation affect the percent of nutrients recovered by a focal tree? (4) In a forest stand, how do different spatial arrangements, tree properties, and environmental properties affect litter sharing between neighboring trees? We hypothesize that taller trees will recover a smaller percent of nutrients because they have a wider litterfall distribution (Staelens et al. 2003, Uriarte et al. 2015) and so, on average, leaves fall farther from the tree. We also expect that environmental conditions that lead to higher advection or diffusion rates such as steep slopes, windiness, or low understory cover will lead to a lower percent of nutrients recovered by the focal tree and more litter sharing with neighbors. Overall, the theory developed here will allow us to make predictions about plant interactions, nutrient limitation under different environmental conditions and with different combinations of plant traits, and inform plant-soil feedback theory.

2 Methods

2.1 Model description

The percent of nutrients that a focal tree can recapture was based on the interplay among the leaf litterfall distribution, subsequent movement of leaves across the ground (random diffusion and non-random advection), leaf immobilization rate (getting physically stopped by trapping or leaf mat formation, then decomposition and mineralization), and tree rooting distribution. Together these properties described how far leaf litter moves from the focal tree before it decomposed and mineralized, as well as how far from its base a focal tree can potentially access the decomposed and mineralized nutrients. Since total litter production is not considered in the model we modeled the percent of nutrients that a focal tree can recapture, however, for brevity we refer to this as litter recapture or φ.

Leaf litterfall, its subsequent movement and decomposition synthesized several processes. There was some literature on leaf litterfall (Ferrari and Sugita 1996, Staelens et al. 2003, Jonard et al. 2006, Uriarte et al. 2015) and extensive literature on leaf litter decomposition (Gholz et al. 2000, Adair et al. 2008, Zhang et al. 2008, Berg 2014, David 2014). The movement of leaf litter across the ground has received little attention though several studies indicated that this could be an important process (Orndorff and Lang 1981, Boerner and Kooser 1989, Porder et al. 2005, Hart et al. 2013). A recent leaf dispersal model demonstrated that wind direction and crown height were key drivers of leaf dispersal patterns and that up to 86% of soil nutrients could originate from the local neighborhood (Nickmans et al. 2019).

This model aimed to understand the mechanisms underlying N recovery in trees by examining leaf litterfall, advection, and diffusion relative to rooting distributions. We assumed that nutrients in leaves that remained within the rooting zone of a tree were potentially available

to the tree after the leaf decomposed and mineralized. But, leaves that moved outside the rooting radius, via any combination of the initial fall, diffusion, and advection, were not available to the focal tree. To investigate litter recovery by a focal tree, we used a reaction-diffusion-advection model to model the dynamics of litterfall distribution, diffusion (random spreading of litter), advection (directed movement of litter), and decomposition (immobilization of litter). Reaction-diffusion modeling has successfully described other problems in spatial ecology such as spore dispersal, fish schooling, and animal home range analysis (Okubo and Levin 2001). We modeled leaf litter movement in the horizontal direction to study the dynamics of leaf litter movement along a landscape after the initial litterfall. Equation 1 is the standard reaction-diffusion-advection equation in a single spatial dimension.

$$\frac{\partial L}{\partial t} = D\frac{\partial^2 L}{\partial x^2} - u\frac{\partial L}{\partial x} - kL \qquad \textbf{(1)}$$

The model framework (Figure 1) included the litter density $L(x,t)$ (kg m^{-2}) at a given distance from tree base x (m) through time, t (y), as determined by the diffusion coefficient, D (m^2 y^{-1}), advection velocity, u (m y^{-1}), and decomposition rate, k (y^{-1}).

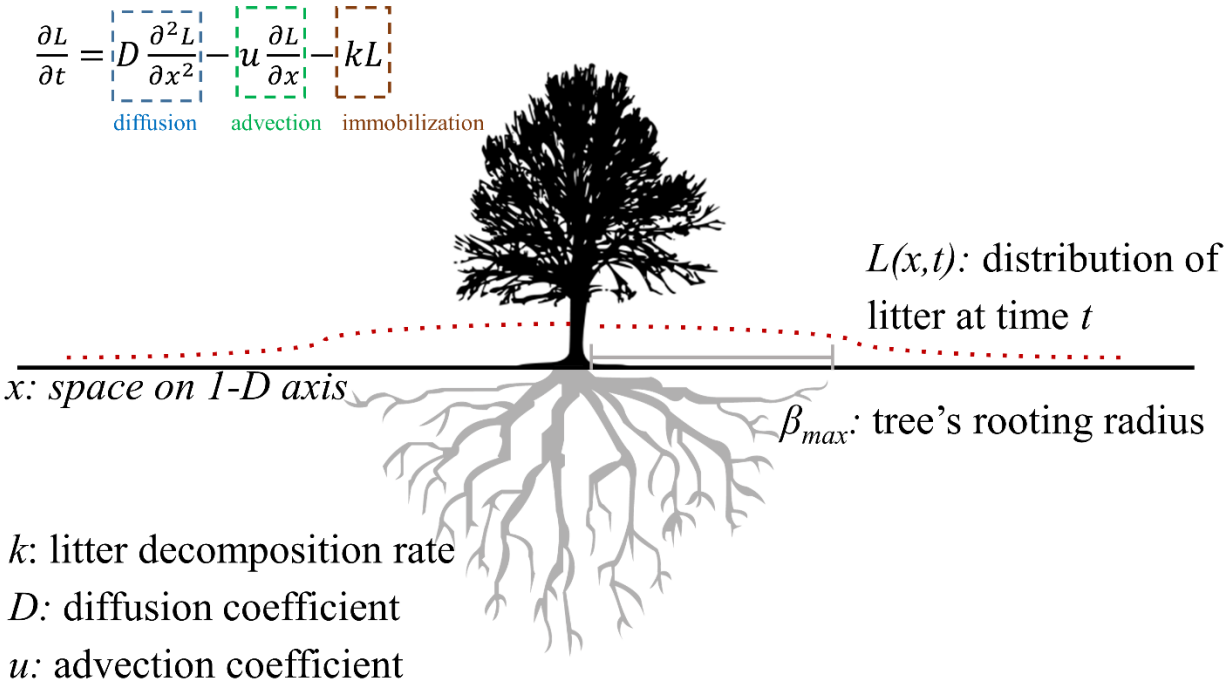

Figure 10. Model framework for an individual tree.
Litter falls in a single pulse at $t = 0$ and moves through advection and diffusion. Litter is immobilized proportional to k. Litter that is immobilized within the tree's roots ($-\beta max$ to βmax) is potentially accessed by the focal tree.

A cohort of litter fell at time 0, simulating autumn litterfall, which subsequently moved across the landscape and eventually decomposed. We only tracked one cohort of litter for simplicity, but this could be expanded into a broader framework of multiple cohorts or continuous litter input. In this equation the net rate of change of litter at a given distance from the focal tree (dL/dt) was given by the flux density of the litter gradient (Laplacian) plus the advection velocity minus the decomposition rate. As litter moves across the landscape it is immobilized when trapped under fallen logs or integrated into leaf mats and eventually decomposes. Though we referred to k as the litter decomposition rate, is also accounted for these processes that cause litter to stop moving.

The model assumed, for simplicity, that the diffusion coefficient, advection coefficient, and decomposition rate were constant across the year and space around the tree. Leaves fell from trees in predictable patterns that can be modeled using an exponential decay equation with asymmetric effects for wind direction (Ferrari and Sugita 1996, Jonard et al. 2006, Uriarte et al. 2015). The initial litterfall distribution ($\varepsilon(x)$) was modeled as the initial condition for solving. Initial litterfall was affected by tree height, total litter production, leaf area (Nickmans et al. 2019) and wind (Staelens et al. 2003). For instance, taller trees tend to increase the width of the litterfall distribution (Ferrari and Sugita 1996, Jonard et al. 2006). Roots did not extend uniformly from the base of a tree outward and the focal tree could only take up nutrients from decomposed leaf litter where it had active roots or mycorrhizae. We added a model term, $\psi(x)$, to account for the distribution of root density which included the possible shift from roots to mycorrhizae as uptake surfaces.

Tree morphology and environmental characteristics influenced the model parameters. Tree morphology dictated the litterfall distribution ($\varepsilon(x)$), root distribution ($\psi(x)$), and litter decomposition rate. Environmental characteristics drove diffusion and advection, and played a role in the decomposition rate. Certainly there is no guarantee that a focal tree will recover its litter nutrients even if they decompose within the rooting radius. Both empirical (Jones et al. 2011) and theoretical work (Dybzinski et al. 2011, Farrior 2019) show that forest trees have extensive root overlap and we incorporated a rooting distribution to account for the decreased probability of nutrient return from nutrients that decompose farther from the base of a focal tree.

2.2 Model analysis

The advection-diffusion-reaction equation was solved numerically using a Crank-Nicolson framework (Dassargues 2018) with initial conditions (describing the litterfall from the tree) and Dirichlet boundary conditions (litter density at end points was 0 kg m^{-2}), constraints necessary to solve the PDE. We tracked both the litter density and litter decomposition (indicating nutrient supply) at each point in space and time. We then calculated the percent of litter that decomposed within the rooting radius by summing the decomposed litter across the rooting radius ($-\beta_{max}$ to β_{max}) and dividing by the total litter. Three initial conditions were considered which allows the distribution of initial litterfall to vary.

To calculate the percent of litter that decomposed within the rooting zone (φ), we divided the decomposed litter within the roots in the first 25 years by the total litter decomposed anywhere. We evaluated the dynamics over 25 years because this is a possible time horizon for a tree to access nutrients before they are taken up by other sinks. Mathematically, φ of the focal plant was the ratio of the density function, *L(x, t)*, spatially integrated across the root extent (-β_{max} to β_{max}) and temporally integrated from time zero to 25 years divided by the density function *L(x, t)* spatially integrated across all space and time (total litter). This ratio was multiplied by *ψ(x)*, the distribution of roots around the tree

$$\varphi_{ultimate} = 100 * \frac{\sum_{t=0}^{25} \sum_{x=-\beta_{max}}^{\beta_{max}} L(x,t)\psi(x)dxdt}{\sum_{t=0}^{\infty} \sum_{x=-\infty}^{\infty} L(x,t)dxdt} \quad (\mathbf{2})$$

Appendix C - SI Figure 1 illustrates the pulse of litter density through time according to our advection-diffusion-reaction model described by equation 1. In addition to the percent of total litter nutrients a tree could recover, we also studied the percent of litter nutrients decomposed at that time that a tree could recover using a modified version of equation 2 where the denominator only included nutrients decomposed up to that time:

$$\varphi_{current} = 100 * \frac{\sum_{t=0}^{25} \sum_{x=-\beta_{max}}^{\beta_{max}} L(x,t)\psi(x)dxdt}{\sum_{t=0}^{25} \sum_{x=-\infty}^{\infty} L(x,t)dxdt} \quad (\mathbf{3})$$

Since roots are not uniform in length or density around a tree, and mycorrhizal networks can further extend the uptake radius, different rooting distributions were considered in the model which were more realistic than a single rooting radius. The rooting distribution ($\psi(x)$) described the probability of finding roots at a given distance from the focal tree.

To evaluate the proportion of nutrients from a focal tree that a second, neighboring tree could potentially capture we defined a variable γ as the proportion of total litter nutrients that decomposed within the second tree's rooting radius after 25 years. A variety of size and space configurations were tested. The details of neighbor tree size and spacing are defined in Appendix C – Text 1.

Solutions were calculated numerically in R (R Core Team 2020) using a runtime of 25 years and spatial extent of 400 m (comparison with 1, 5, and 10 years is shown in Appendix C - Figure SI 10).

2.3 Parameters

We used species-specific parameters to solve the advection-diffusion-reaction model. Tree traits influenced all parameters including initial leaf fall ($\varepsilon(x)$), rooting radius (β, described above) and distribution ($\psi(x)$), diffusion coefficient (D), advection coefficient (u), and immobilization rate (k). Parameters were drawn from a combination of literature and experimentally derived values to simulate four common species from hardwood forests in eastern North America: red oak (*Quercus rubra*), red maple (*Acer rubrum*), American beech (*Fagus grandifolia*), and black locust (*Robinia pseudoacacia*) shown in Table 6. These species were selected to represent typical species with a range of resorption efficiencies and mycorrhizal

associations (see Table 6) found in an eastern hardwood forest. *R. pseudoacacia* was included because it is a nitrogen-fixing tree known to have high N content in litter (White et al. 1988, Hurd et al. 2000) and might, therefore, have different and interesting litter nutrient dynamics. Single species leaf clusters (from *Q. rubra, Q. alba, A. rubrum, R. pseudoacacia,* or *F. grandifolia*) were constructed with 20 spray painted leaves of a single species and tracked across 4 months to observe the diffusion and advection of leaves. The initial litter distribution and decomposition rate for each species was estimated from literature values. Details of parameter estimates and sources are detailed in Appendix C - SI Text 1 and details of the forest stand model are in Appendix C - SI Text 4.

Table 6. Model parameters
for 4 focal temperate tree species where *D* is diffusion coefficient, *u* is advection velocity, *k* is decomposition rate, and mycorrhizal association from Jo et al. (2019) source.

Species	***D*** **($m^2\ y^{-1}$)**	***u*** **($m\ y^{-1}$)**	***u*** **from rank**	***k*** **(y^{-1})**	**Mycorrhizal association**
Q. rubra	196	105	65	0.67	ECM
A. rubrum	180.5	110	115	0.48	AM
F. grandifolia	139.5	111	90	0.55	ECM
R. pseudoacacia	21.6	43.2	40	1.32	AM

3 Results

Overall, of the litter that had decomposed by 25 years, focal trees recovered from 47% to 72% ($\varphi_{current}$) for our base parameters ("Staelens" initial litterfall, "b^x" rooting distribution, k=0.6, D=150 or 50 $m^2\ y^{-1}$, u=75 or 25 $m\ y^{-1}$). On the other hand, litter recovered based on the total litter the tree dropped ($\varphi_{ultimate}$) ranged from 37% to 71% for the same parameter combinations. Within the range of possible parameters, which is wider than the range of base

parameters, the percent of litter nutrients recovered by an individual tree ranged from < 1% to 97%. The litter recovered changed a lot with some parameters (e.g. rooting radius β_{max}, rooting distribution $\psi(x)$, advection velocity u, and diffusion rate D) but not with others (initial litterfall, $\varepsilon(x)$). Here we described some tree properties and environmental characteristics that were important determinants of the litter nutrients recovered by an individual tree.

3.1 Effects of tree properties

Tree properties drove many model parameters, which allowed us to explore how much leaf litter a tree can access depending on its traits. Tree properties included DBH which drove rooting radius (β_{max}) and the initial litterfall ($\varepsilon(x)$), leaf litter decomposition (k), and leaf traits such as SLA and shape that impacted diffusion (D) and advection (u). Without sufficient experimental data it was difficult to incorporate the effect of tree properties on D and u, so we focus on the other parameters here.

Of tree properties, the rooting radius and decomposition rate had the greatest impact on litter recovered. Holding all other parameters constant, varying root length from 1 m to 50 m increased $\varphi_{current}$ from 1% to 48% (*Q. rubra*), 0.8 % to 42% (*A. rubrum*), 0.9 % to 44% (*F. grandifolia*), and 2% to 66% (*R. pseudoacacia*). In 'realistic' simulations, root length was determined based on tree DBH so that larger trees had a wider initial litter distribution and a longer rooting radius. The net effect of larger DBH was that larger trees recovered a greater fraction of litter nutrients. Trees with faster immobilization and decomposition rates (k) recovered more litter nutrients ($\varphi_{current}$). An increase in k from 0.5 y^{-1} to 1.5 y^{-1} for a tree with DBH of 20.6 cm (D = 100 m^2 y^{-1}, u = 50 m y^{-1}) increased $\varphi_{current}$ from 43% to 65%.

The rooting distribution also impacted litter nutrient recovery. When root density dropped off close to the tree, less litter was recovered as shown in Figure 11. For instance, the “uniform” distribution indicated a tree with constant probability of nutrient uptake up to the maximum root length and under this distribution 50% litter nutrient recovery occurred when the root length was 75 m. However, if the roots followed any other rooting distribution explored, the focal tree could never recover 50% of its nutrients. Roots do not grow uniformly, and even when present, tree roots often overlap preventing a focal tree from recovering all of the nutrients that exist within its rooting radius. We did not have sufficient data to quantify the rooting distribution of species studied here so we examined the effect of several theoretical rooting distributions. Reality of the rooting distribution was likely between the extremes presented here and all rooting distributions explored had an important impact on the percent of nutrients recovered.

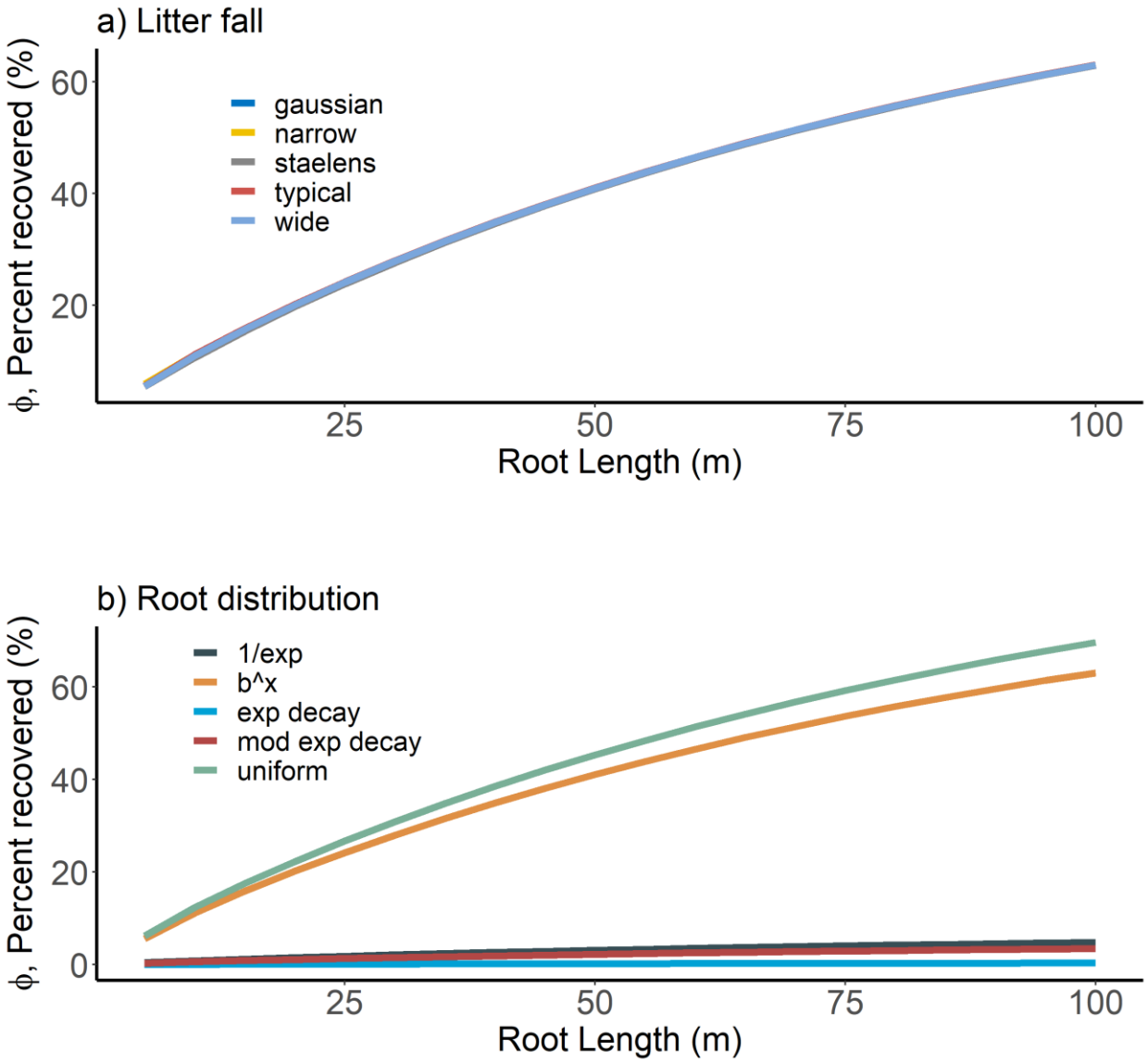

Figure 11. Percent litter recovered
(a) Percent of litter recovered by a focal tree versus root length (β_{max}) under different initial conditions, $\psi(x)$. (b) Percent of litter recovered by a focal tree versus root length (β_{max}) under different rooting distributions. Parameters: k (0.36 y^{-1}), D (100 m^2 y^{-1}), u (100 m y^{-1}), $\varepsilon(x)$ = Uriarte 'typical'.

There was essentially no impact of the initial litterfall distribution on the percent of litter recovered by a focal tree for a given root length as shown in Figure 11a. For example, a 30 cm *Q. rubra* would recover 42.0% with a Gaussian, Uriarte 'wide', Uriarte 'narrow' or 'typical', and

41.9% with ‘Staelens’ (u = 100 m y^{-1}). With a larger tree (DBH = 40 cm) under low wind conditions (u = 40 m y^{-1}) litter recovery was 77.6% (‘Staelens’) and 77.7% with any other initial distribution used.

Parameters interacted in the model so that the relative impact of changing a parameter depended on the values of other parameters. For example, root length and the initial litterfall distribution interacted. When u was 100 m y^{-1} there was little effect of the width of the initial distribution (Appendix C - Figure SI 5a, standard deviation of initial litterfall along the x-axis), however, when u was 1 m y^{-1} there was an effect of initial distribution width where wider distributions led to lower litter recovery (Appendix C - Figure SI 5b).

3.2 Effects of environmental properties

Environmental conditions affected diffusion (D), advection (u), and to an extent decomposition (k) through wind, hill slope, and water. Advection was an important mediator for the percent of litter recovered by a focal tree (Figure 12 and Appendix – SI Figure 4c). A large tree with a fast decomposition rate could recover nearly all of its litter nutrients when u was low, however, as u increased φ dropped below 75%. Very small trees had such small rooting zones that they could not overcome the effect of advection and even at low advection velocities, trees with 1 m rooting radius recovered less than 10% of litter. As a tree’s roots lengthened, the effect of advection interacted more strongly with decomposition (Figure 12).

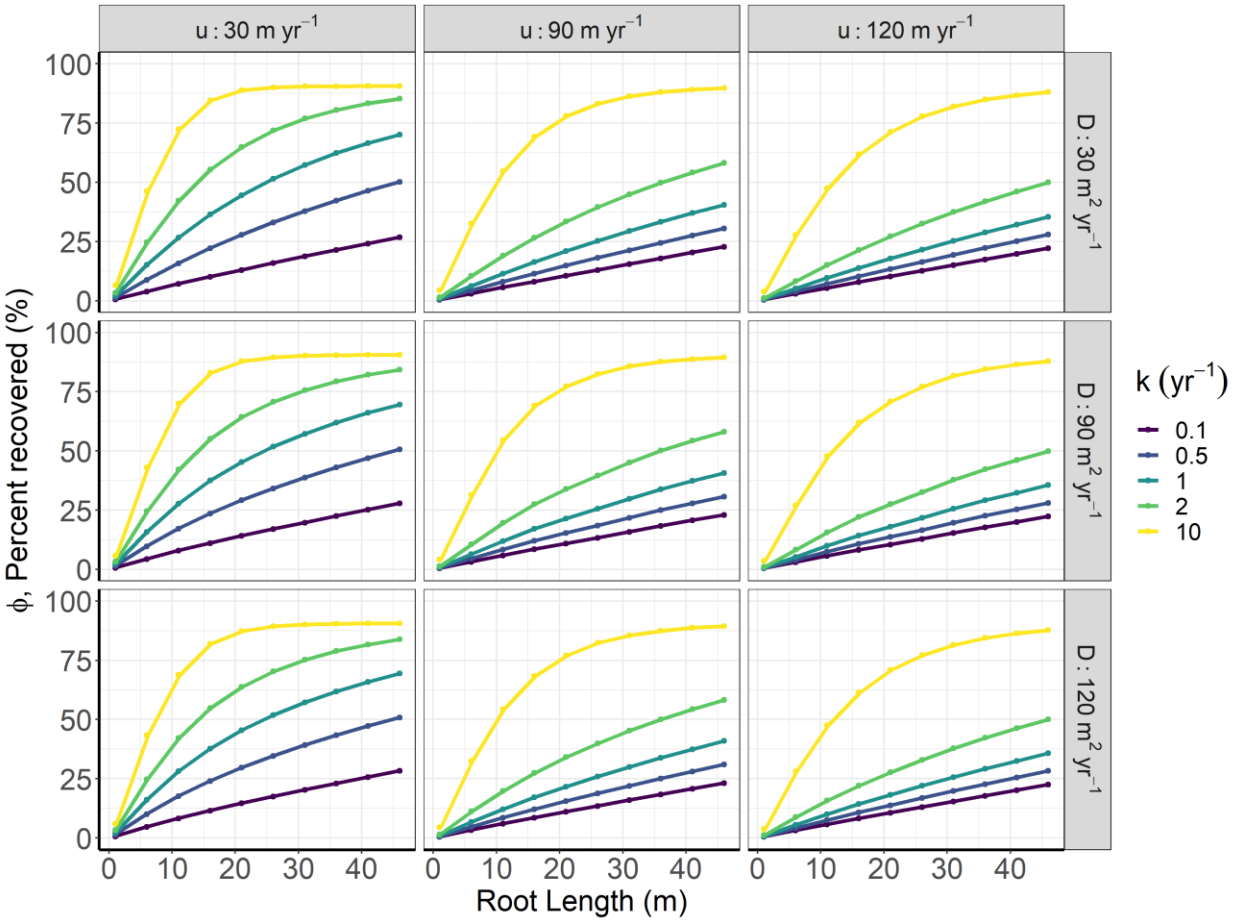

Figure 12. Effect of environmental parameters on the percent of litter potentially recovered by a focal tree.
Across the grid columns *u* (advection velocity) is 30 m y^{-1}, 90 m y^{-1}, and 120 m y^{-1}. Across the grid columns, *D* (diffusion coefficient) is 30 m^2 y^{-1}, 90 m^2 y^{-1}, and 120 m^2 y^{-1}. The decomposition rate (*k*) is shown with different colors. Parameter *k* is a strong driver of $\varphi_{current}$ (the percent of litter recovered).

With a given advection velocity, litter recovered ($\varphi_{current}$) decreased as diffusion (*D*) increased (Figure 12). Again, *k* mediated the relationship between $\varphi_{current}$ and *D*. Since *k* described the immobilization of litter which included both decomposition rate and other possible physical effects such as leaf mats formation and entrapment of leaves under fallen wood, decomposition rate only placed a lower bound on k. Effective values of *k* were likely higher. If

the effective *k* was 10 times greater than the decomposition rate this could lead to a doubling in φ, especially for large trees (Figure 12).

The relative strength of *u* (directed movement) and *D* (random movement) of litter was a key driver of *φ*. For a given rooting zone, as the ratio *u*/*D* increased, *φ* decreased (Appendix C - SI Figure 7a). When the ratio was low diffusion dominated and *φ* was greater. As the ratio increased, advection dominated and *φ* decreased. Since there are likely similar controls on *u* and *D* (wind, precipitation, leaf size, leaf shape, etc.) in nature they likely co-vary.

Parameters interacted to determine *φ*. The interaction of *u*, a predominantly environmentally-controlled parameter, and *k*, a climatic and biotically-mediated parameter, showed that *φ* can be high either when *k* was sufficiently fast or when *u* was sufficiently low. For fast immobilizing litter, trees could experience moderate advection and still recover the majority of their leaf litter (Figure 12, Appendix C – SI Figure 7b).

To synthesize the interaction of all model parameters in a biologically meaningful way, we simulated *φ* for several common eastern forest trees (Figure 13).

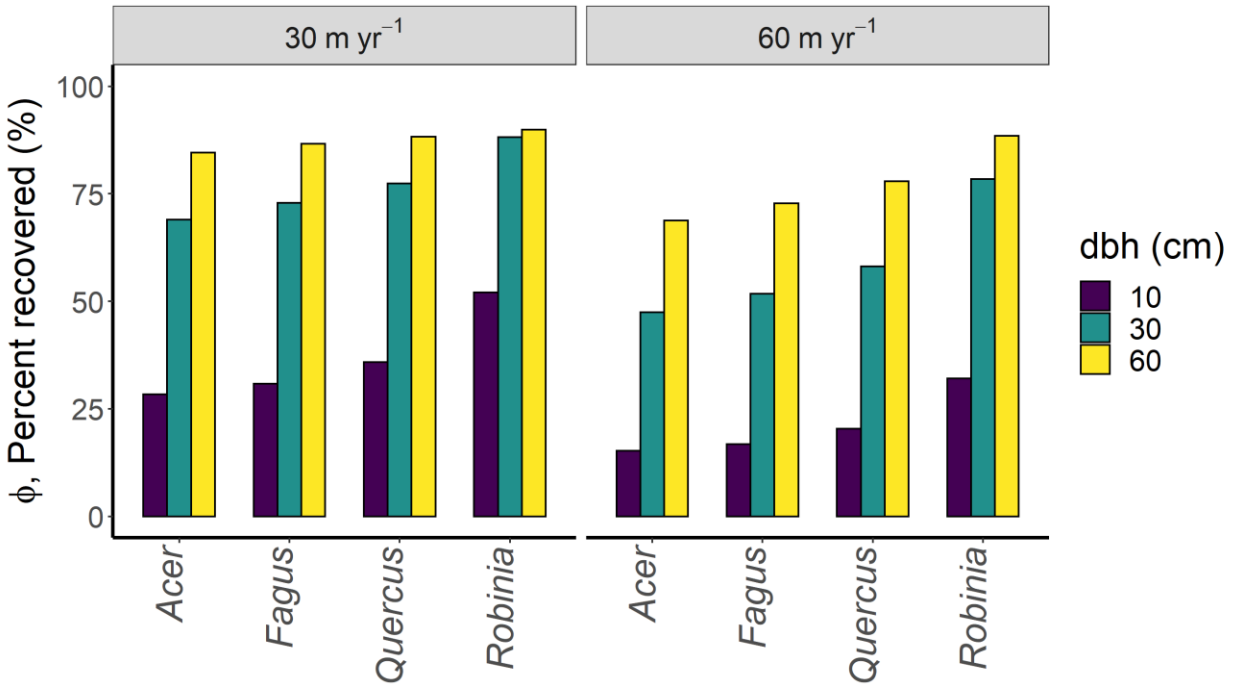

Figure 13. Percent of litter recovered for each of the 4 focal species based on tree dbh. The left facet shows an advection velocity (u) of 30 m y^{-1} and the right facet shows an advection velocity of 60 m y^{-1}. This spans a range of likely wind-induced advection values.

Species all recovered more nutrients in the low wind environment (Figure 13: 30 m y^{-1}) than high wind (Figure 13: 60 m y^{-1}). When tree DBH was 60 cm the roots were sufficiently long to recover most of the nutrients regardless of wind. However, when DBH was 10 cm the decomposition rate (k) was the driver of litter nutrients recovered. For 10 cm DBH trees the order of litter nutrient recovery follows the order of decomposition rates with *Robinia* having the highest decomposition rate and most nutrient recovered.

4 Discussion

4.1 How far do leaves move after they fall and how does this affect nutrient recapture?

Recent work highlighted the overlooked importance of litter redistribution on the forest floor after litterfall and found that 77 to 86% of forest floor litter around focal trees can originate from neighbors (Nickmans et al. 2019). Based on the four species we investigated, individual trees can potentially recover between 3 and 99% of their litter nutrients. Our model predicted a wider range than the Nickmans et al. (2019) model because it considered the full spectrum of plausible species traits and environmental conditions.

4.2 Implications of nutrient recovery for plant-soil feedbacks

Theory suggests that positive plant soil feedbacks occur when an individual's leaf litter remains close (Fang et al. 2019, Png et al. 2019, Veen et al. 2019), adjusting soil conditions (Sayer and Tanner 2010) to increase the individual's fitness. In our model a large φ indicated a positive PSF since leaf litter remained close enough to the focal tree that it could recapture the nutrients and so the litter would decompose close to the focal tree making soil chemistry more favorable for conspecific individuals. This large φ was observed with long rooting radius (Appendix C – Figure SI 6) or large *k* (Figure 12) such as wet, tropical forests (Aerts 1997, Gholz et al. 2000, Powers et al. 2009) or species with low lignin:N (Aerts 1997). Since positive PSFs can decrease stand diversity (Kulmatiski et al. 2008, van der Putten et al. 2013) trees with fast decomposition and long lateral roots could be associated with lower diversity stands. On the other hand, high *u* and *D* minimized φ so PSFs would be less positive in windy or sloped environments. Thus conditions that affect φ simultaneously affect the PSF around a focal tree.

A feedback existed where trees that dropped N rich litter had a greater opportunity to recover that N through root uptake because N rich litter initially decomposed faster for labile C litters (Hobbie 2005, Perakis et al. 2012b, initial decomposition is when much N was liberated)

and thus remained closer to the focal tree. In our model higher *k* (decomposition and litter immobilization) increased nutrient recovery reinforcing this feedback at high litter N. If trees with higher litter N are also observed to have longer roots this could indicate certain species are using a "recycling" strategy for nutrient retention.

To maintain sufficient nutrient levels within the plant to satisfy physiological processes, plants can reduce their nutrient loss in three ways: (1) minimize tissue turnover (reduce), (2) resorb nutrients (Eckstein et al. 1999, Achat et al. 2018) from tissues before they senesce and re-translocate those nutrients for use elsewhere in the plant (reuse), or (3) drop nutrients in leaf litter that decomposes within the rooting radius which the plant can take up from the soil after decomposition and mineralization (recycle). Though nutrient optimization including overcoming nutrient loss is a physiological challenge for plants, little work has investigated the proportion of nutrients that a tree can recapture from the communal soil N pool (recycle). This "recycle" pathway is likely important because the carbon costs of nutrient retention (Kikuzawa and Lechowicz 2011) likely leads some plants toward a nutrient recycling strategy. Based on our model, trees with a high φ can effectively recycle nutrients so that when they drop nutrient rich litter they do not lose access to those nutrients. The range observed in φ suggests that some trees may use the "recycle" strategy while other trees put effort toward "reduce" or "reuse" strategies.

The plant economic spectrum integrates aboveground and belowground traits to predict ecosystem features. The plant economic spectrum predicts that "fast" species would be able to recover a large percent of their nutrients and prevent nutrient access for neighbors so would cause more positive PSFs. "Fast" species tend to combine higher foliar N, faster decomposition rates (Wright et al. 2004), and lower root density (Kramer-Walter et al. 2016). If low root density were correlated with longer roots (since less dense roots could mean more effort to allocate to

length) then the plant economic spectrum would link high foliar N and long rooting radii (β) creating species with distinctly high nutrient return. In our model rooting radius of the focal tree was a critical parameter that drove much of the variation in φ. However, growing long roots requires carbon and energy which could have been used to increase root density. In our model this is effectively like increasing stand density so more root overlap would increase.

4.3 Implications of nutrient recovery for plant competition

Theory suggests that strong competitors draw down key resources (Tilman 1977) which integrates both low litter nutrient input and fast nutrient uptake. According to this theory, high φ individuals should be strong competitors and low φ individuals weak. A tree can recover the majority of its nutrients (high φ) if it has sufficiently high *k*, sufficiently low *u* and *D*, or long root extent. Long roots (*β*) lead to high nutrient return and preempt neighbors from accessing those nutrients (Craine et al. 2005) which make them strong competitors. Although building long roots requires the tree to allocate more effort to root construction and when there is root overlap with neighbors trees might preferentially allocate effort to increasing root density over length (Cabal et al. 2020). Since strong competitors have both large *k* (N rich litter) and long β this leads to a direct trade-off between allocating effort to (1) resorption where the plant does not drop N and risk losing it to neighbors (low *k* and shorter β) and (2) traits that allow nutrient return after N rich litter decomposes such as long roots (high *k* and longer *β*).

Diffusion and advection rates were important determinants of litter nutrient recovery, for instance, a 1.5 times advection velocity decreased nutrient recovery from 57% to 49% for a *Q. rubra* and from 76% to 64% for *R. pseudoacacia*. *R. pseudoacacia* had the smallest *D* and *u* from our field measurements since the leaflets separated from rachis soon after falling from the

tree and were less distributed over the forest floor so recovered more litter nutrient given other parameters. Interestingly, N-fixing plants are inefficient at resorbing N (Killingbeck 1993) so tend to drop more N in their litter and depending on where the litter decomposed could be taken back up by focal N-fixing trees or transported to neighbors where it would fertilize neighbors. Environmental characteristics such as wind speed, hill slope, and precipitation further impacted *D*, *u*, and *k*. Since these parameters were impacted by the same environmental characteristics they were intrinsically linked. For instance, wind increased both the diffusion and advection which caused more leaf litter movement so decreased nutrient recapture by the focal tree. Or, in wet environments diffusion and advection would be lower so *k* would be higher which would increase nutrient recovery a focal tree through several mechanisms (reduced litter movement and faster decomposition).

4.5 Initial litterfall

The initial litter distribution did not drive φ relative to other parameters and subsequent movement of leaf litter after litterfall was much more important. Much of the previous work around litter nutrients focused on the initial litter distribution as leaves fall from trees (Ferrari and Sugita 1996, Staelens et al. 2003, Jonard et al. 2006, Uriarte et al. 2015), however, our model suggested that the movement of leaf litter after it has fallen to the ground is understudied and deserves more attention and field work. This is consistent with work by Hart *et al* (Hart et al. 2013) which found that sites dominated by deciduous, N-rich litter (here high *k*) had more lateral redistribution than coniferous, N-poor litter (here low *k*).

4.6 Conclusion

In conclusion, the advection-diffusion-reaction model was useful for understanding the effect of both plant traits and environmental conditions on potential leaf litter nutrient recovery by trees. Larger trees, species with faster decomposition rates, and low advection environments allowed trees to recover more of their litter nutrients. There was a possible feedback, where litter N increased decomposition rate which in turn increased nutrient recovery, which could make low foliar N resorption adaptive to trees with long roots or in environments where leaf litter was relatively immobile. Litter sharing among neighboring trees can be substantial but was influenced by decomposition and advection rates. When assessing the potential fertilization effects of trees from their leaf litter, stand structure and environmental conditions should be considered. Additional field work should focus on the movement of litter on the ground after it falls as advection rate was identified as a key parameter in this model and limited data exists to parameterize it.

Conclusion

I set out to understand the effect of nitrogen-fixing trees in forests across spatial scales: from the litter nutrient input from N-fixing trees to their neighbors, to the observed stand scale effect of N-fixing trees on neighbor growth and demographic rates, and up to the continental scale to evaluate the magnitude of the tree BNF input compared to other N inputs. Leaf litter transfer is a theoretically possible mechanism of N-fixing trees to fertilize their neighbors. However, N-fixing trees may hoard their litter nutrients and only fertilize neighboring trees after they die and their tissues turn over, highlighting the importance of understanding the effect of nitrogen-fixing trees on different timescales. Nitrogen-fixing trees fix a biologically important fraction of new input to forest where they are present, but they do not have a net effect on forest growth and therefore do not directly impact carbon storage rates. In light of the evidence presented in this thesis, nitrogen-fixing trees are a widespread, important input of nitrogen into forests but the interaction of nitrogen-fixing trees with their neighbors is complicated by the fact that they can either promote or inhibit their neighbors depending on local conditions.

Nitrogen-fixing trees impact forests in varied ways: they are strong competitors that can take advantage of early successional niches often shading out neighbors but also add new biologically available N to ecosystems that can fuel both forest growth (Batterman et al. 2013) and nitrous oxide emissions (Kou-Giesbrecht and Menge 2019). Whether nitrogen-fixing trees should be intentionally planted in managed forests rests on the balance of the effects that they will have on neighboring trees, carbon storage, and nitrous oxide potential. More work is needed

to investigate the temporal dynamics of the nitrogen-fixing tree effects on forest demography. The data that I used (FIA) had only one repeat measurement of biomass and was not a long standing time series which prevented a deeper understanding of time lags and temporal aspects of N-fixer effects. Furthermore, the FIA integrated across the past 5 decades so I was unable to distinguish between effects of nitrogen-fixing trees during earlier periods (1980s) when nitrogen deposition was less than in recent years. Recent work by Helms et al (in prep) demonstrated that there are important time lags between the period when a nitrogen-fixing tree is actively fixing nitrogen and the period when changes in forest demography are observed.

BNF is an important N source in temperate forests. Trees, particularly, often have access to more energy than other types of N-fixers so they have the potential to fix large quantities of N. Since N is often limiting (or co-limiting) to growth in temperate forests this N input could change the local forest properties, which, in sum, could help define large scale forest function. BNF is difficult to quantify at landscape scales since BNF is heterogeneous and it is difficult to measure field rates. Previous work quantified landscape BNF using modeled N demand (Cleveland et al. 2013), isotope modeling (Vitousek et al. 2013), and bottom up scaling biome BNF rates by assumed forest cover (Cleveland et al. 1999, Galloway 2004). We used two complementary, data-based approaches to improve the BNF estimate for the United States by (1) scaling up N-fixing tree abundance (from data) by field measured BNF rates and by (2) calculating the N demand for observed forest growth and scaling by the percent of nitrogen demand met by N-fixation in each N-fixing tree species. Surprisingly, these two methods concluded that tree BNF in the U.S. is lower than previously thought. If tree BNF is lower than expected it could mean that N-fixing trees have less facilitative impact on temperate forests and

could suggest that they may not be such good agroforestry trees from the perspective of N fertilization.

Given that there is less BNF in forests than previously expected, what is the impact of N-fixing trees across the U.S. on forest demographics and basal area? The average trends at the plot and individual scales shows that N-fixing trees do not affect the relative growth rate of neighbors but they do facilitate survival and inhibit recruitment. In sum these average trends suggest that N-fixing trees drive tree turnover. However, the finding that N-fixing trees have no net effect on forest growth in the coterminous U.S. contradicts the prevailing paradigm in biogeochemistry that N-fixing trees improve forest growth. Though facilitation from N-fixing trees is observed locally, the effect does not hold at a regional scale. When strategically managing N-fixing trees the broader context is critical. N-fixing trees facilitate forest growth when they are less likely to be competitive (i.e. locations with high N deposition and high soil moisture) or when they occupy a different niche to neighbors (e.g. high foliar C:N trees and non-fixing trees). Using the Forest Inventory and Analysis data provided a regional look at the effect of N-fixing trees which was gives a new understanding that was not possible to see from previous local studies which spanned the range from N-fixer inhibition to facilitation (Taylor et al. 2017, Lai et al. 2018).

The effect of N-fixing trees represents the balance of the facilitative and inhibitory effects that they have on their neighbors. Like all trees, N-fixers compete with their neighbors for limited resources: light, water, and nutrients. Though they have access to a unique N pool, they are still constrained by soil available P and other micronutrients. Since N-fixing trees access a unique N pool they have the potential to either inhibit their neighbors by outcompeting the neighbors for other resources or to facilitate their neighbors by spreading N rich litter that relieves N limitation for neighbors and facilitates growth. One (often cited) mechanism by which

N-fixing trees could spread this N is through their litter after litterfall. I used theoretical modeling to assess whether this is a plausible mechanism for N-fixing trees to fertilize their neighbors and under what conditions they would be most likely to do so. The model considered (1) the initial litter fall from trees after leaf senescence which changes based on a tree's size and the physical properties of the leaves, (2) the subsequent movement of litter across the forest floor as a result of wind, water movement, and (3) other advective forces, and the immobilization and decomposition rate of litter. The model shows that whether litter N could reach neighbors depends greatly on tree architecture, advection rate, and decomposition rate. A tree could share almost none of its litter N or most of its litter N depending on the combination of those three factors (tree architecture, advection rate, and decomposition rate). Under conditions of high wind or water movement and slow decomposition rate then litter from N-fixing trees may be an important source of N for neighbors. However, it is likely that N-fixing trees do not share a large fraction of their litter N with neighbors and instead fertilize forests only after death when their tissues decompose.

The biogeochemistry community needs better quantification of BNF across scales. This thesis provides a framework for how tree BNF can be estimated in large geographic regions. For the United States it provides a spatially explicit representation of tree BNF that can be an input to biogeochemical models or used to understand the local N cycle. Given that past investigation of the effect of N-fixing trees on forests resulted in conflicting findings (facilitation, no effect, and inhibition), this work which teases apart some contexts in which N-fixing trees facilitate or inhibit forest growth is an important contribution. When explaining the mechanism by which N-fixers facilitate neighbors, leaf litter transfer is often cited as a plausible example. Evidence suggests nutrient transfer through leaf litter happens in controlled experiments (Notaro et al.

2014). This thesis adds a theoretical exploration of this mechanism and describes the conditions under which leaf litter transfer may be an important source of nutrients for trees and when individuals are likely to retain much of their nutrient. This theoretical exploration is a stepping stone to uncovering the conditions under which N-fixing trees should be planted to facilitate forest growth or augment agroforestry schemes. It also helps describe the conditions under which N-fixing trees would not facilitate forest growth which is important for forest managers to know since N-fixing trees can have other adverse effects (e.g. nitrous oxide emissions; Kou-Giesbrecht and Menge 2019). Furthermore, the theoretical exploration of litter movement uncovered a possible feedback mechanism where the distance that leaf litter moves is inversely related to the litter nitrogen content so trees that drop more N-rich leaf litter have a greater opportunity to recycle that N in a future growing year. This testable question merits further investigation and could have important implications for tree competition and community structure.

References

Abrahamson, I. 2019. Fire Effects Informatoin System (FEIS).

Achat, D., N. Pousse, M. Nicolas, and L. Augusto. 2018. Nutrient remobilization in tree foliage as affected by soil nutrients and leaf life span. Ecological Monographs 0:1–21.

Ackerly, D. 2004. Functional strategies of chaparral shrubs in relation to seasonal water deficit and disturbance. Ecological Monographs 74:25–44.

Adair, E. C., W. J. Parton, S. J. Del Grosso, W. L. Silver, M. E. Harmon, S. A. Hall, I. C. Burke, and S. C. Hart. 2008. Simple three-pool model accurately describes patterns of long-term litter decomposition in diverse climates. Global Change Biology 14:2636–2660.

Adams, M. A., T. L. Turnbull, J. I. Sprent, N. Buchmann, T. L. Turnbulla, J. I. Sprent, Nina Buchmannc, T. L. Turnbull, J. I. Sprent, and N. Buchmann. 2016. Legumes are different: Leaf nitrogen, photosynthesis, and water use efficiency. Proceedings of the National Academy of Sciences 113:4098–4103.

Aerts, R. 1996. Nutrient resorption from senescing leaves of perennials: Are there general patterns? Journal of Ecology 84:597–608.

Aerts, R. 1997. Climate, leaf litter chemistry and leaf litter decomposition in terrestrial ecosystems: A triangular relationship. Oikos 79:439.

Antoine, E. 2004. An ecophysiological approach to quantifying nitrogen fixation by *Lobaria oregana*. The Bryologist 107:82–87.

Azani, N., M. Babineau, C. D. Bailye, H. Banks, A. Barbosa, R. B. Pinto, J. S. Boatwright, L. M. Borges, G. K. Brown, A. Bruneau, and E. Al. 2017. A new subfamily classification of the Leguminosae based on a taxonomically comprehensive phylogeny – The Legume Phylogeny Working Group (LPWG). Taxon 66:44–77.

Ballantyne, F. I., D. N. L. Menge, A. Ostling, and P. Hosseini. 2008. Nutrient Recycling Affects Autotroph and Ecosystem Stoichiometry. The American Naturalist 171:511–523.

Barot, S., S. Bornhofen, S. Boudsocq, X. Raynaud, and N. Loeuille. 2016. Evolution of nutrient acquisition: When space matters. Functional Ecology 30:283–294.

Batterman, S. A., L. O. Hedin, M. van Breugel, J. Ransijn, D. J. Craven, and J. S. Hall. 2013. Key role of symbiotic dinitrogen fixation in tropical forest secondary succession. Nature 502:224–227.

Bennett, J., and J. Klironomos. 2018. Mechanisms of plant-soil feedback: interactions among biotic and abiotic drivers. New Phytologist.

Berg, B. 2014. Decomposition patterns for foliar litter - A theory for influencing factors. Soil Biology and Biochemistry 78:222–232.

Binkley, D. 2003. Seven decades of stand development in mixed and pure stands of conifers and nitrogen-fixing red alder. Canadian Journal of Forest Research 33:2274–2279.

Binkley, D., K. Cromack, and D. D. Backer. 1994. Nitrogen fixation by red alder: Biology, rates, and controls. Pages 57–72 *in* D. Hibbs, D. DeBell, and R. Tarrant, editors. The Biology and Managment of Red Alder. Oregon State University Press, Corvallis.

Binkley, D., K. A. Dunkin, D. DeBell, and M. G. Ryan. 1992. Production and nutrient cycling in mixed plantations of *Eucalyptus* and *Albizia* in Hawaii. Forest Science 38:393–408.

Binkley, D., and C. Giardina. 1997. Nitrogen fixation in tropical forest plantations. Pages 297–337 Management of soil, nutrients and water in tropical plantation forests.

Binkley, D., and C. Giardina. 1998. Why do tree species affect soils? The warp and woof of tree-soil interactions. Biogeochemistry 42:89–106.

Boerner, R. E. J., and J. G. Kooser. 1989. Leaf litter redistribution among forest patches within an Allegheny Plateau watershed. Landscape Ecology 2:81–92.

Bormann, B. T., K. Cromack, Jr, and W. O. Russell III. 1994. Influences of red alder on soils and long-term ecosystem productivity. Pages 47–56 The biology and management of red alder.

Bormann, B. T., and J. C. Gordon. 1984. Stand density effects in young red alder plantations: Productivity, photosynthate partioning, and nitrogen fixation. Ecology 65:394–402.

Boudsocq, S., S. Barot, and N. Loeuille. 2011. Evolution of nutrient acquisition: when adaptation fills the gap between contrasting ecological theories. Proceedings of the Royal Society B: Biological Sciences 278:449–457.

Boudsocq, S., A. Niboyet, J. C. Lata, X. Raynaud, N. Loeuille, J. Mathieu, M. Blouin, L. Abbadie, and S. Barot. 2012. Plant Preference for Ammonium versus Nitrate: A Neglected Determinant of Ecosystem Functioning? The American Naturalist 180:60–69.

Boyden, S., D. Binkley, and R. Senock. 2005. Competition and facilitation between Eucalyptus and nitrogen-fixing Falcataria in relation to soil fertility. Ecology 86:992–1001.

Brookshire, E. N. J., S. Gerber, D. N. L. Menge, and L. O. Hedin. 2012. Large losses of inorganic nitrogen from tropical rainforests suggest a lack of nitrogen limitation. Ecology Letters 15:9–16.

Brookshire, E. N. J., N. Wurzburger, B. Currey, D. N. L. Menge, M. P. Oatham, and C. Roberts. 2019. Symbiotic N fixation is sufficient to support net aboveground biomass accumulation in a humid tropical forest. Scientific Reports 9:7571.

Burrill, E., A. Wilson, J. Turner, S. A. Pugh, J. Menlove, G. Christensen, B. Conkling, and W. David. 2017. The Forest Inventory and Analysis Database: Database Description and User Guide for Phase 2.

Cabal, C., R. Martínez-García, A. de Castro Aguilar, F. Valladares, and S. W. Pacala. 2020. The exploitative segregation of plant roots. Science (New York, N.Y.) 370:1197–1199.

Canham, C. D., P. T. LePage, and D. K. Coates. 2004. A neighborhood analysis of canopy tree competition: Effects of shading versus crowding. Canadian Journal of Forest Research 34:778–787.

Canham, C. D., M. J. Papaik, M. Uriarte, W. H. McWilliams, J. C. Jenkins, and M. J. Twery. 2006. Neighborhood analyses of canopy tree competition along environmental gradients in New England forests. Ecological Applications 16:540–554.

Carranca, C., G. Brunetto, and M. Tagliavini. 2018. Nitrogen nutrition of fruit trees to reconcile productivity and environmental concerns. Plants 7:4.

Chadwick, O. a, L. a Derry, P. M. Vitousek, B. J. Huebert, and L. O. Hedin. 1999. Changing sources of nutrients during four million years of ecosystem development. Nature 397:491–497.

Chapin, F. S., L. R. Walker, C. L. Fastie, C. Lewis, and L. C. Sharman. 1994. Mechanisms of primary succession following deglaciation at Glacier Bay, Alaska. Ecological Monographs 64:149–175.

Chapin III, F. S., P. A. Matson, and H. A. Mooney. 2011. Principles of Terrestrial Ecosystem Ecology. Page BioScience. 2nd edition. London.

Chapman, S. K., J. A. Langley, S. C. Hart, and G. W. Koch. 2006. Plants actively control nitrogen cycling: Uncorking the microbial bottleneck. New Phytologist 169:27–34.

Chapman, W. K., and L. Paul. 2012. Evidence that northern pioneering pines with tuberculate mycorrhizae are unaffected by varying soil nitrogen levels. Microbial Ecology 64:964–972.

Chazdon, R. L. 2008. Beyond deforestation: Restoring forests and ecosystem services on degraded lands. Science 320:1458–1460.

Chen, W., R. T. Koide, T. S. Adams, J. L. DeForest, L. Cheng, and D. M. Eissenstat. 2016. Root morphology and mycorrhizal symbioses together shape nutrient foraging strategies of temperate trees. PNAS 113:8741–8746.

Ciais, P., P. P. Tans, M. Trolier, J. W. C. White, and R. J. Francey. 1995. A Large Northern Hemisphere Terrestrial CO_2 Sink Indicated by the $^{13}C/^{12}C$ Ratio of Atmospheric CO2. Science 269:1098–1102.

Clark, B. R., S. E. Hartley, K. N. Suding, and C. de Mazancourt. 2005. The effect of recycling on plant competitive hierarchies. The American Naturalist 165:609–622.

Cleveland, C. C., B. Z. Houlton, W. K. Smith, A. R. Marklein, S. C. Reed, W. J. Parton, S. J. Del Grosso, and S. W. Running. 2013. Patterns of new versus recycled primary production in the terrestrial biosphere. Proceedings of the National Academy of Sciences 110:12733–12737.

Cleveland, C. C., A. R. Townsend, D. S. Schimel, H. Fisher, L. O. Hedin, S. Perakis, E. F. Latty, C. Von Fischer, A. Elseroad, and M. F. Wasson. 1999. Global patterns of terrestrial biological nitrogen (N2) fixation in natural ecosystems. Global Biochemical Cycles 13:623–645.

Condit, R., P. Ashton, S. Bunyavejchewin, H. S. Dattaraja, and S. J. Davies. 2006. The importance of demographic niches to tree diversity. Science 313:98–101.

Coskun, D., D. T. Britto, and H. J. Kronzucker. 2016. Nutrient constraints on terrestrial carbon fixation: The role of nitrogen. Journal of Plant Physiology 203:95–109.

Craine, J. M., and R. Dybzinski. 2013. Mechanisms of plant competition for nutrients, water and light. Functional Ecology 27:833–840.

Craine, J. M., J. Fargione, and S. Sugita. 2005. Supply pre-emption, not concentration reduction, is the mechanism of competition for nutrients. New Phytologist 166:933–940.

Cross, A., and S. S. Perakis. 2011. Complementary Models of Tree Species-Soil Relationships in Old-Growth Temperate Forests. Ecosystems 14:248–260.

Dassargues, A. 2018. Hydrogeology: Groundwater Science and Engineering. CRC Press.

David, J. F. 2014. The role of litter-feeding macroarthropods in decomposition processes: A reappraisal of common views. Soil Biology and Biochemistry 76:109–118.

Deal, R. L., E. H. Orlikowska, D. V. D. Amore, and P. E. Hennon. 2017. Red alder-conifer stands in Alaska: An example of mixed species management to enhance structural and biological

complexity. Forests 8:1–25.

DeLuca, T. H., O. Zackrisson, F. Gentili, A. Sellstedt, and M. C. Nilsson. 2007. Ecosystem controls on nitrogen fixation in boreal feather moss communities. Oecologia 152:121–130.

Doty, S. L., A. W. Sher, N. D. Fleck, M. Khorasani, R. E. Bumgarner, Z. Khan, A. W. K. Ko, S. H. Kim, and T. H. DeLuca. 2016. Variable nitrogen fixation in wild Populus. PLoS ONE 11:1–22.

Du, E., and W. de Vries. 2018. Nitrogen-induced new net primary production and carbon sequestration in global forests. Environmental Pollution 242:1476–1487.

Dybzinski, R., C. Farrior, A. Wolf, P. B. Reich, and S. W. Pacala. 2011. Evolutionarily stable strategy carbon allocation to foliage, wood, and fine roots in trees competing for light and nitrogen: An analytically tractable, individual-based model and quantitative comparisons to data. American Naturalist 177:153–166.

Eckstein, R. L., P. S. Karlsson, and M. Weih. 1999. Leaf life span and nutrient resorption as determinants of plant nutrient conservation in temperate-arctic regions. New Phytologist 143:177–189.

Ehrenfeld, J. G., B. Ravit, and K. Elgersma. 2005. Feedback in the plant-soil system. Annual Review of Environment and Resources 30:75–115.

Elser, J. J., M. E. S. Bracken, E. E. Cleland, D. S. Gruner, W. S. Harpole, H. Hillebrand, J. T. Ngai, E. W. Seabloom, J. B. Shurin, and J. E. Smith. 2007. Global analysis of nitrogen and phosphorus limitation of primary producers in freshwater, marine and terrestrial ecosystems. Ecology Letters 10:1135–1142.

ESRI. 2011. ArcGIS Desktop: Relase 10. Environmental Systems Research Institute, Redlands, CA.

Fang, K., L. Chen, J. Zhou, Z. Yang, X. Dong, and H. Zhang. 2019. Plant – soil – foliage feedbacks on seed germination and seedling growth of the invasive plant Ageratina adenophora. Proc. R. Soc. B 286.

Farrior, C. E. 2019. Theory predicts plants grow roots to compete with only their closest neighbours. Proceedings of the Royal Society B: Biological Sciences 286.

Ferrari, J., and S. Sugita. 1996. A spatially explicit model of leaf litter fall in hemlock-hardwood forests. Can. J. For. Res. 26:1905–1913.

Forrester, D. I., J. Bauhus, A. L. Cowie, and J. K. Vanclay. 2006. Mixed-species plantations of Eucalyptus with nitrogen-fixing trees: A review. Forest Ecology and Management 233:211–230.

Fowler, D., M. Coyle, U. Skiba, M. A. Sutton, J. N. Cape, S. Reis, L. J. Sheppard, A. Jenkins, B. Grizzetti, J. N. Galloway, P. M. Vitousek, A. Leach, A. F. Bouwman, K. Butterbach-bahl, F. Dentener, D. Stevenson, M. Amann, M. Voss, N. Galloway, P. M. Vitousek, A. Leach, A. F. Bouwman, K. Butterbach-bahl, F. Dentener, D. Stevenson, M. Amann, M. Voss, J. N. Galloway, D. Fowler, J. N. Galloway, P. M. Vitousek, A. Leach, A. F. Bouwman, K. Butterbach-bahl, F. Dentener, D. Stevenson, M. Amann, and M. Voss. 2013a. The global nitrogen cycle in the twenty-first century. Phil Trans R Soc B 368:1–13.

Fowler, D., M. Coyle, U. Skiba, M. A. Sutton, J. N. Cape, S. Reis, L. J. Sheppard, A. Jenkins, B. Grizzetti, J. N. Galloway, P. M. Vitousek, A. Leach, A. F. Bouwman, K. Butterbach-bahl, F. Dentener, D. Stevenson, M. Amann, M. Voss, N. Galloway, P. M. Vitousek, A. Leach, A. F. Bouwman, K. Butterbach-bahl, F. Dentener, D. Stevenson, M. Amann, M. Voss, J. N. Galloway, D. Fowler, J. N. Galloway, P. M. Vitousek, A. Leach, A. F. Bouwman, K. Butterbach-bahl, F. Dentener, D. Stevenson, M. Amann, and M. Voss. 2013b. The global nitrogen cycle in the twenty-first century. Phil Trans R Soc B 368:1–13.

Franklin, O., R. E. McMurtrie, C. M. Iversen, K. Y. Crous, A. C. Finzi, D. T. Tissue, D. S. Ellsworth, R. Oren, and R. J. Norby. 2009. Forest fine-root production and nitrogen use under elevated CO2: Contrasting responses in evergreen and deciduous trees explained by a common principle. Global Change Biology 15:132–144.

Freschet, G. T., J. H. C. Cornelissen, R. S. P. van Logtestijn, and R. Aerts. 2010. Evidence of the "plant economics spectrum" in a subarctic flora. Journal of Ecology 98:362–373.

Fyllas, N. M., S. Patino, T. R. Baker, G. Bielefeld Nardoto, L. A. Martinelli, C. A. Quesada, R. Paiva, M. Schwarz, V. Horna, L. M. Mercado, A. Santos, L. Arroyo, E. M. Jiměnez, F. J. Luizao, D. A. Neill, N. Silva, A. Prieto, A. Rudas, M. Silviera, I. C. G. Vieira, G. Lopez-Gonzalez, Y. Malhi, O. L. Phillips, J. Lloyd, S. Patiño, T. R. Baker, G. Bielefeld Nardoto, L. A. Martinelli, C. A. Quesada, R. Paiva, M. Schwarz, V. Horna, L. M. Mercado, A. Santos, L. Arroyo, E. M. Jiménez, F. J. Luizão, D. A. Neill, N. Silva, A. Prieto, A. Rudas, M. Silviera, I. C. G. Vieira, G. Lopez-Gonzalez, Y. Malhi, O. L. Phillips, J. Lloyd, S. Patino, T. R. Baker, G. Bielefeld Nardoto, L. A. Martinelli, C. A. Quesada, R. Paiva, M. Schwarz, V. Horna, L. M. Mercado, A. Santos, L. Arroyo, E. M. Jiměnez, F. J. Luizao, D. A. Neill, N. Silva, A. Prieto, A. Rudas, M. Silviera, I. C. G. Vieira, G. Lopez-Gonzalez, Y. Malhi, O. L. Phillips, J. Lloyd, S. Patiño, T. R. Baker, G. Bielefeld Nardoto, L. A. Martinelli, C. A. Quesada, R. Paiva, M. Schwarz, V. Horna, L. M. Mercado, A. Santos, L. Arroyo, E. M. Jiménez, F. J. Luizão, D. A. Neill, N. Silva, A. Prieto, A. Rudas, M. Silviera, I. C. G. Vieira, G. Lopez-Gonzalez, Y. Malhi, O. L. Phillips, and J. Lloyd. 2009. Basin-wide variations in foliar properties of Amazonian forest: Phylogeny, soils and climate. Biogeosciences 6:2677–2708.

Galloway, J. N., and E. Cowling. 2002. Reactive nitrogen and the world: 200 years of change. Ambio: A Journal of the Human Environment 31:64–71.

Galloway, J. N., F. J. Dentener, D. G. Capone, E. W. Boyer, R. W. Howarth, S. P. Seitzinger, G. P.

Asner, C. C. Cleveland, P. A. Green, E. A. Holland, D. M. Karl, A. F. Michaels, J. H. Porter, A. R. Townsend, and C. J. Vörösmarty. 2004. Nitrogen cycles: Past, present, and future. Biogeochemistry 70:153–226.

Galloway, J. N., A. R. Townsend, J. W. Erisman, M. Bekunda, Z. Cai, J. R. Freney, L. A. Martinelli, S. P. Seitzinger, and M. A. Sutton. 2008. Transformation of the nitrogen cycle: Recent trends, questions, and potential solutions. Science 320:889–892.

Gerber, S., L. O. Hedin, S. G. Keel, S. W. Pacala, and E. Shevliakova. 2013. Land use change and nitrogen feedbacks constrain the trajectory of the land carbon sink. Geophysical Research Letters 40:5218–5222.

Gerber, S., L. O. Hedin, M. Oppenheimer, S. W. Pacala, and E. Shevliakova. 2010. Nitrogen cycling and feedbacks in a global dynamic land model. Global Biogeochemical Cycles 24:1–15.

Gholz, H. L., D. A. Wedin, S. M. Smitherman, M. E. Harmon, and W. J. Parton. 2000. Long-term dynamics of pine and hardwood litter in contrasting environments: toward a global model of decomposition. Global Change Biology 6:751–756.

Giller, K. 2001. Assessment of the role of N2 fixation. 2nd edition. CABI Publishing, Wallingford, UK.

Goodale, C. L., M. J. Apps, R. A. Birdsey, C. B. Field, L. S. Heath, R. Houghton, J. C. Jenkins, G. Kohlmaier, W. Kurz, S. Liu, G.-J. Nabuurs, S. Nillson, and A. Shvidenko. 2002. Forest carbon sinks in the Northern Hemisphere. Ecological Applications 12:891–899.

Gordon, W. S., and R. B. Jackson. 2000. Nutrient concentrations in fine roots. Ecology 81:275–280.

Gruber, N., and J. N. Galloway. 2008. An Earth-system perspective of the global nitrogen cycle. Nature 451:293–296.

Gutschick, V. P. 1981. Evolved strategies in nitrogen acquisition by plants. The American Naturalist 118:607–637.

Gyaneshwar, P., A. M. Hirsch, L. Moulin, W.-M. Chen, G. N. Elliott, C. Bontemps, P. Estrada-de los Santos, E. Gross, F. B. dos Reis, J. I. Sprent, J. P. W. Young, and E. K. James. 2011. Legume-nodulating Betaproteobacteria: Diversity, host range, and future prospects. Molecular Plant-Microbe Interactions 24:1276–1288.

Hajek, P., D. Hertel, and C. Leuschner. 2013. Intraspecific variation in root and leaf traits and leaf-root trait linkages in eight aspen demes (populus tremula and p tremuloides). Frontiers in Plant Science 4:1–11.

Hallik, L., Ü. Niinemets, and I. J. Wright. 2009. Are species shade and drought tolerance reflected in leaf-level structural and functional differentiation in Northern Hemisphere temperate woody flora? New Phytologist 184:257–274.

Hansen, M. C., R. S. Defries, J. R. G. Townshend, and R. Sohlberg. 2000. Global land cover classification at 1 km spatial resolution using a classification tree approach. Page International Journal of Remote Sensing.

Hart, S. K., D. E. Hibbs, and S. S. Perakis. 2013. Riparian litter inputs to streams in the central Oregon Coast Range. Freshwater Science 32:343–358.

Heilman, P., and R. F. Stettler. 1983. Phytomass production in young mixed plantations of Alnus rubra (Bong.) and cottonwood in western Washington. Canadian Journal of Microbiology 29:1007–1013.

Heilman, P., and R. F. Stettler. 1985. Mixed, short-rotation culture of red alder and black cottonwood: growth, coppicing, nitrogen fixation, and allelopathy. Forest Science 31:607–616.

Hijmans, R. J. 2017. raster: Geographic Data Analysis and Modeling.

Hobbie, S. E. 2005. Contrasting Effects of Substrate and Fertilizer Nitrogen on the Early Stages of Litter Decomposition. Ecosystems 8:644–656.

Hobbie, S. E. 2015. Plant species effects on nutrient cycling: revisiting litter feedbacks. Trends in Ecology and Evolution 30:357–363.

Horn, K. J., R. Q. Thomas, C. M. Clark, L. H. Pardo, M. E. Fenn, G. B. Lawrence, S. S. Perakis, E. A. H. Smithwick, D. Baldwin, S. Braun, A. Nordin, C. H. Perry, J. N. Phelan, P. G. Schaberg, S. B. St. Clair, R. Warby, and S. Watmough. 2018. Growth and survival relationships of 71 tree species with nitrogen and sulfur deposition across the conterminous U.S. Plos One 13:e0205296.

Houghton, R. A., J. L. Hackler, and K. T. Lawrence. 1999. The U.S. Carbon budget: contributions from land-use change. Science (New York, N.Y.) 285:574–8.

Houlton, B. Z., S. L. Morford, and R. A. Dahlgren. 2018. Convergent evidence for widespread rock nitrogen sources in Earth's surface environment. Science 62:58–62.

Hruska, J., J. Cermák, and S. Sustek. 1999. Mapping tree root systems with ground-penetrating radar. Tree Physiology 19:125–130.

Hungate, B. A., J. S. Dukes, M. R. Shaw, Y. Luo, C. B. Field, J. S. Dunkes, M. R. Shaw, Y. Luo, and C. B. Field. 2003. Nitrogen and climate change. Science 302:1512–1513.

Hurd, T. M., D. J. Raynal, and C. R. Schwintzer. 2000. Symbiotic N_2 fixation of *Alnus incana* ssp.

rugosa in shrub wetlands of the Adirondack Mountains, New York, USA. Oecologia 126:94–103.

Huss-Danell, K. 1997. Actinorhizal symbioses and their N_2 fixation. New Phytologist 136:375–405.

Jackson, R. B., H. A. Mooney, and E. D. Schulze. 1997. A global budget for fine root biomass, surface area, and nutrient contents. Proceedings of the National Academy of Sciences of the United States of America 94:7362–7366.

Jenkins, J. C., D. C. Chojnacky, L. S. Heath, and R. A. Birdsey. 2003. National-scale biomass estimators for United States tree species. Forest Science 49:12–30.

Jo, I., S. Fei, C. M. Oswalt, G. M. Domke, and R. P. Phillips. 2019. Shifts in dominant tree mycorrhizal associations in response to anthropogenic impacts. Science Advances 5:eaav6358.

Jonard, M., F. Andre, and Q. Ponette. 2006. Modeling leaf dispersal in mixed hardwood forests using a ballistic approach. Ecology 87:2306–2318.

Jones, F. A., D. L. Erickson, M. A. Bernal, E. Bermingham, W. J. Kress, E. A. Herre, H. C. Muller-Landau, and B. L. Turner. 2011. The roots of diversity: Below ground species richness and rooting distributions in a tropical forest revealed by DNA barcodes and inverse modeling. PLoS ONE 6.

Jordan, T. E., and D. E. Weller. 1996. Human contributions to terrestrial nitrogen flux. BioScience 46:655–664.

Kalliokoski, T., P. Nygren, and R. Sievänen. 2008. Coarse root architecture of three boreal tree species growing in mixed stands. Silva Fennica 42:189–210.

Kardol, P., G. F. C. (Ciska) Veen, F. P. F. P. Teste, and M. P. Perring. 2015. Peeking into the black box: A trait-based approach to predicting plant-soil feedback. New Phytologist 206:1–4.

Van Kessel, C., R. E. Farrell, J. P. Roskoski, and K. M. Keane. 1994. Recycling of the naturally-occurring 15N in an established stand of Leucaena leucocephala. Soil Biology and Biochemistry 26:757–762.

Kikuzawa, K., and M. J. Lechowicz. 2011. Ecology of Leaf Longevity. Page (Y. Iwasa, Ed.). Springer Tokyo, Tokyo.

Killingbeck, K. T. 1993. Inefficient nitrogen resorption in genets of the actinorhizal nitrogen fixing shrub Comptonia peregrina: physiological ineptitude or evolutionary tradeoff? Oecologia 94:542–549.

Klausmeier, C. A., E. Litchman, T. Daufresne, and S. A. Levin. 2004. Optimal nitrogen-to-

phosphorus stoichiometry of phytoplankton. Nature 429:171–174.

Kou-Giesbrecht, S., and D. Menge. 2019. Nitrogen-fixing trees could exacerbate climate change under elevated nitrogen deposition. Nature Communications 10:1–8.

Kramer-Walter, K. R., P. J. Bellingham, T. R. Millar, R. D. Smissen, S. J. Richardson, and D. C. Laughlin. 2016. Root traits are multidimensional: specific root length is independent from root tissue density and the plant economic spectrum. Journal of Ecology 104:1299–1310.

Kulmatiski, A., K. H. Beard, J. R. Stevens, and S. M. Cobbold. 2008. Plant-soil feedbacks: A meta-analytical review. Ecology Letters 11:980–992.

Lai, H. R., J. S. Hall, S. A. Batterman, B. L. Turner, and M. van Breugel. 2018. Nitrogen fixer abundance has no effect on biomass recovery during tropical secondary forest succession. Journal of Ecology 106:1415–1427.

Lawrence, D. M., R. A. Fisher, C. D. Koven, K. W. Oleson, S. C. Swenson, G. Bonan, N. Collier, B. Ghimire, L. Kampenhout, D. Kennedy, E. Kluzek, P. J. Lawrence, F. Li, H. Li, D. Lombardozzi, W. J. Riley, W. J. Sacks, M. Shi, M. Vertenstein, W. R. Wieder, C. Xu, A. A. Ali, A. M. Badger, G. Bisht, M. Broeke, M. A. Brunke, S. P. Burns, J. Buzan, M. Clark, A. Craig, K. Dahlin, B. Drewniak, J. B. Fisher, M. Flanner, A. M. Fox, P. Gentine, F. Hoffman, G. Keppel-Aleks, R. Knox, S. Kumar, J. Lenaerts, L. R. Leung, W. H. Lipscomb, Y. Lu, A. Pandey, J. D. Pelletier, J. Perket, J. T. Randerson, D. M. Ricciuto, B. M. Sanderson, A. Slater, Z. M. Subin, J. Tang, R. Q. Thomas, M. Val Martin, and X. Zeng. 2019. The Community Land Model version 5: Description of new features, benchmarking, and impact of forcing uncertainty. Journal of Advances in Modeling Earth Systems 2:1–43.

LeBauer, D. S., and K. K. Treseder. 2008. Nitrogen limitation of net primary productivity in terrestrial ecosystems is globally distributed. Ecology 89:371–379.

Li, Z., W. A. Kurz, M. J. Apps, and S. J. Beukema. 2003. Belowground biomass dynamics in the Carbon Budget Model of the Canadian Forest Sector: recent improvements and implications for the estimation of NPP and NEP. Canadian Journal of Forest Research 136:126–136.

Liao, W., and D. N. L. Menge. 2016. Demography of symbiotic nitrogen-fixing trees explains their rarity and successional decline in temperate forests in the United States. PLoS ONE 11:1–13.

De Long, J. R., E. L. Fry, G. F. Veen, and P. Kardol. 2019. Why are plant–soil feedbacks so unpredictable, and what to do about it? Functional Ecology 33:118–128.

Lovett, G. M., L. M. Christenson, P. M. Groffman, C. G. Jones, J. E. Hart, and M. J. Mitchell. 2002. Insect defoliation and nitrogen cycling in forests. BioScience 52:335.

Marleau, J. N., F. Guichard, and M. Loreau. 2015. Emergence of nutrient co-limitation through movement in stoichiometric meta-ecosystems. Ecology Letters 18:1163–1173.

Mattson, W. J. 1980. Herbivory in relation to plant nitrogen content. Annual Review of Ecology and Systematics 11:119–161.

McGroddy, M. E., T. Daufresne, and L. O. Hedin. 2004. Scaling of C:N:P stoichiometry in forests worldwide: Implications of terrestrial Redfield-type ratios. Ecology 85:2390–2401.

McHargue, L. A. 1999. Factors affecting the nodulation and growth of tropical woody legume seedlings. Florida International University.

Menge, D. N. L., S. A. Batterman, L. O. Hedin, W. Liao, S. W. Pacala, and B. N. Taylor. 2017a. Why are nitrogen-fixing trees rare at higher compared to lower latitudes? Ecology 98:0–22.

Menge, D. N. L., S. A. Batterman, W. Liao, B. N. Taylor, J. W. Lichstein, and G. Ángeles-Pérez. 2017b. Nitrogen-fixing tree abundance in higher-latitude North America is not constrained by diversity.

Menge, D. N. L., J. L. Denoyer, and J. W. Lichstein. 2010. Phylogenetic constraints do not explain the rarity of nitrogen-fixing trees in late-successional temperate forests. PLoS ONE 5.

Menge, D. N. L., and L. O. Hedin. 2009. Nitrogen fixation in different biogeochemical niches along a 120 000-year chronosequence in New Zealand. Ecology 90:2190–2201.

Menge, D. N. L., L. O. Hedin, and S. W. Pacala. 2012. Nitrogen and phosphorus limitation over long-term ecosystem development in terrestrial ecosystems. PLoS ONE 7.

Menge, D. N. L., and S. A. Levin. 2017. Spatial heterogeneity can resolve the nitrogen paradox of tropical forests. Ecology 98:1049–1061.

Menge, D. N. L., S. A. Levin, and L. O. Hedin. 2008. Evolutionary tradeoffs can select against nitrogen fixation and thereby maintain nitrogen limitation. PNAS 105:1573–1578.

Menge, D. N. L., S. A. Levin, and L. O. Hedin. 2009a. Facultative versus obligate nitrogen fixation strategies and their ecosystem consequences. The American Naturalist 174:465–477.

Menge, D. N. L., S. W. Pacala, and L. O. Hedin. 2009b. Emergence and Maintenance of Nutrient Limitation over Multiple Timescales in Terrestrial Ecosystems. The American Naturalist 173:164–175.

Menge, D. N. L., A. A. Wolf, and J. L. Funk. 2015. Diversity of nitrogen fixation strategies in Mediterranean legumes. Nature Plants 1:15064.

Meyerholt, J., S. Zaehle, and M. J. Smith. 2016. Variability of projected terrestrial biosphere

responses to elevated levels of atmospheric CO2 due to uncertainty in biological nitrogen fixation. Biogeosciences 13:1491–1518.

Miki, T., and M. Kondoh. 2002. Feedbacks between nutrient cycling and vegetation predict plant species coexistence and invasion. Ecology Letters 5:624–633.

Miki, T., M. Ushio, S. Fukui, and M. Kondoh. 2010. Functional diversity of microbial decomposers facilitates plant coexistence in a plant-microbe-soil feedback model. Proceedings of the National Academy of Sciences of the United States of America 107:14251–14256.

Mitchell, J. S., and R. W. Ruess. 2009. Seasonal patterns of climate controls over nitrogen fixation by *Alnus viridis* subsp *fruticosa* in a secondary successional chronosequence in interior Alaska. Ecoscience 16:341–351.

Moyes, A. B., L. M. Kueppers, J. Pett-Ridge, D. L. Carper, N. Vandehey, J. O'Neil, and A. C. Frank. 2016. Evidence for foliar endophytic nitrogen fixation in a widely distributed subalpine conifer. New Phytologist 210:657–668.

Myster, R. W. 2006. Light and nutrient effects on growth and allocation of *Inga vera* (Leguminosae), a successional tree of Puerto Rico. Canadian Journal of Forest Research 36:1121–1128.

Nadelhoffer, K. J., J. D. Aber, and J. M. Melillo. 1985. Fine Roots, Net Primary Production, and Soil Nitrogen Availability: A New Hypothesis. Ecology 66:1377–1390.

Nadelhoffer, K. J., and J. W. Raich. 1992. Fine Root Production Estimates and Belowground Carbon Allocation in Forest Ecosystems. Ecology 73:1139–1147.

Nasto, M. K., S. Alvarez-Clare, Y. Lekberg, B. W. Sullivan, A. R. Townsend, and C. C. Cleveland. 2014. Interactions among nitrogen fixation and soil phosphorus acquisition strategies in lowland tropical rain forests. Ecology Letters 17:1282–1289.

Neumann, M., L. Ukonmaanaho, J. Johnson, S. Benham, L. Vesterdal, R. Novotný, A. Verstraeten, L. Lundin, A. Thimonier, P. Michopoulos, and H. Hasenauer. 2018. Quantifying Carbon and Nutrient Input from Litterfall in European Forests using Field Observations and Modelling. Global Biogeochemical Cycles:1–15.

Nickmans, H., M. Jonard, K. Verheyen, and Q. Ponette. 2019. Modelling leaf dispersal and nutrient return in tree species mixtures. Forest Ecology and Management 436:68–78.

Norby, R. J., J. M. Warren, C. M. Iversen, B. E. Medlyn, and R. E. McMurtrie. 2010. CO_2 enhancement of forest productivity constrained by limited nitrogen availability. Proceedings of the National Academy of Sciences 107:19368–19373.

Notaro, K. de A., E. V. de Medeiros, G. P. Duda, A. O. Silva, and P. M. de Moura. 2014. Agroforestry systems, nutrients in litter and microbial activity in soils cultivated with coffee at high altitude. Scientia Agricola 71:87–95.

Okubo, A., and S. A. Levin. 2001. Diffusion and Ecological Problems: Modern Perspectives. 2nd edition. Springer-Verlag, New York.

Orndorff, K. A., and G. E. Lang. 1981. Leaf litter redistribution in a West Virginia hardwood forest. Journal of Ecology 69:225–235.

Pacala, S. W., G. C. Hurtt, D. Baker, P. Peylin, R. A. Houghton, R. A. Birdsey, L. S. Heath, E. T. Sundquist, R. F. Stallard, P. Ciais, P. R. Moorcroft, J. P. Caspersen, E. Shevliakova, B. Moore, G. Kohlmaier, E. Holland, M. Gloor, M. E. Harmon, S. M. Fan, J. L. Sarmiento, C. L. Goodale, D. S. Schimel, and C. B. Field. 2001. Consistent land-and atmosphere-based U.S. carbon sink estimates. Science 292:2316–2320.

Padda, K. P., A. Puri, and C. Chanway. 2019. Endophytic nitrogen fixation – a possible 'hidden' source of nitrogen for lodgepole pine trees growing at unreclaimed gravel mining sites. FEMS Microbiology Ecology 95.

Pan, Y., R. A. Birdsey, J. Fang, R. Houghton, P. E. Kauppi, W. A. Kurz, O. L. Phillips, A. Shvidenko, S. L. Lewis, J. G. Canadell, P. Ciais, R. B. Jackson, S. W. Pacala, A. D. McGuire, S. Piao, A. Rautiainen, S. Sitch, D. Hayes, R. Bridsey, J. Fang, R. Houghton, P. E. Kauppi, W. A. Kurz, O. L. Phillips, A. Shvidenko, S. L. Lewis, J. G. Canadell, P. Ciais, R. B. Jackson, S. W. Pacala, A. D. McGuire, S. Piao, A. Rautiainen, S. Sitch, D. Hayes, R. A. Birdsey, J. Fang, R. Houghton, P. E. Kauppi, W. A. Kurz, O. L. Phillips, A. Shvidenko, S. L. Lewis, J. G. Canadell, P. Ciais, R. B. Jackson, S. W. Pacala, A. D. McGuire, S. Piao, A. Rautiainen, S. Sitch, and D. Hayes. 2011. A large and persistent carbon sink in the world's forests. Science 333:988–993.

Parrotta, J. A., D. D. Baker, and M. Fried. 1996. Changes in dinitrogen fixation in maturing stands of *Casuarina equisetifolia* and *Leucaena leucocephala*. Canadian Journal of Forest Research 26:1684–1691.

Paul, L. R., B. K. Chapman, and C. P. Chanway. 2007. Nitrogen fixation associated with *Suillus tomentosus* tuberculate ectomycorrhizae on *Pinus contorta* var. latifolia. Annals of Botany 99:1101–1109.

Pebesma, E. J., and R. S. Bivand. 2005. Classes and methods for spatial data in R. R News.

Peng, J., L. Dan, Y. P. Wang, X. Tang, X. Yang, F. Yang, X. Lu, and B. Pak. 2018. Role contribution of biological nitrogen fixation to future terrestrial net land carbon accumulation under warming condition at centennial scale. Journal of Cleaner Production 202:1158–1166.

Perakis, S. S., J. J. Matkins, and D. E. Hibbs. 2012a. N_2-fixing red alder indirectly accelerates ecosystem nitrogen cycling. Ecosystems 15:1182–1193.

Perakis, S. S., J. J. Matkins, and D. E. Hibbs. 2012b. Interactions of tissue and fertilizer nitrogen on decomposition dynamics of lignin-rich conifer litter. Ecosphere 3:art54.

Perakis, S. S., and E. R. Sinkhorn. 2011. Biogeochemistry of a temperate forest nitrogen gradient. Ecology 92:1481–1491.

Perakis, S. S., E. R. Sinkhorn, and J. E. Compton. 2011. $\delta^{15}N$ constraints on long-term nitrogen balances in temperate forests. Oecologia 167:793–807.

Perakis, S. S., A. J. Tepley, and J. E. Compton. 2015. Disturbance and topography shape nitrogen availability and $\delta^{15}N$ over long-term forest succession. Ecosystems 18:573–588.

Pérez, C. A., M. R. Carmona, and J. J. Armesto. 2010. Non-symbiotic nitrogen fixation during leaf litter decomposition in an old-growth temperate rain forest of Chiloé Island, southern Chile: Effects of single versus mixed species litter. Austral Ecology 35:148–156.

Phillips, R. P., E. Brzostek, and M. G. Midgley. 2013. The mycorrhizal-associated nutrient economy: A new framework for predicting carbon-nutrient couplings in temperate forests. New Phytologist 199:41–51.

Png, G. K., H. Lambers, P. Kardol, B. L. Turner, D. A. Wardle, and E. Laliberte. 2019. Biotic and abiotic plant-soil feedback depends on nitrogen-acquisition strategy and shifts during long-term ecosystem development. Journal of Ecology 107:142–153.

Porder, S., G. P. Asner, and P. M. Vitousek. 2005. Ground-based and remotely sensed nutrient availability across a tropical landscape. PNAS 102:10909–10912.

Powers, J. S., R. A. Montgomery, E. C. Adair, F. Q. Brearley, S. J. Dewalt, C. T. Castanho, J. Chave, E. Deinert, J. U. Ganzhorn, M. E. Gilbert, J. A. González-Iturbe, S. Bunyavejchewin, H. R. Grau, K. E. Harms, A. Hiremath, S. Iriarte-Vivar, E. Manzane, A. A. De Oliveira, L. Poorter, J. B. Ramanamanjato, C. Salk, A. Varela, G. D. Weiblen, and M. T. Lerdau. 2009. Decomposition in tropical forests: A pan-tropical study of the effects of litter type, litter placement and mesofaunal exclusion across a precipitation gradient. Journal of Ecology 97:801–811.

van der Putten, W. H., R. D. Bardgett, J. D. Bever, T. M. Bezemer, B. B. Casper, T. Fukami, P. Kardol, J. N. Klironomos, A. Kulmatiski, J. A. Schweitzer, K. N. Suding, T. F. J. Van de Voorde, and D. A. Wardle. 2013. Plant-soil feedbacks: The past, the present and future challenges. Journal of Ecology 101:265–276.

R Core Team. 2020. R: A language and environment for statistical computing. R Foundation for Statistical Computing, Vienna, Austria.

Reed, S. C., C. C. Cleveland, and A. R. Townsend. 2007. Controls over Leaf Litter and Soil Nitrogen Fixation in Two Lowland Tropical Rain Forests. Biotropica 39:585–592.

Reed, S. C., C. C. Cleveland, and A. R. Townsend. 2011. Functional ecology of free-living nitrogen fixation: A contemporary perspective. Annual Review of Ecology, Evolution, and Systematics 42:489–512.

Reed, S. C., A. R. Townsend, C. C. Cleveland, and D. R. Nemergut. 2010. Microbial community shifts influence patterns in tropical forest nitrogen fixation. Oecologia 164:521–531.

Roumet, C., M. Birouste, C. Picon-Cochard, M. Ghestem, N. Osman, S. Vrignon-Brenas, K. fang Cao, and A. Stokes. 2016. Root structure-function relationships in 74 species: Evidence of a root economics spectrum related to carbon economy. New Phytologist 210:815–826.

Ruess, R. W., J. M. McFarland, L. M. Trummer, and J. K. Rohrs-Richey. 2009. Disease-mediated declines in N-fixation inputs by Alnus tenuifolia to early-successional floodplains in interior and south-central Alaska. Ecosystems 12:489–502.

Rufat, J., and T. M. DeJong. 2001. Estimating seasonal nitrogen dynamics in peach trees in response to nitrogen availability. Tree Physiology 21:1133–1140.

Russo, R. O. 2005. Nitrogen fixing trees with actinorhiza in forestry and agroforestry. Pages 143–171 *in* D. Werner and W. E. Newton, editors. Nitrogen fixation in agriculture, forestry, ecology, and the environment. Springer, Berlin/Heidelberg.

Sabo, R., C. Clark, J. Bash, D. Sobota, E. Cooter, J. Dobrowolski, B. Houlton, A. Rea, D. Schwede, S. Morford, and J. Compton. 2019. Decadal shift in nitrogen inputs and fluxes across the contiguous United States: 2002-2012. Biogeosciences 124:3104–3124.

Sayer, E. J., and E. V. J. Tanner. 2010. Experimental investigation of the importance of litterfall in lowland semi-evergreen tropical forest nutrient cycling. Journal of Ecology 98:1052–1062.

Schenk, H. J., and R. B. Jackson. 2002. Rooting Depths, Lateral Root Spreads and Below-Ground / Above-Ground Allometries of Plants in Water-Limited Ecosystems. Journal of Ecology 90:480–494.

Schwede, D. B., and G. G. Lear. 2014. A novel hybrid approach for estimating total deposition in the United States. Atmospheric Environment 92:207–220.

Shearer, G., D. H. Kohl, J. R. Jones, and D. H. Kohl. 1986. N_2-fixation in field settings: Estimations based on natural ^{15}N abundance. Aust. J. Plant Physiol. 13:699–756.

Shi, Z., Y. Yang, X. Zhou, E. Weng, A. C. Finzi, and Y. Luo. 2016. Inverse analysis of coupled carbon-nitrogen cycles against multiple datasets at ambient and elevated CO_2. Journal of Plant Ecology 9:285–295.

Siddique, I., V. L. Engel, J. A. Parrotta, D. Lamb, G. B. Nardoto, J. P. H. B. Ometto, L. A. Martinelli, and S. Schmidt. 2008. Dominance of legume trees alters nutrient relations in mixed species forest restoration plantings within seven years. Biogeochemistry 88:89–101.

Silvester, W. B. 1983. 6. Analysis of nitrogen fixation.

Simard, S. W., and D. M. Durall. 2004. Mycorrhizal networks: A review of their extent, function, and importance. Canadian Journal of Botany 82:1140–1165.

Sobota, D. J., J. E. Compton, and J. A. Harrison. 2013. Reactive nitrogen inputs to US lands and waterways: how certain are we about sources and fluxes? Frontiers in Ecology and the Environment 11:82–90.

Sokolov, A. P., D. W. Kicklighter, J. M. Melillo, B. S. Felzer, C. A. Schlosser, and T. W. Cronin. 2008. Consequences of considering carbon-nitrogen interactions on the feedbacks between climate and the terrestrial carbon cycle. Journal of Climate 21:3776–3796.

Sprent, J. I. 2009. Legume Nodulation: A Global Perspective. Wiley-Blackwell, Ames, IA.

Staelens, J., L. Nachtergale, S. Luyssaert, and N. Lust. 2003. A model of wind-influenced leaf litterfall in a mixed hardwood forest. Canadian Journal of Forest Research 33:201–209.

Stocker, B. D., I. C. Prentice, S. E. Cornell, T. Davies-Barnard, A. C. Finzi, O. Franklin, I. Janssens, T. Larmola, S. Manzoni, T. Näsholm, J. A. Raven, K. T. Rebel, S. C. Reed, S. Vicca, A. Wiltshire, and S. Zaehle. 2016. Terrestrial nitrogen cycling in Earth system models revisited. New Phytologist 210:1165–1168.

Stout, B. B. 1956. Studies of the root systems of deciduous trees. Black Rock Forest Bulletin:3–45.

Sulman, B. N., E. Shevliakova, E. R. Brzostek, N. Stephanie, S. Malyshev, D. N. L. Menge, and X. Zhang. 2019. Diverse mycorrhizal associations enhance terrestrial C storage in a global model. Global biogeochemical Cycles:0–3.

Tans, P. P. 1990. Atmospheric CO_2 budget. Science 247:1431–1438.

Taylor, B. N., R. L. Chazdon, B. Bachelot, and D. N. L. Menge. 2017. Nitrogen-fixing trees inhibit growth of regenerating Costa Rican rainforests. Proceedings of the National Academy of Sciences 114:8817–8822.

Taylor, B. N., and D. N. L. Menge. 2018. Light regulates tropical symbiotic nitrogen fixation more strongly than soil nitrogen. Nature Plants 4.

Terrer, C., S. Vicca, B. D. Stocker, B. A. Hungate, R. P. Phillips, P. B. Reich, A. C. Finzi, and I. C. Prentice. 2017. Ecosystem responses to elevated CO_2 governed by plant – soil interactions and the cost of nitrogen acquisition. New Phytologist:1–16.

Thomas, R. Q., E. N. J. Brookshire, and S. Gerber. 2015. Nitrogen limitation on land: How can it occur in Earth system models? Global Change Biology 21:1777–1793.

Thomas, R. Q., S. Zaehle, P. H. Templer, and C. L. Goodale. 2013. Global patterns of nitrogen limitation: Confronting two global biogeochemical models with observations. Global Change Biology 19:2986–2998.

Thornton, P. E., J. F. Lamarque, N. A. Rosenbloom, and N. M. Mahowald. 2007. Influence of carbon-nitrogen cycle coupling on land model response to CO_2 fertilization and climate variability. Global Biogeochemical Cycles 21:1–15.

Tilman, D. 1977. Resource Competition between Plankton Algae: An Experimental and Theoretical Approach. Ecology 58:338–348.

Tilman, D. 1980. Resources: A Graphical-Mechanistic Approach to Competition and Predation. The American Naturalist 116:362–393.

Tilman, D. 1982. Resource Competition and Community Structure. Princeton University Press, Princeton, NJ.

Tilman, D. 2003. Mechanisms of plant competition for nutrients: the elements of a predictive theory of competition. Pages 117–141 *in* J. Grace and D. Tilman, editors. Perspectives on Plant Competition. The Blackburn Press, New Jersey.

Toselli, M., J. A. Flore, C. Zavalloni, and B. Marangoni. 2000. Nitrogen partitioning in apple trees as affected by application time. HortTechnology 10:136–141.

Treseder, K. K. 2013. The extent of mycorrhizal colonization of roots and its influence on plant growth and phosphorus content. Plant and Soil 371:1–13.

Turchin, P. 1998. Quantitative analysis of movement - measuring and modeling population redistribution in animals. Sinauer, Sunderland, MA.

Turetsky, M. R. 2003. The role of bryophytes in carbon and nitrogen cycling. The Bryologist 106:395–409.

Uliassi, D. D., and R. W. Ruess. 2002. Limitations to symbiotic nitrogen fixation in primary succession on the Tanana River floodplain. Ecology 83:88–103.

Uriarte, M., and D. Menge. 2018. Variation between individuals fosters regional species coexistence. Ecology Letters 21:1496–1504.

Uriarte, M., B. L. Turner, J. Thompson, and J. K. Zimmerman. 2015. Linking spatial patterns of leaf litterfall and soil nutrients in a tropical forest: A neighborhood approach. Ecological Applications 25:2022–2034.

USGS. 2000. Forest Cover Types. Reston, VA.

Veen, G. F., E. L. Fry, F. C. ten Hooven, P. Kardol, E. Morriën, and J. R. De Long. 2019. The Role of Plant Litter in Driving Plant-Soil Feedbacks. Frontiers in Environmental Science 7:1–10.

Vergutz, L., S. Manzoni, A. Porporato, R. F. Novais, and R. B. Jackson. 2012. Global resorption efficiencies and concentrations of carbon and nutrients in leaves of terrestrial plants. Ecological Monographs 82:205–220.

Vitousek, P. M., J. D. Aber, R. W. Howarth, G. E. Likens, A. Matson, D. W. Schindler, W. H. Schlesinger, D. G. Tilman, M. P. A, D. W. Schindler, W. H. Schlesinger, and D. G. Tilman. 1997. Human alteration of the global nitrogen cycle: Sources and consequences. Ecological Applications 7:737–750.

Vitousek, P. M., and R. W. Howarth. 1991. Nitrogen limitation on land and in the sea: how can it occur? Biogeochemistry 13:87–115.

Vitousek, P. M., D. N. L. Menge, S. C. Reed, and C. C. Cleveland. 2013. Biological nitrogen fixation: rates, patterns and ecological controls in terrestrial ecosystems. Phil Trans R Soc B 368.

Wali, M., F. Evrendilek, and M. S. Fennessy. 2009. The Environment: Science, Issues, and Solutions. CRC Press.

Wedin, D. A., and D. Tilman. 1990. Species effects on nitrogen cycling: a test with perennial grasses. Oecologia 84:433–441.

White, D. L., B. L. Haines, and L. Boring. 1988. Litter decomposition in southern Appalachian black locust and pine-hardwood stands: litter quality and nitrogen dynamics. Canadian Journal of Forest Research 18:54–63.

Wieder, W. R., C. C. Cleveland, W. K. Smith, and K. Todd-Brown. 2015. Future productivity and carbon storage limited by terrestrial nutrient availability. Nature Geoscience 8:441–444.

Winbourne, J., M. Harrison, B. W. Sullivan, L. Alvarez-Clare, S. R. Lins, L. Martinelli, M. Nasto, D. Piotto, S. Rolim, M. Wong, and S. Porder. 2018. A new framework for evaluating estimates of symbiotic nitrogen fixation in forests. American Naturalist 192.

Wise, D. R., and H. M. Johnson. 2011. Surface-Water Nutrient Conditions and Sources in the United States Pacific Northwest. Journal of the American Water Resources Association 47:1110–1135.

Wright, I. J., P. B. Reich, M. Westoby, D. D. Ackerly, Z. Baruch, F. Bongers, J. Cavender-Bares, T. Chapin, J. H. C. Cornelissen, M. Diemer, J. Flexas, E. Garnier, P. K. Groom, J. Gulias, K. Hikosaka, B. B. Lamont, T. Lee, W. Lee, C. Lusk, J. J. Midgley, M.-L. Navas, U. Niinemets, J.

Oleksyn, N. Osada, H. Poorter, P. Poot, L. Prior, V. I. Pyankov, C. Roumet, S. C. Thomas, M. G. Tjoelker, E. J. Veneklaas, and R. Villar. 2004. The worldwide leaf economics spectrum. Nature 428:821–827.

Wurzburger, N. 2016. Old-growth temperate forests harbor hidden nitrogen-fixing bacteria. New Phytologist 210:374–376.

Xu-Ri, and I. C. Prentice. 2017. Modelling the demand for new nitrogen fixation by terrestrial ecosystems. Biogeosciences 14:2003–2017.

Xu, H., M. Detto, S. Fang, R. L. Chazdon, Y. Li, B. C. H. Hau, G. A. Fischer, G. D. Weiblen, J. A. Hogan, J. K. Zimmerman, M. Uriarte, J. Thompson, J. Lian, K. Cao, D. Kenfack, A. Alonso, P. Bissiengou, H. R. Memiaghe, R. Valencia, S. L. Yap, S. J. Davies, X. Mi, and T. L. Yao. 2020. Soil nitrogen concentration mediates the relationship between leguminous trees and neighbor diversity in tropical forests. Communications Biology 3:1–8.

Yelenik, S., S. Perakis, and D. Hibbs. 2013. Regional constraints to biological nitrogen fixation in post-fire forest communities. Ecology 94:739–750.

Zaehle, S., P. Friedlingstein, and A. D. Friend. 2010. Terrestrial nitrogen feedbacks may accelerate future climate change. Geophysical Research Letters 37:1–5.

Zhang, D. Q., D. F. Hui, Y. Luo, and G. Y. Zhou. 2008. Rates of litter decomposition in terrestrial ecosystems: global patterns and controlling factors. Journal of Plant Ecology 1:85–93.

Appendix A – Supplementary Information for Chapter 1

Introduction

The supplementary information provides details on the methods used to find the basal area-BNF rate regression, the specific literature that was used to derive both these regressions and the $\%N_{dfa}$ for different genera. The text describes further methods used to compare previous global estimates of BNF to the conterminous US scale and to examine the relevance of *P. contorta* as an additional source of N.

Text S1. Basal area-BNF regression method

This section explains additional details of the basal area-BNF regression method. The N fixation rate per basal area was determined using a linear regression between BNF rate (kg N ha^{-1} yr^{-1}) and basal area (m^2 ha^{-1}) for each N-fixing genus independently. A literature search was conducted, where, for each genus, both the basal area of that genus and the BNF rate were recorded. All of the data collected from the literature search were combined into a linear regression. The regression was bootstrapped to account for the relatively small and variable sample for BNF in each genus from the literature search. *Acacia* and *Prosopis* had sufficient literature values to obtain the estimate of slope and intercept. *Robinia* and *Alnus* did not exhibit a relationship between basal area and BNF so a slope of zero was used. This meant that if any *Robinia* were present in the plot it would result in the same BNF rate and if any *Alnus* were

present in the plot it would result in a set BNF rate. The average of *Acacia*, *Alnus*, *Prosopis*, and *Robinia* data were used as an estimate for all other genera (all other genera comprised only 10% of stems so the estimate had low sensitivity to this assumption). To get the confidence interval around this estimate, ten thousand random samples were drawn from a normal distribution where $\mu = mean$ and $\sigma = standard\ error$ of the range of fixation rates and the 95% confidence interval of the estimate was obtained.

Text S2. BNF rate literature review sources

This section gives the extended list of citations from the literature review of BNF rates used in the analysis.

1. Bernhard-Reversat, F. (1996). Nitrogen cycling in tree plantations grown on a poor sandy savanna soil in Congo. *Applied Soil Ecology*, *4*(2), 161–172. https://doi.org/10.1016/0929-1393(96)00096-0

2. Forrester, D. I., Schortemeyer, M., Stock, W. D., Bauhus, J., Khanna, P. K., & Cowie, A. L. (2007). Assessing nitrogen fixation in mixed-and single-species plantations of *Eucalyptus globulus* and *Acacia mearnsii*. *Tree Physiology*, *27*(9), 1319.

3. Chikowo, R. (2004). *Nitrogen cycling in agroforestry systems of sub-humid Zimbabwe: Closing the loop*. Wageningen University.

4. Rundel, P. W., Nilsen, E. T., Sharifi, M. R., Virginia, R. A., Jarrell, W. M., Kohl, D. H., & Shearer, G. B. (1982). Seasonal dynamics of nitrogen cycling for a *Prosopis* woodland in the Sonoran Desert. *Plant and Soil*, *67*(1–3), 343–353. https://doi.org/10.1007/BF02182781

5. Soper, F. M. (2016). *Effects of woody legume (*Prosopis glandulosa*) encroachment on nitrogen fixation, storage and gas loss in a subtropical, semi-arid savana*. Cornell University.

6. Soper, F. M., & Sparks, J. P. (2017). Estimating Ecosystem Nitrogen Addition by a Leguminous Tree: A Mass Balance Approach Using a Woody Encroachment Chronosequence. *Ecosystems*, *20*(6), 1164–1178. https://doi.org/10.1007/s10021-016-0100-1

7. Boring, L. R., & Swank, W. T. (1984). The role of black locust (*Robinia pseudoacacia*) in forest succession. *Journal of Ecology*, *72*, 749–766.

8. Newton, M., Hassan, B. A. E., & Zavitkovski, J. (1968). Role of red alder in western Oregon forest succession. In J. M. Trappe, F. Franklin, R. F. Tarrant, & G. M. Hansen (Eds.), *Biology of alder* (pp. 73–83). Portland, OR: USDA For. Serv., PNW For. Range Exp. Sta.

9. Luken, J. O., & Fonda, R. W. (1983). Nitrogen accumulation in a chronosequence of red alder communities along the Hoh River, Olympic National Park, Washington. *Can. J. For. Res.*, *13*(6), 1228–1237. https://doi.org/10.1139/x83-161

10. de Bell, D. S., & Radwan, M. A. (1979). Growth and nitrogen relations of coppiced Black Cottonwood and Red Alder in pure and mixed plantings. *Botanical Gazette, 140*, S97–S101. https://doi.org/10.1086/337043

11. Binkley, D. (1983). Ecosystem production in Douglas-fir plantations: Interaction of red alder and site fertility. *Forest Ecology and Management*, *5*(3), 215–227. https://doi.org/10.1016/0378-1127(83)90073-7

12. Malcolm, D. C., Hooker, J. E., & Wheeler, C. T. (1985). Frankia symbiosis as a source of nitrogen in forestry: a case study of symbiotic nitrogen-fixation in a mixed *Alnus-Picea* plantation in Scotland. *Proceedings of the Royal Society of Edinburgh. Section B. Biological Sciences*, *85B*, 263–282. https://doi.org/10.1017/s0269727000004061

13. Heilman, P., & Stettler, R. F. (1985). Mixed, short-rotation culture of red alder and black cottonwood: growth, coppicing, nitrogen fixation, and allelopathy. *Forest Science*, *31*(3), 607–616. https://doi.org/10.1093/forestscience/31.3.607

14. Van Cleve, K., Viereck, L. A., & Schlentner, R. L. (1971). Accumulation of nitrogen in Alder (*Alnus*) ecosystems near Fairbanks, Alaska. *Arctic and Alpine Research*, *3*(2), 101–114. https://doi.org/10.2307/1549980

15. Daly, G. T. (1966). Nitrogen fixation by nodulated *Alnus rugosa*. *Canadian Journal of Botany*, *44*, 1607–1621.

16. Binkley, D., Sollins, P., Bell, R., Sachs, D., & Myrold, D. (1992). Biogeochemistry of adjacent conifer and alder-conifer stands. *Ecology*, *73*(6), 2022–2033. https://doi.org/10.2307/1941452

17. Tarrant, R. F., & Miller, R. E. (1963). Accumulation of organic matter and soil nitrogen beneath a plantation of Red Alder and Douglas-Fir. *Soil Science Society of America Proceedings*, *27*(2), 231–234. https://doi.org/10.2136/sssaj1963.03615995002700020041x

18. Chikowo, R. (2004). *Nitrogen cycling in agroforestry systems of sub-humid Zimbabwe: Closing the loop*. Wageningen University.

19. Aronson, J., Ovalle, C., Avendaño, J., Longeri, L., & Del Pozo, A. (2002). Agroforestry tree selection in central Chile: Biological nitrogen fixation and early plant growth in six dryland species. *Agroforestry Systems*, *56*(2), 155–166. https://doi.org/10.1023/A:1021345318008

20. Bouillet, J. P., Laclau, J. P., Gonçalves, J. L. M., Moreira, M. Z., Trivelin, P. C. O., Jourdan, C., et al. (2008). Mixed-species plantations of *Acacia mangium* and *Eucalyptus grandis* in Brazil. 2: Nitrogen accumulation in the stands and biological N_2 fixation. *Forest Ecology and Management*, *255*(12), 3918–3930. https://doi.org/10.1016/j.foreco.2007.10.050

21. Galiana, A., Gnahoua, G. M., Chaumont, J., Lesueur, D., Prin, Y., & Mallet, B. (1998). Improvement of nitrogen fixation in *Acacia mangium* through inoculation with rhizobium. *Agroforestry Systems*, *40*(3), 297–307. https://doi.org/10.1023/A:1006006410174

22. Mercado, A. R., Van Noordwijk, M., & Cadisch, G. (2011). Positive nitrogen balance of *Acacia mangium* woodlots as fallows in the Philippines based on ^{15}N natural abundance data of N_2 fixation. *Agroforestry Systems*, *81*(3), 221–233. https://doi.org/10.1007/s10457-010-9309-8

23. Raddad, E. A. Y., Salih, A. A., Ahmed, M., Fadl, M. A. El, Kaarakka, V., & Luukkanen, O. (2005). Symbiotic nitrogen fixation in eight *Acacia senegal* provenances in dryland clays of the Blue Nile Sudan estimated by the ^{15}N natural abundance method. *Plant and Soil*, *275*(1/2), 261–269.

24. Fox-Dobbs, K., Doak, D. F., Brody, A. K., & Palmer, T. M. (2010). Termites create spatial structure and govern ecosystem function by affecting N_2 fixation in an East African savanna. *Ecology*, *91*(5), 1296–1307.

25. Ndoye, I., Gueye, M., Danso, S. K. A., & Dreyfus, B. (1995). Nitrogen fixation in *Faidherbia albida*, *Acacia raddiana*, *Acacia senegal* and *Acacia seyal* estimated using the ^{15}N isotope dilution technique. *Plant and Soil*, *172*(2), 175–180. https://doi.org/10.1007/BF00011319

26. Cramer, M. D., Van Cauter, A., & Bond, W. J. (2010). Growth of N_2-fixing African savanna *Acacia* species is constrained by below-ground competition with grass. *Journal of Ecology*, *98*(1), 156–167. https://doi.org/10.1111/j.1365-2745.2009.01594.x

27. Raddad, E. A. Y., Salih, A. A., Ahmed, M., Fadl, M. A. El, Kaarakka, V., & Luukkanen, O. (2005). Symbiotic nitrogen fixation in eight *Acacia senegal* provenances in dryland clays of the Blue Nile Sudan estimated by the ^{15}N natural abundance method. *Plant and Soil*, *275*(1/2), 261–269.

28. Forrester, D. I., Schortemeyer, M., Stock, W. D., Bauhus, J., Khanna, P. K., & Cowie, A. L. (2007). Assessing nitrogen fixation in mixed-and single-species plantations of *Eucalyptus globulus* and *Acacia mearnsii*. *Tree Physiology*, *27*(9), 1319.

29. Paparcikova, K., Brienza jun., S., Kato, O. R., & Vlek, P. L. G. (2002). Field estimation of biological N_2-fixation by five tropical tree species using two ^{15}N isotope dilution methods. In R. Lieberi, H. Bianchi, V. Boehm, & C. Reisdorff (Eds.), *Neotropical Ecosystems, Proceedings of the German-Brazilian Workshop* (pp. 639–643). Hamburg: GKSS-Forschungszentrum Geesthacht GmbH.

30. Ovalle, C., Longeri, L., Aronson, J., Herrera, A., & Avendano, J. (1996). N_2-Fixation, nodule

efficiency and biomass accumulation after two years in three Chilean legume trees and Tagasaste *Chamaecytisus proliferus* subsp. *palmensis*. *Plant and Soil*, *179*(1), 131–140. https://doi.org/10.1007/BF00011650

31. Kadiata, B. D., Mulongoy, K., & Isirimah, N. O. (1997). Influence of pruning frequency of *Albizia lebbeck, Gliricidia sepium* and *Leucaena leucocephala* on nodulation and potential nitrogen fixation. *Biology and Fertility of Soils*, *24*(3), 255–260. https://doi.org/10.1007/s003740050240

32. Rundel, P. W., Nilsen, E. T., Sharifi, M. R., Virginia, R. A., Jarrell, W. M., Kohl, D. H., & Shearer, G. B. (1982). Seasonal dynamics of nitrogen cycling for a *Prosopis* woodland in the Sonoran Desert. *Plant and Soil*, *67*(1–3), 343–353. https://doi.org/10.1007/BF02182781

33. Villagra, G. M. L., & Felker, P. (1997). Influence of understory removal, thinning and P fertilization on N_2 fixation in a mature mesquite (*Prosopis glandulosa* var. *glandulosa*) stand. *Journal of Arid Environments*, *36*(4), 591–610. https://doi.org/10.1006/jare.1996.0219

34. Shearer, G., Kohl, D. H., Virginia, R. a., Bryan, B. a., Skeeters, J. L., Nilsen, E. T., et al. (1983). Estimates of N_2-fixation from variation in the natural abundance of ^{15}N in Sonoran desert ecosystems. *Oecologia*, *56*(2–3), 365–373. https://doi.org/10.1007/BF00379714

35. Aronson, J., Ovalle, C., Avendaño, J., Longeri, L., & Del Pozo, A. (2002). Agroforestry tree selection in central Chile: Biological nitrogen fixation and early plant growth in six dryland species. *Agroforestry Systems*, *56*(2), 155–166. https://doi.org/10.1023/A:1021345318008

36. Ovalle, C., Longeri, L., Aronson, J., Herrera, A., & Avendano, J. (1996). N_2-Fixation, nodule efficiency and biomass accumulation after two years in three Chilean legume trees and Tagasaste *Chamaecytisus proliferus* subsp. *palmensis*. *Plant and Soil*, *179*(1), 131–140. https://doi.org/10.1007/BF00011650

37. Ovalle, C., Arrendono, S., Aronson, J., Longeri, L., & Avendano, J. (1998). *The use of nuclear techniques in the management of nitrogen fixation by trees to enhance fertility of fragile tropical soils*. Vienna, Austria.

38. Danso, S. K. A., Zapata, F., & Awonaike, O. (1995). Measurement of biological N_2 fixation in field-grown *Robinia pseudoacacia L*. *Soil Biology and Biochemistry*, *27*(4/5), 415–419.

39. Marron, N., Gana, C., Gérant, D., Maillard, P., Priault, P., & Epron, D. (2018). Estimating symbiotic N_2 fixation in *Robinia pseudoacacia*. *Journal of Plant Nutrition and Soil Science*, *181*(2), 296–304. https://doi.org/10.1002/jpln.201700503

40. Mantovani, D., Veste, M., Boldt-Burisch, K., Fritsch, S., Koning, L. A., & Freese, D. (2015). Carbon allocation, nodulation, and biological nitrogen fixation of black locust (*Robinia pseudoacacia L.*) under soil water limitation. *Annals of Forest Research*, *58*(2), 259–274. https://doi.org/10.15287/afr.2015.420

41. Veste, M., Böhm, C., Quinkenstein, A., & Freese, D. (2012). Estimation of biological

nitrogen fixation by black locust in short-rotation forests using natural ^{15}N abundance method. *Geophysical Research Abstracts*, *14*, 4186.

42. Djumaeva, D., Vlek, P. L. G., & Khamzina, A. (2011). *The effect of phosphorus amendments on nitrogen fixation and growth of trees on salt-affected croplands in the lower reaches of Amu Darya, Uzbekistan*. *Landwirtschaftliche Fakultät*.

43. Hoosbeek, M. R., Lukac, M., Velthorst, E., Smith, A. R., & Godbold, D. L. (2011). Free atmospheric CO_2 enrichment increased above ground biomass but did not affect symbiotic N_2-fixation and soil carbon dynamics in a mixed deciduous stand in Wales. *Biogeosciences*, *8*(2), 353–364. https://doi.org/10.5194/bg-8-353-2011

44. Coté, B., & Camire, C. (1984). Growth, nitrogen accumulation, and symbiotic dinitrogen fixation in pure and mixed plantings of hybrid poplar and black alder. *Plant and Soil*, *78*(1–2), 209–220. https://doi.org/10.1007/BF02277852

45. Domenach, A. M., Kurdali, F., & Bardin, R. (1989). Estimation of symbiotic dinitrogen fixation in alder forest by the method based on natural ^{15}N abundance. *Plant and Soil*, *118*(1–2), 51–59. https://doi.org/10.1007/BF02232790

46. Hurd, T. M., Raynal, D. J., & Schwintzer, C. R. (2001). Symbiotic N_2 fixation of *Alnus incana* ssp. *rugosa* in shrub wetlands of the Adirondack Mountains, New York, USA. *Oecologia*, *126*(1), 94–103. https://doi.org/10.1007/s004420000500

47. Millett, J., Godbold, D., Smith, A., & Grant, H. (2012). N_2 fixation and cycling in *Alnus glutinosa*, *Betula pendula* and *Fagus sylvatica* woodland exposed to free air CO_2 enrichment. *Oecologia*, *169*(2), 541–552.

48. Mead, D., & Preston, C. (1992). Nitrogen fixation in Sitka alder by ^{15}N isotope dilution after eight growing seasons in a lodgepole pine site. *Canadian Journal of Forest Research*, *22*, 1192–1194.

49. Kurdali, F., Domenach, A. M., & Bardin, R. (1990). Alder-poplar associations: Determination of plant nitrogen sources by isotope techniques. *Biology and Fertility of Soils*, *9*(4), 321–329. https://doi.org/10.1007/BF00634109

50. Khamzina, A., Lamers, J. P. A., & Vlek, P. L. G. (2009). Nitrogen fixation by *Elaeagnus angustifolia* in the reclamation of degraded croplands of Central Asia. *Tree Physiology*, *29*(6), 1–10. https://doi.org/10.1093/treephys/tpp017

Text S3. Scaling past BNF estimates to US

This section gives full details on how we used past biome-specific or global estimates of BNF to calculate BNF at the scale of the US. For all estimates, the biome-specific or global estimate of

fixed N (Tg N yr^{-1}) was scaled to the extent of the conterminous US. Then we calculated the BNF rate per forest area by dividing the fixed N in the US by forest area in the US.

$$BNF\ per\ forest\ area = \frac{F_{US}}{forest\ area_{US}}$$

The forest area in the US is 2.09 x 10^6 hectares (USGS 2000). Some estimates reported BNF by biome. For these estimates we scaled to the US using two methods: (1) by land area where the fraction of land area in the US relative to the globe was used to scale down the global BNF estimate, and (2) the fraction of each reported biome that occurs in the US was used to scale the biome-specific BNF estimates.

Global land area was 148,429,000 km^2 and was obtained from Wali et al. (2009). The forest area and land area in the US were obtained from the USGS land cover data (USGS 2000). The proportion of symbiotic to asymbiotic fixation was 0.76 (Cleveland et al. 2013). The proportion of tree fixation to understory fixation was assumed to be 0.75. The abbreviations used below are F_{global}: total global BNF; land $area_{US}$: land area of the US; land $area_{global}$: land area of the entire globe; forest $area_{US}$: forest area within the US; land $area_{US}$: total land area in the US; BNF_{symb}: symbiotic nitrogen fixation; $BNF_{symb+asymb}$: total biological nitrogen fixation including symbiotic and asymbiotic; BNF_{tree}: nitrogen fixation from N-fixing trees; $BNF_{tree+understory}$: nitrogen fixation from N-fixing trees and understory plants.

Vitousek et al. (2013):

$$F_{US} = F_{global} * \frac{land\ area_{US}}{land\ area_{global}} * \frac{forest\ area_{US}}{land\ area_{US}} * \frac{BNF_{symb}}{BNF_{symb+asymb}} * \frac{BNF_{tree}}{BNF_{tree+understory}}$$

The overall global estimate comes straight from Vitousek et al. (2013): F_{global} = 58 Tg N yr^{-1}. This calculation assumes that the overall BNF rate is similar across the globe.

Cleveland, et al (2013):

Biome area scaling:

$$F_{US} = \sum_{i=1}^{\#\ biomes} BNF_i * \frac{biome\ area_{US,i}}{biome\ area_{global,i}}$$

The biome area globally (indexed with *i*) and biome-specific BNF rates (BNF_i) were calculated by Cleveland, et al (2013). The biome area in the US was determined analyzing land cover data from the University of Maryland (Hansen et al. 2000) using ArcGIS (ESRI 2011).

Land area scaling:

$$F_{US} = F_{global} * \frac{land\ area_{US}}{land\ area_{global}} * \frac{forest\ area_{US}}{land\ area_{US}} * \frac{BNF_{symb}}{BNF_{symb+asymb}} * \frac{BNF_{tree}}{BNF_{tree+understory}}$$

$$F_{global} = 105\ Tg\ N\ yr^{-1}$$

Cleveland, et al (1999):

Biome area scaling:

$$F_{US} = BNF\ rate * forest\ area_{US} * 1x10^{-9}$$

Cleveland et al (1999) used 16.04 kg N ha^{-1} yr^{-1} as the BNF rate across all temperate forests.

Land area scaling:

$$F_{US} = F_{global} * \frac{land\ area_{US}}{land\ area_{global}} * \frac{forest\ area_{US}}{land\ area_{US}} * \frac{BNF_{symb}}{BNF_{symb+asymb}} * \frac{BNF_{tree}}{BNF_{tree+understory}}$$

$$F_{global} = 195\ Tg\ N\ yr^{-1}$$

Galloway, et al (2004):

Land area scaling:

$$F_{US} = F_{global} * \frac{land\ area_{US}}{land\ area_{global}} * \frac{forest\ area_{US}}{land\ area_{US}} * \frac{BNF_{symb}}{BNF_{symb+asymb}} * \frac{BNF_{tree}}{BNF_{tree+understory}}$$

$$F_{global} = 107\ Tg\ N\ yr^{-1}$$

Constants:

$$\frac{BNF_{symb}}{BNF_{symb+asymb}} = 0.76\ (from\ Cleveland, et\ al\ (2013)\ DBF, DNF, EBF, ENF, MIX\ biomes)$$

$$\frac{land\ area_{US}}{land\ area_{global}} = \frac{747726000\ ha}{14842900000\ ha} = 0.05$$

$$\frac{BNF_{tree}}{BNF_{tree+understory}} = 0.75$$

Text S4. Method for *Pinus contorta* calculation

This section gives the full details on the calculation of BNF from *Pinus contorta*. Recent work indicates that *P. contorta* fixes N at rates up to 10% of those observed in *Alnus rubra* (Paul et al. 2007). This could be a relevant source of symbiotically fixed N. We tested the impact of including *P. contorta* by assuming that it fixed at a certain rate. We evaluated three different percentages to capture the range of likely importance: 10% of the per-basal area rate of *Alnus rubra* (the highest rates observed by Paul et al., 2007), 1%, and 0.5%. Overall, the impact on the BNF estimate from trees was increased by 5.05 (± 0.08)%, 1.04 (± 0.05)%, and 0.52 (± 0.03)% respectively. This suggests that *P. contorta* is only a minor contributor on the scale of the continental US, although it could be an important source of fixed N in some biomes (Fig. S3).

Text S5. Scaling up to the coterminous US

To scale tree BNF estimates from the plot scale to the US we took the average plot BNF rate across a 1-degree grid cell and multiplied by the forest area in that grid cell. An alternate method of scaling up would be to use the FIA designated scaling factors. These scaling factors are defined for a given plot in a given year and depend on the number of other plots that were sampled in the region that year. Since we used plots from many years to maximize the number of plots used and the FIA scaling factors critically depend on which plots are being included, the FIA scaling factors over accounted for forest area in our project. For example, in a census window, if 50 plots were measured in 5,000,000 ha of forest, the plot expansion factor for these trees would, on average, be one plot represents 100,000 ha (though individual plot expansion factors would vary around this average). Then, in a census window ten years later if 500 plots were measured in the same area each plot would on average have an expansion factor of 10,000 ha per plot. For plots that have been measured more than once we used the most recent plot so plots were selected from different census intervals with different expansion factors over counting forest. We concluded that scaling using known forest cover over a one-degree grid cell was a more reliable method for scaling up.

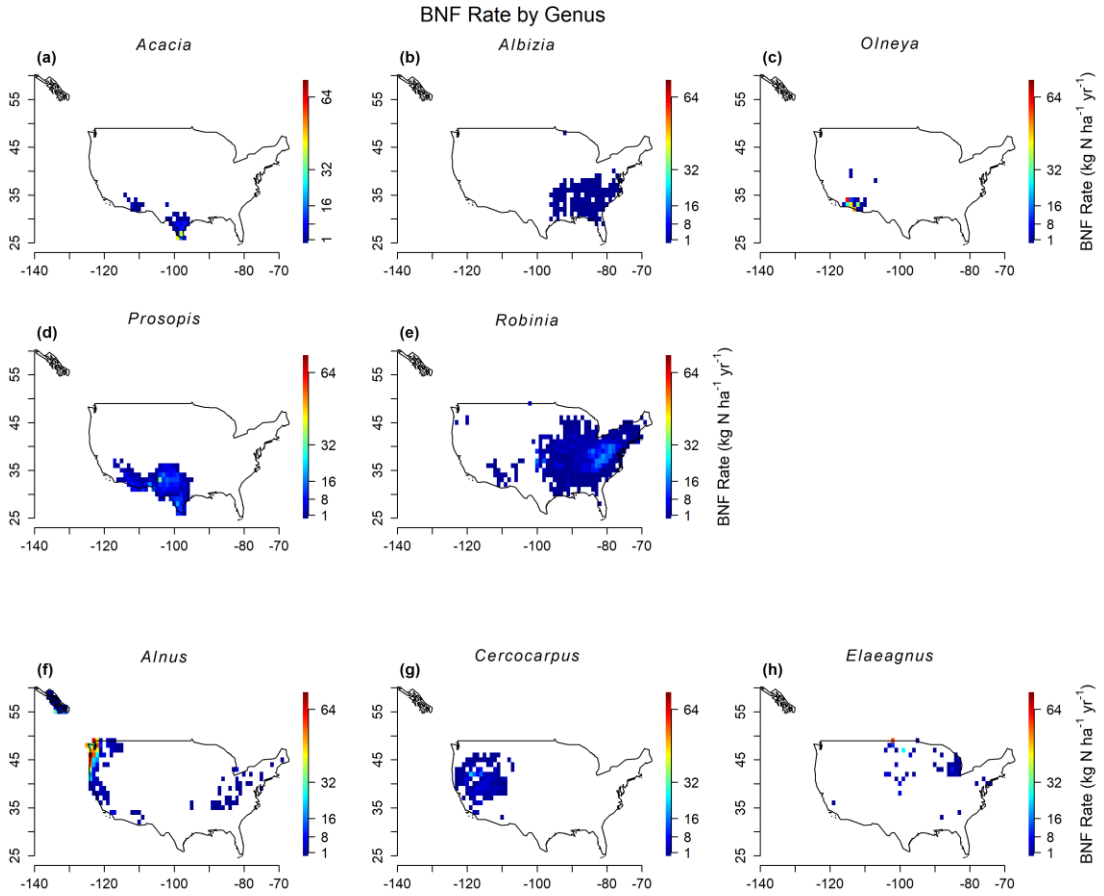

Figure S1. Nitrogen fixation by genus in kg N per hectare ground area per year. This integrates both the BNF rate and the abundance of forest. Panels a-e are for rhizobial N-fixers: a) *Acacia*, b) *Albizia*, c) *Olneya*, d) *Prosopis*, and e) *Robinia*. Panels f-i are for actinorhizal N-fixers: f) *Alnus*, g) *Cercocarpus*, and h) *Elaeagnus*.

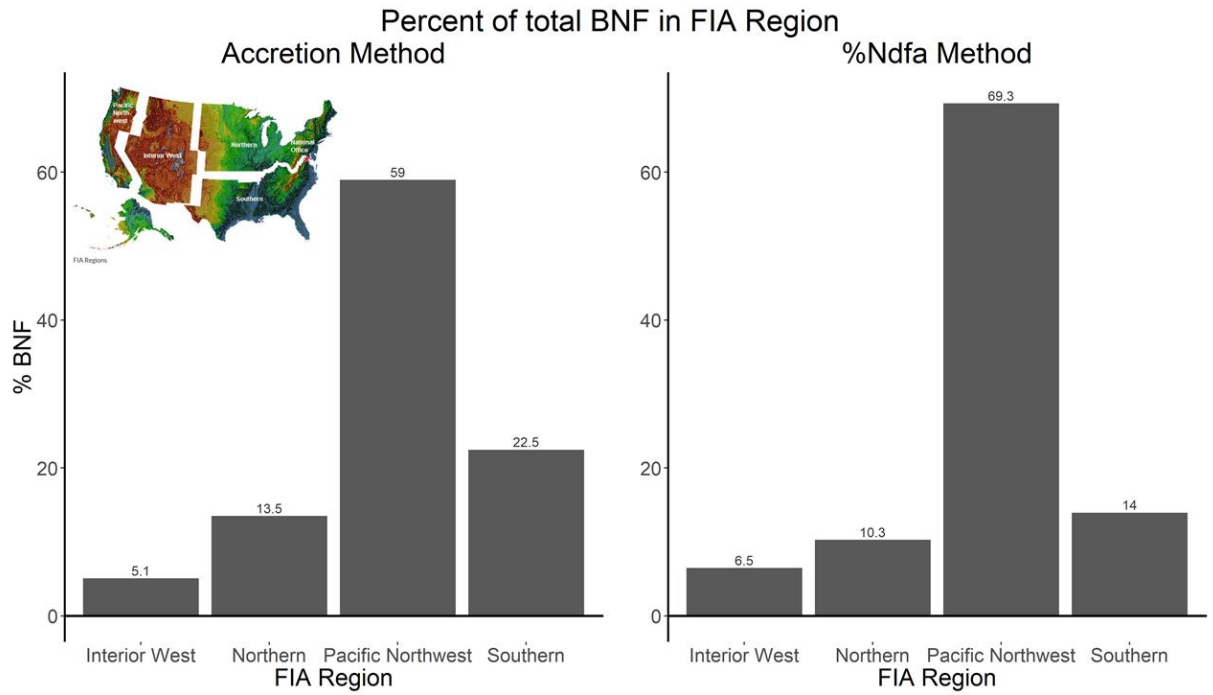

Figure S2. Tree BNF by region. The regions are defined by the FIA administrative regions and colors on the inset represent topography. Error bars were show the standard deviation of the analysis bootstrapped 1000 times at the continent scale.

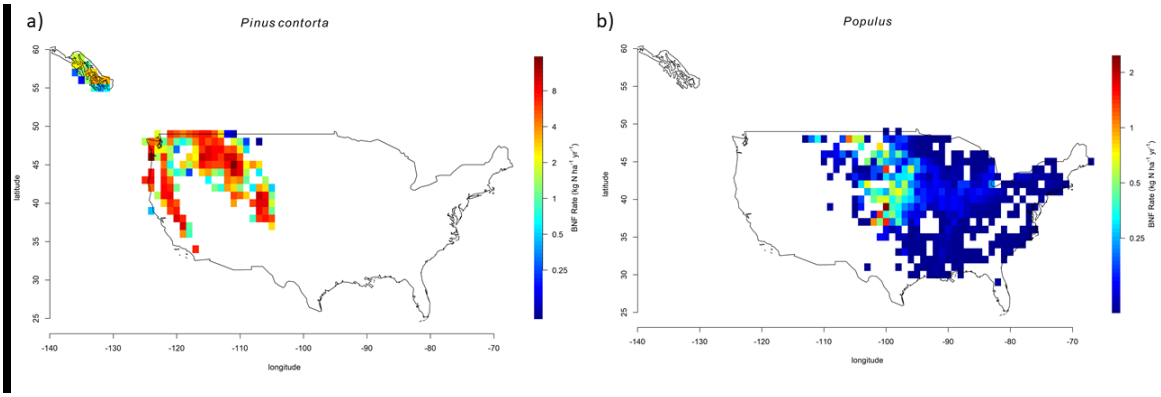

Figure S3. Nitrogen fixation by genus in kg N per hectare ground area per year for Pinus contorta (a) and Populus (b). This integrates both the BNF rate and the abundance of forest.

Table S1. Data sources for genus-specific fixation rate data sources (accretion & %Ndfa). Numbers refer to the citations in Text S2. The number range indicates the papers from the reference list above. The number in brackets represents the number of data points extracted from those papers (including several species, locations, ages, or aspects examined within the papers).

Genus	Accretion	$\%N_{dfa}$
Acacia	1 – 3 [6]	18-30 [45]
Albizia	--	31 [2]
Prosopis	4-6 [4]	32-37 [24]

Robinia	7 [3]	38-43 [11]
Alnus	8-17 [17]	44-49 [9]
Elaeagnus	--	50 [2]

Table S2. Data for %Ndfa method from the literature search.

Location	Genus	Species	Reference Plant	BNF Rate (%N_{dfa})	Treatment	Source
Pot/glasshouse	*Acacia*	*senegal*	Uninoculated *A. senegal*	39	High P	Isaac et al 2011
Pot/glasshouse	*Acacia*	*senegal*	Uninoculated *A. senegal*	33	High P	Isaac et al 2011
Zimbabwe	*Acacia*	*angustisima*	*Hyparrhenia*	48	Upper limit	Chikowo et al 2004
Zimbabwe	*Acacia*	*angustisima*	*Hyparrhenia*	79	Lower limit	Chikowo et al 2004
Dry, plantation	*Acacia*	*caven*	*Schinus polygamous*, *Fraxinus excelsior*	50		Aronson et al 2002
Subhumid, mixed plantation	*Acacia*	*mangium*	*Eucalyptus grandis*	59		Bouillet et al 2008
Humid, plantation	*Acacia*	*mangium*	*Eucalyptus urophylla*	42	Upper limit	Galiana et al 1998
Humid, plantation	*Acacia*	*mangium*	*Eucalyptus urophylla*	62	Lower limit, strain Aust 13c	Galiana et al 1998
Humid, improved fallow	*Acacia*	*mangium*	Understory *Chromolaena odorata*	57	Year 12	Mercado et al 2011
Dry, arabic gum production	*Acacia*	*senegal*	*Balanites aegyptiaca*	24	Upper limit	Raddad et al 2005
Dry, arabic gum production	*Acacia*	*senegal*	*Balanites aegyptiaca*	61	lower limit	Raddad et al 2005
France	*Acacia*	*senegal*	Uninoculated *A. senegal*	50	Lower limit	Isaac et al 2011
France	*Acacia*	*senegal*	Uninoculated *A. senegal*	72	Upper limit	Isaac et al 2011
glasshouse	*Acacia*	*senegal*	Uninoculated *A. senegal*	74	Low P	Isaac et al 2011
glasshouse	*Acacia*	*senegal*	Uninoculated *A. senegal*	67	Med P	Isaac et al 2011

glasshouse	*Acacia*	*senegal*	Uninoculated *A. senegal*	52	High P	Isaac et al 2011
Kenya	*Acacia*	*drepanolobium*	*Aerva*	55	Lower limit	Fox-Dobbs et al 2010
Kenya	*Acacia*	*drepanolobium*	*Aerva*	80	Upper limit	Fox-Dobbs et al 2010
Kenya	*Acacia*	*drepanolobium*	*Aerva*	40	Lower limit	Fox-Dobbs et al 2010
Kenya	*Acacia*	*drepanolobium*	*Aerva*	50	Upper limit	Fox-Dobbs et al 2010
Greenhouse	*Acacia*	*raddiana*	*P. biglobosa*	58.1	Ref species 1	Ndoye et al 1995
Greenhouse	*Acacia*	*raddiana*	*T. indica*	66.8	Ref species 2	Ndoye et al 1995
Greenhouse	*Acacia*	*senegal*	*P. biglobosa*	27.2	Ref species 1	Ndoye et al 1995
Greenhouse	*Acacia*	*senegal*	*T. indica*	41.6	Ref species 2	Ndoye et al 1995
Greenhouse	*Acacia*	*seyal*	*P. biglobosa*	59.7	Ref species 1	Ndoye et al 1995
Greenhouse	*Acacia*	*seyal*	*T. indica*	66.7	Ref species 2	Ndoye et al 1995
Greenhouse	*Acacia*	*albida*	*P. biglobosa*	30.4	Ref species 1	Ndoye et al 1995
Greenhouse	*Acacia*	*albida*	*T. indica*	44.2	Ref species 2	Ndoye et al 1995
S Africa, Hluhluwe	*Acacia*	*nilotica*	Non-nodulating *A. ataxacantha, A. schweinfurthii, A. brevispica*	17		Cramer et al 2010
S Africa, False Bay	*Acacia*	*nilotica*	Non-nodulating *A. ataxacantha, A. schweinfurthii, A. brevispica*	46		Cramer et al 2010
S Africa, Hluhluwe	*Acacia*	*tortilis*	Non-nodulating *A.*	8		Cramer et al 2010

			ataxacantha, A. schweinfurthii, A. brevispica			
S Africa, False Bay	*Acacia*	*tortilis*	Non-nodulating *A. ataxacantha, A. schweinfurthii, A. brevispica*	62		Cramer et al 2010
S Africa, Hluhluwe	*Acacia*	*nigrescens*	Non-nodulating *A. ataxacantha, A. schweinfurthii, A. brevispica*	-1		Cramer et al 2010
S Africa, False Bay	*Acacia*	*nigrescens*	Non-nodulating *A. ataxacantha, A. schweinfurthii, A. brevispica*	39		Cramer et al 2010
S Africa, Hluhluwe	*Acacia*	*karroo*	Non-nodulating *A. ataxacantha, A. schweinfurthii, A. brevispica*	23		Cramer et al 2010
S Africa, False Bay	*Acacia*	*karroo*	Non-nodulating *A. ataxacantha, A. schweinfurthii, A. brevispica*	52		Cramer et al 2010
Sudan	*Acacia*	*senegal*	*Balanites aegyptiaca*	24	Mazmoon provenance	Amin et al 2005
Sudan	*Acacia*	*senegal*	*Balanites aegyptiaca*	61	Rahad provenance	Amin et al 2005

Victoria, Australia	*Acacia*	*mearnsii*	*Eucalyptus globulus*	10	mixed stand (*Eucalyptus globulus*)	Forrester et al 2007
Victoria, Australia	*Acacia*	*mearnsii*	*Eucalyptus globulus*	63	pure stand	Forrester et al 2007
Brazil	*Acacia*	*mangium*	*Eucalypthus urophylla, Jacaranda coaia, Schyzolobium amazonicum*	91	^{15}N enriched	Paprcikova et al 2002
Brazil	*Acacia*	*mangium*	*Eucalypthus urophylla, Jacaranda coaia, Schyzolobium amazonicum*	47	Natural abundance method	Paprcikova et al 2002
Brazil	*Acacia*	*angustissima*	*Eucalypthus urophylla, Jacaranda coaia, Schyzolobium amazonicum*	72	^{15}N enriched	Paprcikova et al 2002
Brazil	*Acacia*	*angustissima*	*Eucalypthus urophylla, Jacaranda coaia, Schyzolobium amazonicum*	86	Natural abundance method	Paprcikova et al 2002
Chile	*Acacia*	*caven*	*Fraxinus excelsior, Schinus polygamus*	84.375		Ovalle et al 1996
Nigeria	*Albizia*	*lebbeck*	*Senna siamea*	74	Lower limit	Kadiata et all 1997
Nigeria	*Albizia*	*lebbeck*	*Senna siamea*	83	Upper limit	Kadiata et all 1997
Wales, UK	*Alnus*	*glutinosa*	*Betula*	60.5		Hoosbeek et al 2011
Quebec	*Alnus*	*glutinosa*	Black Alder	68		Cote & Camire 1984
France	*Alnus*	*glutinosa*	*Acer pseudoplatanus*	97		Domenach et al 1989

France	*Alnus*	*incana*	*Acer pseudoplatanus*	75		Domenach et al 1989
New York	*Alnus*	*incana*	*Betula alleghaniensis*	86		Hurd 2001
pot	*Alnus*	*incana*	air	8	High N	Ekblad & Huss-Danell 1995
pot	*Alnus*	*incana*	air	46	Low P	Ekblad & Huss-Danell 1995
pot	*Alnus*	*incana*	air	90	High P, low N	Ekblad & Huss-Danell 1995
Bangor, UK	*Alnus*	*glutinosa*	*Betula pendula, Fraxinus sylvatica*	62	mixture	Millett et al 2012
Bangor, UK	*Alnus*	*glutinosa*	*Betula pendula, Fraxinus sylvatica*	61	monoculture	Millett et al 2012
Spillimacheen, BC, Canada	*Alnus*	*sinuata*	Understory *Salix, Spirea betulifolia, Epilobium angustifolium, Cornus canadensis*	96		Mead & Preston 1992
pot	*Alnus*	*glutinosa*		70	grown with *Populus nigra*	Kuradli et al 1990
pot	*Alnus*	*glutinosa*		43	monoculture	Kuradli et al 1990
Uzbekistan	*Elaeagnus*	*angustifolia*	*Gleditsia triacanthos*	68	Ref species 1	Khamzina et al 2010
Uzbekistan	*Elaeagnus*	*angustifolia*	*Ulmus pumila*	79	Ref species 2	Khamzina et al 2010
Salton Sea, CA	*Prosopis*	*glandulosa*		50		Rundel et al 1982

Texas	*Prosopis*	*glandulosa*	*Dyospiros texana*	69.4	Ref species 1	Villagra & Felker 1996
Texas	*Prosopis*	*glandulosa*	*Celtis pallidae*	64.7	Ref species 2	Villagra & Felker 1996
Texas	*Prosopis*	*glandulosa*	*Zanthoxylum fagara*	48.2	Ref species 3	Villagra & Felker 1996
Texas	*Prosopis*	*glandulosa*	*Setaria beneath*	59.4	Ref species 4	Villagra & Felker 1996
Texas	*Prosopis*	*glandulosa*	*Setaria open*	72.7	Ref species 5	Villagra & Felker 1996
Harper's well	*Prosopis*		*Larrea tridentate, Tamarix pentandra, Atriplex polycarpa, Haplopappus acradenius*	43	Site 1	Shearer 1983
Harper's Well	*Prosopis*		*Larrea tridentate, Tamarix pentandra, Atriplex polycarpa, Haplopappus acradenius*	61	Ste 2	Shearer 1983
Borrego Sink	*Prosopis*		*Suaeda torryana, Atriplex polycarpa, Allenrolfia occidentalis, Happlopappus acradenius*	60	Site 3	Shearer 1983
Carrizo Badlands	*Prosopis*		*Larrea tridentate, Atriplex polycarpa*	57	Site 4	Shearer 1983
Clark Dry Lake	*Prosopis*		*Tamarix pentandra, Encelia*	58	Site 5	Shearer 1983

			farinose, Suaeda torreyana, Atriplex polycarpa			
	Prosopis	*alba*	*Schinus polyganus*	10	plantation, 6 yrs	Aronson et al 2002
	Prosopis	*chilensis*	*Schinus polyganus*	30	plantation, 6 yrs	Aronson et al 2002
Chile	*Prosopis*	*alba*	*Schinus polygamous, Fraxinus excelsior*	42.86		Ovalle et al 1996
Chile	*Prosopis*	*chilensis*	*Schinus polygamous, Fraxinus excelsior*	23.53		Ovalle et al 1996
Chile	*Prosopis*	*chilensis*	*Schinus polygamous, Fraxinus excelsior*	31.8	1992	Ovalle et al 1998
Chile	*Prosopis*	*chilensis*	*Schinus polygamous, Fraxinus excelsior*	69.7	1993	Ovalle et al 1998
Chile	*Prosopis*	*chilensis*	*Schinus polygamous, Fraxinus excelsior*	28	1994	Ovalle et al 1998
Chile	*Prosopis*	*chilensis*	*Schinus polygamous, Fraxinus excelsior*	16	1995	Ovalle et al 1998
Chile	*Prosopis*	*chilensis*	*Schinus polygamous, Fraxinus excelsior*	16.8	1996	Ovalle et al 1998
Chile	*Prosopis*	*alba*	*Schinus polygamous, Fraxinus excelsior*	25.8	1992	Ovalle et al 1998
Chile	*Prosopis*	*alba*	*Schinus polygamous, Fraxinus excelsior*	52.4	1993	Ovalle et al 1998

Chile	*Prosopis*	*alba*	*Schinus polygamous, Fraxinus excelsior*	19	1994	Ovalle et al 1998
Chile	*Prosopis*	*alba*	*Schinus polygamous, Fraxinus excelsior*	7.8	1995	Ovalle et al 1998
Chile	*Prosopis*	*alba*	*Schinus polygamous, Fraxinus excelsior*	1.25	1996	Ovalle et al 1998
Austria	*Robinia*	*pseudoacacia*	*Ligustrum vulgaris, Syringa vulgare*	65	Year 1	Danso et al 1995
Austria	*Robinia*	*pseudoacacia*	*Ligustrum vulgaris, Syringa vulgare*	90	Year 2	Danso et al 1995
France	*Robinia*	*pseudoacacia*	*Populus euramericana*	76	23 months	Marron et al 2018
France	*Robinia*	*pseudoacacia*	*Populus euramericana*	67	28 months	Marron et al 2018
France	*Robinia*	*pseudoacacia*	*Populus euramericana*	59	40 months	Marron et al 2018
France	*Robinia*	*pseudoacacia*	*Populus euramericana*	71	52 months	Marron et al 2018
Welzow-Sud, Germany	*Robinia*	*pseudoacacia*	Soil	91	High water	Montovani et al 2015
Welzow-Sud, Germany	*Robinia*	*pseudoacacia*	Soil	83	Low water	Montovani et al 2015
Welzow-Sud, Germany	*Robinia*	*pseudoacacia*	Soil	76	High water - drought cycle	Montovani et al 2015
Welzow-Sud, Germany	*Robinia*	*pseudoacacia*	Soil	87	Low water - drought cycle	Montovani et al 2015
pots	*Robinia*	*pseudoacacia*		0	seeds from Semnan	Moshki & Lamersdorf 2011
pots	*Robinia*	*pseudoacacia*		39.89	seeds from Sanandaj	Moshki & Lamersdorf 2011

pots	*Robinia*	*pseudoacacia*		50.81	seeds from Karaj	Moshki & Lamersdorf 2011
pots	*Robinia*	*pseudoacacia*		44.59	seeds from Hosszupalyi	Moshki & Lamersdorf 2011
Germany	*Robinia*	*pseudoacacia*		73	midrange	Veste et al 2012
Uzbekistan	*Robinia*	*pseudoacacia*	*Gleditsia triacanthos*	82		Djumaeva 2011

Table S3. Data for the accretion method from the literature search.

Location	***Genus***	**Species**	**BA (m^2 ha^{-1})**	**BNF Rate (kg N ha^{-1} yr^{-1})**	**Treatment**	**Source**
W. Oregon	*Alnus*	*rubra*	35.8	320	Pure alder	Newton 1968
Hoh River, WA	*Alnus*	*rubra*	19.8	164	0-14 years	Luken & Fonda 1983
Hoh River, WA	*Alnus*	*rubra*	34.2	58	15-24 years	Luken & Fonda 1983
Hoh River, WA	*Alnus*	*rubra*	44.2	25	25-65 years	Luken & Fonda 1983
Lady Island, WA	*Alnus*	*rubra*	2.3	80	Pure alder	DeBell & Rodwan 1979
Mt. Benson, BC	*Alnus*	*rubra*	16.5	65		Binkley 1983
Skykomis, WA	*Alnus*	*rubra*	9.9	42		Binkley 1983
Scotland, UK	*Alnus*	*rubra*	10.29	36		Malcolm 1985
Toutle River, WA	*Alnus*	*rubra*	8.39	56		Heilman 1990
Lady Island, WA	*Alnus*	*rubra*	2.3	32	Mixed stand	DeBell & Radwan 1979
AK boreal	*Alnus*	*incana*	15.4	361.6	5 years	Van Cleve 1971
AK boreal	*Alnus*	*incana*	14.78	74.6	15 years	Van Cleve 1971

AK boreal	*Alnus*	*incana*	28.9	114.8	20 years	Van Cleve 1971
Montreal Island	*Alnus*	*rugosa*	10	168		Daly 1966
Cascade Head, OR	*Alnus*	*rubra*	35	73		Binkley 1992
Wind River, WA	*Alnus*	*rubra*	19.5	54		Binkley 1992
Wind River, WA	*Alnus*	*rubra*	35	40.3		Tarrant & Miller 1963
Senegal	*Acacia*	*senegal*	8.72	5.25		Deans 1999
Pointe Noire, Congo	*Acacia*	*auriculiformis*	16.8	140		Bernhard-Reversat 1996
Pointe Noire, Congo	*Acacia*	*mangium*	16.8	115		Bernhard-Reversat 1996
Victoria, Australia	*Acacia*	*mearnsii*	9.7	38	Mixed stand	Forrester 2007
Victoria, Australia	*Acacia*	*mearnsii*	14	86	Pure stand	Forrester 2007
Zimbabwe	*Acacia*	*angustissima*	2.50	61		Chikowo 2004
N. Carolina, USA	*Robinia*	*pseudoacacia*	8.2	48	Year 4	Boring and Swank 1984
N. Carolina USA	*Robinia*	*pseudoacacia*	32.1	75	Year 17	Boring and Swank 1984
N. Carolina, USA	*Robinia*	*pseudoacacia*	52.1	33	Year 38	Boring and Swank 1984
California	*Prosopis*	*glandulosa*	9.64	30		Rundel 1982
Texas	*Prosopis*	*glandulosa*	3.37	9.2		Soper 2016

Table S4. Data for N-fixing tree genera in the FIA database including the number of stems in the database, the total N fixed by each genus as determined by the accretion method and N demand method.

Genus	**Fixer type**	**# stems in FIA (saplings & mature trees)**	**Total N fixed Accretion method**	**Total N fixed**

			(Tg N yr^{-1}) [SE]	**N demand method (Gg N yr^{-1}) [SE]**
Acacia	Rhizobial	1,439	0.005 [0.001]	0.684 [0.010]
Albizia	Rhizobial	1,582	0.024 [0.004]	1.290 [0.056]
Alnus	Actinorhizal	18,396	0.184 [0.002]	97.036 [3.342]
Cercocarpus	Actinorhizal	18,326	0.020 [0.008]	18.257 [0.212]
Elaeagnus	Actinorhizal	2,298	0.011 [0.001]	0.610 [0.030]
Olneya	Rhizobial	254	0.004 [0.0001]	0.267 [0.003]
Prosopis	Rhizobial	34,772	0.031 [0.001]	18.201 [0.430]
Robinia	Rhizobial	50,982	0.548 [0.002]	167.834 [2.896]

Table S5. Data for species that are represented in the FIA database for each genus.

Genus	**Species present in FIA**
Acacia	*farnesiana, spp*
Albizia	*julibrissin*
Alnus	*rubra, rhombifolia, oblongifolia, glutinosa*
Cercocarpus	*ledifolius*
Elaeagnus	*angustifolia*
Olneya	*tesota*
Prosopis	*velutina, glandulosa, pubescens, spp*
Robinia	*pseudoacacia, neomexicana*

Appendix B – Supplementary Information for Chapter 2

SI Text 1. NCI & NCI weighting

To account for the fact that trees in denser stands experience greater competition regardless of their neighbors' identities, we isolated the impact of N-fixers by comparing individual-scale demographic rates as functions of the proportion of neighborhood crowding index (NCI) from N-fixing trees. NCI is the sum of the competitive effects of all trees within a specified radius (here, 7.3 m), which incorporates the spatial distribution of trees within a plot (Canham et al. 2004). To investigate the impact of crowding from N-fixing trees compared to non-fixing trees, we calculated the fraction of total NCI from N-fixers following Taylor et al. (2017) and Canham et al. (2006) as shown in equation SI-1.

$$NCI_{prop-i} = \frac{NCI_{fixers}}{NCI_{total}} = \frac{\sum_{j=1}^{n} \frac{DBH_{j-fixers}^2}{d_{i,j-fixers}^2}}{\sum_{j=1}^{n} \frac{DBH_{j-total}^2}{d_{i,j-total}^2}} \quad \textbf{(SI-1)}$$

where *i* is the focal individual and the *j*s are the other individuals in the plot.

Since the calculation of NCI is based on a fixed radius neighborhood (7.3 m) but the FIA subplots are 7.3 m radius in total, NCI values were weighted based on the fraction of the neighborhood that was sampled. The weighting parameter was calculated as the area of neighborhood sampled divided by the area of a complete neighborhood. The area of neighborhood sampled was calculated as the intersection of the subplot with the complete radius

around a given tree: $a_{neighborhood} = 2r^2 cos^{-1}\left(\frac{d}{2r}\right) - 0.5d\sqrt{-d^2 + 4r^2}$ where *d* is the distance between the focal tree and plot center and *r* is the neighborhood radius (7.3 m).

SI Text 2. Model details

The percent of basal area comprised of N-fixing trees (BA_{pct}) is used as the measure of the relative prevalence of N-fixing trees in the plot-scale analysis:

$$BA_{pct} = \frac{\sum BA_{N-fixers}}{\sum BA_{N-fixers} + \sum BA_{non-fixers}} \quad \textbf{(SI-2)}$$

where $\sum BA_{N\text{-}fixers}$ is the total basal area ($BA = \pi\left(\frac{DBH}{2}\right)^2$) of N-fixing trees in the plot and $\sum BA_{non\text{-}fixers}$ is the total basal area of non-fixing trees in the plot.

At the plot scale, basal area increment (*BAI*), which is the annual change in total basal area of trees in the plot was examined as a response variable:

$$BAI = \frac{\sum_{i=1}^{n_2} BA_i - \sum_{j=1}^{n_1} BA_j}{\Delta t} \quad \textbf{(SI-3)}$$

where *i* is each tree in the plot at the second census, *j* is each tree in the plot at the first census, n_1 is the total number of trees in the plot at the first census, n_2 is the total number of trees in the plot at the second census, and Δt is the interval between census dates.

Plot-scale recruitment rate (*R*) was examined as a response variable:

$$R = \frac{recruits_{t2}}{n_1 * \Delta t} \quad \textbf{(SI-4)}$$

where $recruits_{t2}$ is the number of trees recorded in the second census that were not recorded in the first census.

Plot-scale survival rate (*S*) was examined as a response variable:

$$S = \frac{survivors_{t2}}{n_1 * \Delta t} \quad \textbf{(SI-5)}$$

where $survivors_{t2}$ is the number of trees recorded in both the first and second censuses.

To assess the effects of N-fixing trees on plot-level basal area increment, we calculated the basal area of the plot for two FIA census points and divided by the census interval. Individual tree basal area was calculated from measured diameters, assuming circular stems, then summed to get plot-level basal area. Similar to the individual-scale method, apparent negative changes in tree *DBH* were positivized. We used a linear mixed-effect model to investigate the effect of N-fixing trees on plot-level basal area increment, including fixed effects for the percent of basal area from N-fixing trees (BA_{pct}) and the total basal area in the first census interval (BA_{total}), as well as a random effect for state to account for climatic or vegetation differences among regions. In the linear mixed-effect models, *BAI*, *R* and *S* were modeled as a normally distributed response variable:

$$BAI = \mu_s + \beta_1 BA_{pct} + \beta_2 BA_{total} + \varepsilon \quad \textbf{(SI-6)}$$

$$R = \mu_s + \beta_1 BA_{pct} + \beta_2 BA_{total} + \varepsilon \quad \textbf{(SI-7)}$$

$$S = \mu_s + \beta_1 BA_{pct} + \beta_2 BA_{total} + \varepsilon \quad \textbf{(SI-8)}$$

where μ_s is the state-specific intercept, β_1 through β_4 are the regression coefficients, BA_{total} is the total basal area at the first census point, and ε is the normally distributed residual error.

The plot-scale N-fixer effect on each response variable was calculated as $100 * \left(\frac{metric_{100\%\, BA_{pct}} - metric_{0\%\, BA_{pct}}}{metric_{0\%\, BA_{pct}}}\right)$ where $metric_{100\%\, BA_{pct}}$ is the value of the response variable predicted by the linear mixed-effect model at $BA_{pct} = 100$ and $metric_{0\%\, BA_{pct}}$ is the value of the response variable predicted by the linear mixed-effect model at $BA_{pct} = 0$.

At the individual scale, the relative growth rate (*RGR*) was examined as a response variable:

$$RGR_i = \frac{\ln(DBH_{i,t2}) - \ln(DBH_{i,t1})}{\Delta t} \quad \textbf{(SI-9)}$$

where *i* is the focal tree, $DBH_{i,t2}$ is the *DBH* of the focal tree at the second census, and $DBH_{i,t1}$ is the *DBH* of the focal tree at the first census. Apparent negative relative growth rates were positivized because we assumed that measurement error was a greater source of negative growth rate measurements than actual tree shrinkage. Positivized growth for an individual tree was $DBH_{j+1} = \frac{Minimum\ Detection\ Limit}{2} + DBH_j$ where the minimum detection limit was 0.05 cm following Condit *et al.* (2006). Individual-scale recruitment rate (*r*) and survival rate (*s*) were also examined as response variables. Recruitment, *r*, is 1 if a tree that was not recorded in the first census is recorded in the second census. Survival, *s*, is 1 if a tree that was recorded in the first census is also recorded in the second census.

In the linear mixed-effect model, RGR_i was modeled as a normally distributed response variable, and *r* and *s* were modelled as binomially distributed response variables. Model selection was done on the set of possibly relevant terms including *NCI*, NCI^2, NCI_{prop}, *DBH*, and the interaction between *NCI* and NCI_{prop} (SI Table 2). According to model selection, the best model (and therefore the one we used) for relative growth rate had fixed effects for the proportion of NCI from N-fixing trees, the DBH of the focal tree, and the NCI^2, as well as a random effect for the plot ID:

$$RGR_i = \mu_p + \beta_1 NCI_{prop-i} + \beta_2 NCI_{total-i} + \beta_3 NCI_{total-i}^2 + \beta_4 DBH_i + \beta_5 NCI_{total-i} * DBH_i + \beta_6 DBH_i * NCI_{prop-i} + \varepsilon \quad \textbf{(SI-10)}$$

$$r_i \sim \mu_p + \beta_1 NCI_{prop-i} + \beta_2 NCI_{total-i} + \beta_3 NCI_{total-i}^2 + \beta_4 DBH_i + \beta_5 NCI_{total-i} * NCI_{prop-i} + \varepsilon \quad \textbf{(SI-11)}$$

$$s_i \sim \mu_p + \beta_1 NCI_{prop-i} + \beta_2 NCI_{total-i} + \beta_3 NCI_{total-i}^2 + \beta_4 DBH_i + \beta_5 NCI_{total-i} * DBH_i + \beta_5 NCI_{total-i} * NCI_{prop-i} + \varepsilon \quad \textbf{(SI-12)}$$

where μ_p is the plot-specific intercept. The random effect for plot ID accounts for variation in climate and vegetation dynamics across the continental US. The coefficient for NCI_{prop} (the proportion of crowding that comes from N-fixers) addresses our primary question. A positive coefficient would indicate that N-fixers enhance or weakly inhibit neighboring tree growth, whereas a negative coefficient would indicate that N-fixers inhibit neighboring tree growth.

The individual-scale N-fixer effect on each response variable was calculated as $100 * \left(\frac{demographic\ rate_{100\%\ NCI_{prop-i}} - demographic\ rate_{0\%\ NCI_{prop-i}}}{demographic\ rate_{0\%\ NCI_{prop-i}}}\right)$ where $demographic\ rate_{100\%\ NCI_{prop-i}}$ is the value of the response variable predicted by the linear mixed-effect model at $NCI_{prop-i} = 100$ and $demographic\ rate_{0\%\ NCI_{prop-i}}$ is the value of the response variable predicted by the linear mixed-effect model at $NCI_{prop-i} = 0$.

After running the statistical models for each of the individual-level and plot-level metrics, we calculated the N-fixer effect for each metric. The N-fixer effect was calculated as the expected percent change in a demographic rate or basal area increment between a plot that contained only N-fixing trees and a plot that contained only non-fixing trees. Equation SI-9 shows the general model fit for any of the plot-level metrics, with parameters for the intercept (β_0), the percent basal area comprised of N-fixers (β_1), and the total basal area of trees in the plot (β_2). To get the estimated demographic rate (y) for either 100% or 0% of basal area comprised of N-fixers ($y_{all\ N\text{-}fixers}$ or $y_{all\ non\text{-}fixers}$, respectively), we plugged in 1 (Equation SI-10) or 0 (Equation SI-15) for the fraction of basal area comprised of N-fixers. We also plugged in the average BA_{total} of all plots to express the effect for an average plot. (Analogously, for individual-level metrics

we used the averages of NCI and DBH to express NFEs for average-sized trees with average crowding.)

$$y = \beta_0 + \beta_1 * BA_{pct} + \beta_2 * BA_{total} \quad \textbf{(SI-13)}$$

$$y_{all\ N-fixers} = BAI_{100\%\ BA_{pct-i}} = \beta_0 + \beta_1 * 1 + \beta_2 * \overline{BA_{total}} \quad \textbf{(SI-14)}$$

$$y_{all\ non-fixers} = BAI_{0\%\ BA_{pct-i}} = \beta_0 + \beta_1 * 0 + \beta_2 * \overline{BA_{total}} \quad \textbf{(SI-15)}$$

$$BAI_{NFE} = 100 * \left(\frac{BAI_{100\%\ BA_{pct-i}} - BAI_{0\%\ BA_{pct-i}}}{BAI_{0\%\ BA_{pct-i}}}\right) = 100 * \left(\frac{\beta_1}{\beta_0 + \beta_2 * \overline{BA_{total}}}\right) \quad \textbf{(SI-16)}$$

The expected effect for BAI_n (the basal area increment of non-fixers) for a plot with all N-fixers is unintuitive. Even though it is not biologically possible to have 100% basal area comprised on N-fixers when looking at the basal area increment on non-fixers (because there would not be any non-fixers in the plot), we still used this comparison from the statistical fit to enable comparison of the NFE on other demographic rates.

When we used the statistical model to evaluate whether abiotic conditions or biotic traits could drive the NFE we modified the model to include an interaction between NCI_{prop} and the trait of interest. For example, when evaluating whether mycorrhizal association (MR_{type}) was a possible driver of RGR_{NFE} we modified the model:

$$RGR \sim NCI_{prop} + NCI + DBH + NCI^2 + NCI * DBH + NCI_{prop} * DBH + NCI_{prop} * MR_{type} + (1|plot\ ID) + \varepsilon \quad \textbf{(SI-17)}$$

When mycorrhizal type was AM then MR_{type} = 1 and when mycorrhizal type was EM then MR_{type} = 0. To get the estimated demographic rate (*RGR*) for either AM or EM, we plugged in 1 or 0 (Equation SI-13) for the MR_{type}. We also plugged in the average covariate value for other parameters to express the effect for an average tree. To obtain the NFE for each mycorrhizal type

we followed the same method described above (and SI-12) with NCI_{prop} = 0% and NCI_{prop} = 100%.

SI Text 3. Deciduous vs evergreen data sources

Categorization of species as deciduous or evergreen was assigned based on a compilation of 12 databases. For species that did not occur in any of the 13 databases, the species habit was assigned based on the majority or other species in the genus. When sources disagreed on a species it was categorized as deciduous. The 12 databases were:

FEIS Fire database	Abrahamson, I. (2019). Fire Effects Information System (FEIS). Retrieved from https://www.feis-crs.org/feis/
UFL plants database	Florida, U. of. (2018). Tree fact sheets. Retrieved from http://hort.ufl.edu/database/trees/trees_scientific.shtml
USDA plants fact sheet	USDA, N. (2019). The PLANTS Database. Greensboro, NC USA: National Plant Data Team. Retrieved from http://plants.usda.gov
Oregon State plants database	Breen, P. (2019). Landscape plants. Retrieved from https://landscapeplants.oregonstate.edu/species
International Oak Society	Cameron, R. (2018). Species spotlight: *Quercus rugosa*. Retrieved from https://www.internationaloaksociety.org/content/species-spotlight-quercus-rugosa-née-0
TAMU	Texas A & M System. (2019). Virtual herbarium. Retrieved April 2019, from https://rangeplants.tamu.edu/scientific-name-index/
Cal Poly select tree	SelecTree. (1995-2019). Tree Record. Retrieved April 2019, from https://selectree.calpoly.edu/tree-detail/
UCONN plants database	Brand, M. (2019). University of Connecticut Plant Database. Storrs, CT: Department of Plant Science and Landscape Architecture. Retrieved from http://hort.uconn.edu/plants
Cornell Woody plants	Cornell University. (2019). Woody plants database. Retrieved from http://woodyplants.cals.cornell.edu/plant/
CA Martin plants	Martin, C. A. (2019). Virtual library of Phoenix landscape plants. Retrieved from http://www.public.asu.edu/~camartin/Martin landscape plant library.htm
Wildflower database	Lady Bird Johnson Wildflower Center (2019). Native plants database. Retrieved from https://www.wildflower.org/plants/
Missouri Plant Finder	Missouri Botanical Garden. (2019). Plant finder. Retrieved from http://www.missouribotanicalgarden.org/PlantFinder/PlantFinderSearch.aspx

SI Table 1. Frequency of each taxon

Species	**n**
Albizia julibrissin	87
Alnus glutinosa	23
Alnus oblongifolia	8
Alnus rubra	126
Cercocarpus ledifolius	718

Elaeagnus angustifolia	33
Prosopis glandulosa	23
Prosopis pubescens	2
Prosopis velutina	222
Robinia pseudoacacia	7050

SI Table 2. Model Selection ΔAIC_cs**.** Table shows different fixed effect formulations. All individual-scale models included a random effect for plot ID to account for geographic and climatic differences among plots. All plot-scale models included a random effect for state to account for geographic and climatic differences among regions. ΔAIC_c values were calculated as the difference between models using the $AIC_c()$ command (stats package, R Core Team, 2017) from the full model.

Model	**ΔAIC_c**
Plot Scale	
$BAI \sim BA_{pct} + BA_{total}$	0
$BAI \sim BA_{pct}$	3534
$BAI_n \sim BA_{pct} + BA_{total}$	0
$BAI_n \sim BA_{pct}$	3510
$Survival \sim BA_{pct} + BA_{total}$	0
$Survival \sim BA_{pct}$	351
$Recruitment \sim BA_{pct} + BA_{total}$	0
$Recruitment \sim BA_{pct}$	468
Individual Scale	
$RGR \sim NCI_{prop} + NCI + NCI^2 + DBH + NCI*NCI_{prop} + NCI*DBH$	0
$RGR \sim NCI_{prop} + NCI + NCI^2 + DBH + NCI*NCI_{prop}$	19
$RGR \sim NCI_{prop} + NCI + NCI^2 + DBH + NCI*DBH$	0
$RGR \sim NCI_{prop} + NCI + NCI^2 + DBH$	17
$RGR \sim NCI_{prop} + DBH$	21
$RGR \sim NCI_{prop} + NCI + NCI^2$	85276
$RGR \sim NCI_{prop} + NCI + DBH$	17
$Recruitment \sim NCI_{prop} + NCI + NCI^2 + DBH + NCI*NCI_{prop} + NCI*DBH$	1
$Recruitment \sim NCI_{prop} + NCI + NCI^2 + DBH + NCI*NCI_{prop}$	0
$Recruitment \sim NCI_{prop} + NCI + NCI^2 + DBH + NCI*DBH$	263
$Recruitment \sim NCI_{prop} + NCI + NCI^2 + DBH$	262
$Recruitment \sim NCI + NCI^2 + DBH$	282
$Recruitment \sim NCI_{prop} + DBH$	270
$Recruitment \sim NCI_{prop} + NCI + NCI^2$	113626
$Recruitment \sim NCI_{prop} + NCI + DBH$	262
$Survival \sim NCI_{prop} + NCI + NCI^2 + DBH + NCI*NCI_{prop} + NCI*DBH$	0
$Survival \sim NCI_{prop} + NCI + NCI^2 + DBH + NCI*NCI_{prop}$	248
$Survival \sim NCI_{prop} + NCI + NCI^2 + DBH + NCI*DBH$	2
$Survival \sim NCI_{prop} + NCI + NCI^2 + DBH$	251
$Survival \sim NCI + NCI^2 + DBH$	249
$Survival \sim NCI_{prop} + DBH$	439
$Survival \sim NCI_{prop} + NCI + NCI^2$	586
$Survival \sim NCI_{prop} + NCI + DBH$	251

Note: we selected the model with the lowest ΔAIC_c that included either NCI_{prop} or BA_{pct} (for individual-scale and plot-scale respectively).

SI Table 3. Model parameters and fit (results for β_1) where significant parameters are in bold.

Response Variable (plot scale)	**Parameters**	**Parameter estimates**	**95% CI**	**Marginal** R^2_{GLMM}	**Conditional** R^2_{GLMM}
BAI	BA pct	0.04253	(-0.440217, 0.525294)	0.0352	0.5282
	BA total	**-0.00085**	(-0.000887, -0.000832)		
BAI_n	BA pct	**0.495886**	(0.013382, 0.978391)	0.0640	0.1471
	BA total	**-0.000856**	(-0.000884, -0.000828)		
Recruitment	BA pct	**0.0290**	(0.010117, 0.047884)	0.0073	0.2995
	BA total	**-0.000012**	(-0.000013, -0.000011)		
Survival	BA pct	**-0.013148**	(-0.024977, -0.001318)	0.0009	0.8781
	BA total	**0.000006**	(0.000006, 0.000007)		

Response Variable (individual scale)	**Parameters**	**Parameter estimates**	**95% CI**	**Marginal** R^2_{GLMM}	**Conditional** R^2_{GLMM}
RGR	NCI prop	-0.000253	(-0.00089, 0.00038)	0.0272	0.5870
	NCI	7.595e-7	(-0.000001, 0.000002)		
	DBH	**-0.00040**	(-0.00040, -0.00040)		
Recruitment	NCI prop	**0.00025**	(0.00011, 0.00039)	0.0403	0.2634
	NCI	**0.00079**	(0.00068, 0.00091)		
	DBH	**-0.01891**	(-0.01903, -0.01879)		
Survival	NCI prop	-0.00010	(-0.00023, 0.000016)	0.00014	0.5949
	NCI	**-0.00095**	(-0.00105, -0.00084)		
	DBH	**0.00075**	(0.00065, 0.00085)		

SI Table 4. P-values for Moran's I test for spatial autocorrelation

Demographic rate	p-value
Plot scale	
BAI	0.4427
BAI_n	0.5227
Recruitment	0.8264
Survival	0.5824
Individual scale	
RGR	0.5459
Recruitment	0.8408
Survival	0.8368

SI Table 5. P-values for differences among groups

Scale	Demographic rate	Group	p-value	Significant
Plot	BAI	N Deposition	**0.0273**	*
		Age	0.5168	NS
		Soil moisture	**0.0341**	*
Plot	BAI_n	N Deposition	**0.0273**	*
		Age	0.5168	NS
		Soil moisture	**0.0341**	*
Plot	Recruitment	N deposition	0.7034	NS
		Age	0.7659	NS
		Soil moisture	**0.0202**	*
Plot	Survival	N deposition	**0.0120**	*
		Age	0.3477	NS
		Soil moisture	**0.0296**	*
Individual	RGR	Fixer vs. non-fixer	**1.0e-8**	***
		Canopy position	**<2.2e-16**	****
		Deciduousness	**4.1e-7**	****
		Foliar C:N	**<2.2e-16**	***
		Mycorrhizae (AM to EM)	0.5365	NS
Individual	Recruitment	Fixer vs. non-fixer	0.5787	NS
		Canopy position	**7.78e-6**	***
		Deciduousness	0.9567	NS
		Foliar C:N	**0.0027**	**
		Mycorrhizae (AM to EM)	0.2914	NS
Individual	Survival	Fixer vs. non-fixer	0.1798	NS
		Canopy position	0.5235	NS
		Deciduousness	**2.55e-9**	***
		Foliar C:N	**0.0060**	**
		Mycorrhizae (AM to EM)	**0.0066**	**

Where * indicates $p < 0.05$, ** $p < 0.01$, *** $p < 0.001$

SI Table 6. Covariation

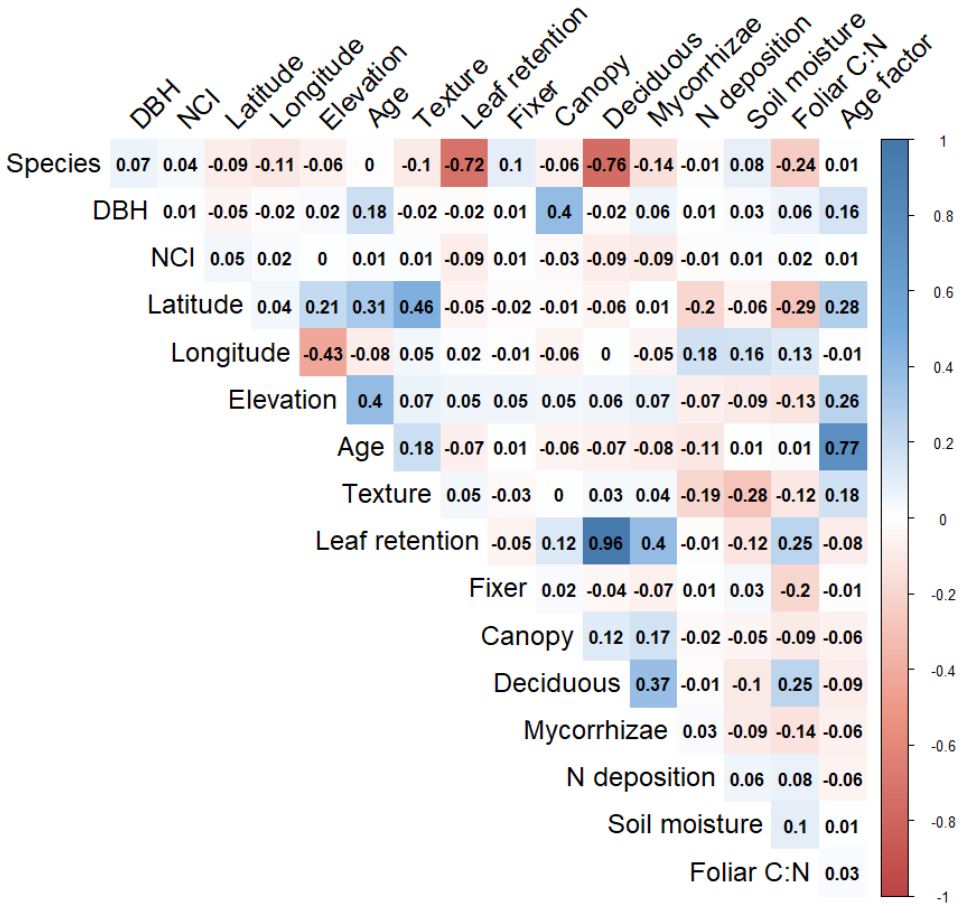
DBH
NCI
Latitude
Longitude
Elevation
Age
Texture
Leaf retention
Fixer
Canopy
Deciduous
Mycorrhizae
N deposition
Soil moisture
Foliar C:N
Age factor
Species 0.07 0.04 -0.09 -0.11 -0.06 0 -0.1 -0.72 0.1 -0.06 -0.76 -0.14 -0.01 0.08 -0.24 0.01
DBH 0.01 -0.05 -0.02 0.02 0.18 -0.02 -0.02 0.01 0.4 -0.02 0.06 0.01 0.03 0.06 0.16
NCI 0.05 0.02 0 0.01 0.01 -0.09 0.01 -0.03 -0.09 -0.09 -0.01 0.01 0.02 0.01
Latitude 0.04 0.21 0.31 0.46 -0.05 -0.02 -0.01 -0.06 0.01 -0.2 -0.06 -0.29 0.28
Longitude -0.43 -0.08 0.05 0.02 -0.01 -0.06 0 -0.05 0.18 0.16 0.13 -0.01
Elevation 0.4 0.07 0.05 0.05 0.05 0.06 0.07 -0.07 -0.09 -0.13 0.26
Age 0.18 -0.07 0.01 -0.06 -0.07 -0.08 -0.11 0.01 0.01 0.77
Texture 0.05 -0.03 0 0.03 0.04 -0.19 -0.28 -0.12 0.18
Leaf retention -0.05 0.12 0.96 0.4 -0.01 -0.12 0.25 -0.08
Fixer 0.02 -0.04 -0.07 0.01 0.03 -0.2 -0.01
Canopy 0.12 0.17 -0.02 -0.05 -0.09 -0.06
Deciduous 0.37 -0.01 -0.1 0.25 -0.09
Mycorrhizae 0.03 -0.09 -0.14 -0.06
N deposition 0.06 0.08 -0.06
Soil moisture 0.1 0.01
Foliar C:N 0.03
1
0.8
0.6
0.4
0.2
0
-0.2
-0.4
-0.6
-0.8
-1

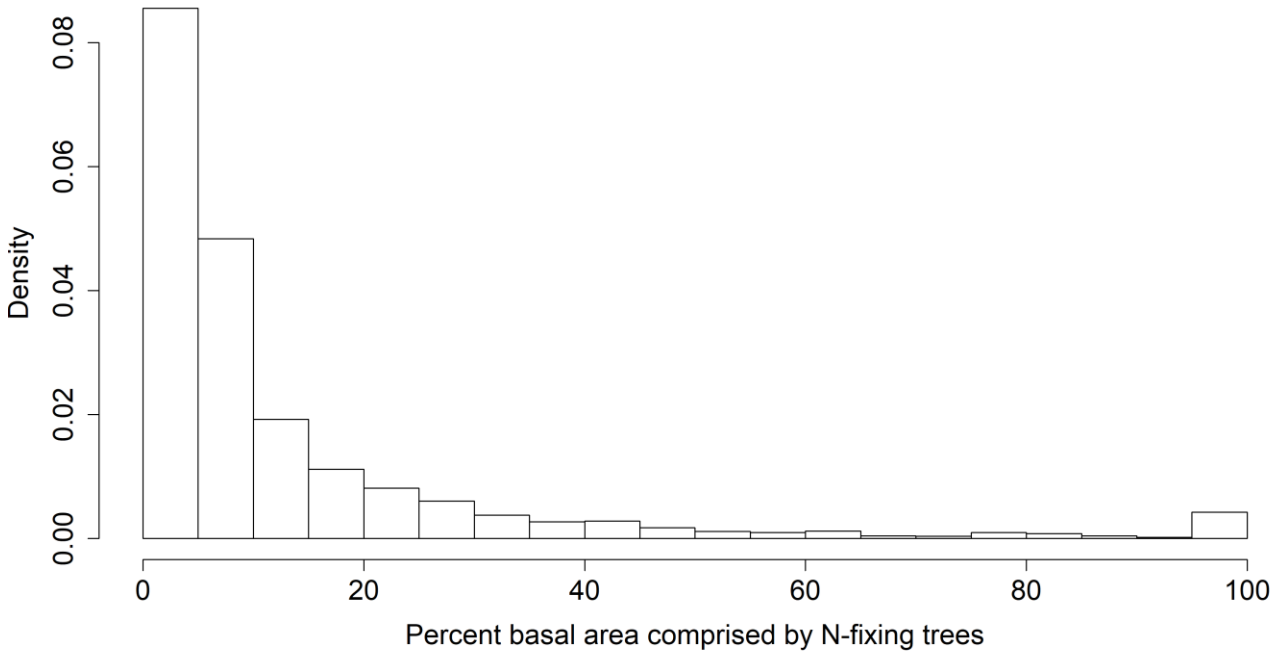

SI Figure 1. Histogram showing the percent of basal area comprised of N-fixing trees at the plot-scale in the FIA database. When percent basal area is 0% all trees in the plot were non-fixers. When the percent basal area is 100% all trees in the plot were N-fixers.

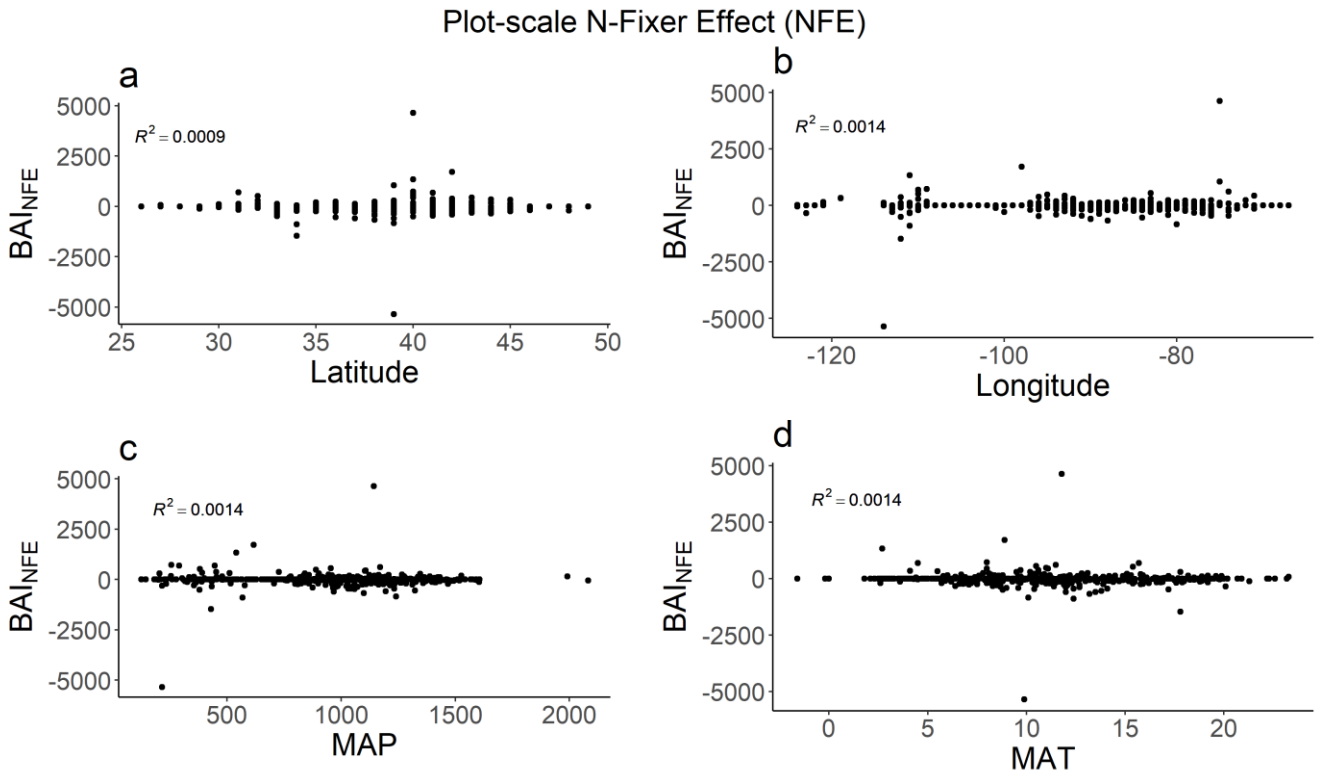
Plot-scale N-Fixer Effect (NFE)
a
b
c
d
BAI_{NFE}
$R^2 = 0.0009$
$R^2 = 0.0014$
$R^2 = 0.0014$
$R^2 = 0.0014$
Latitude
Longitude
MAP
MAT

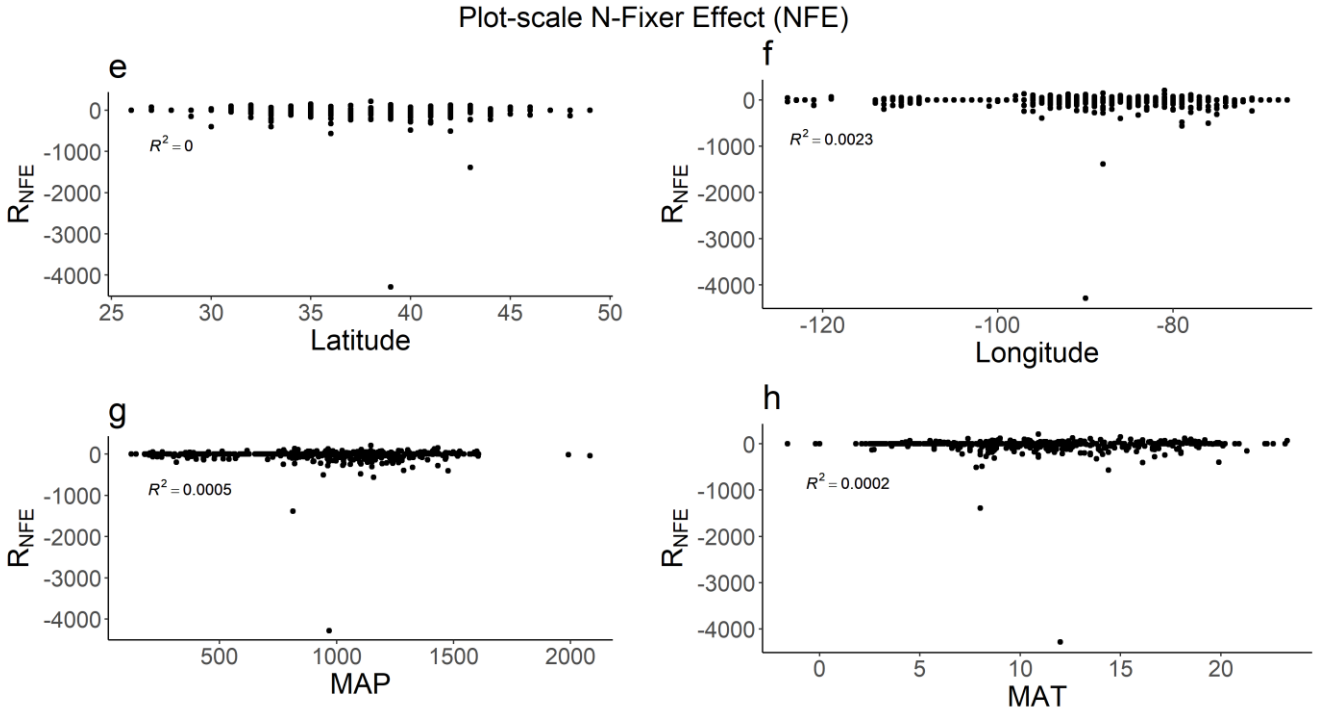
Plot-scale N-Fixer Effect (NFE)
e
f
g
h
R_{NFE}
$R^2 = 0$
$R^2 = 0.0023$
$R^2 = 0.0005$
$R^2 = 0.0002$
Latitude
Longitude
MAP
MAT

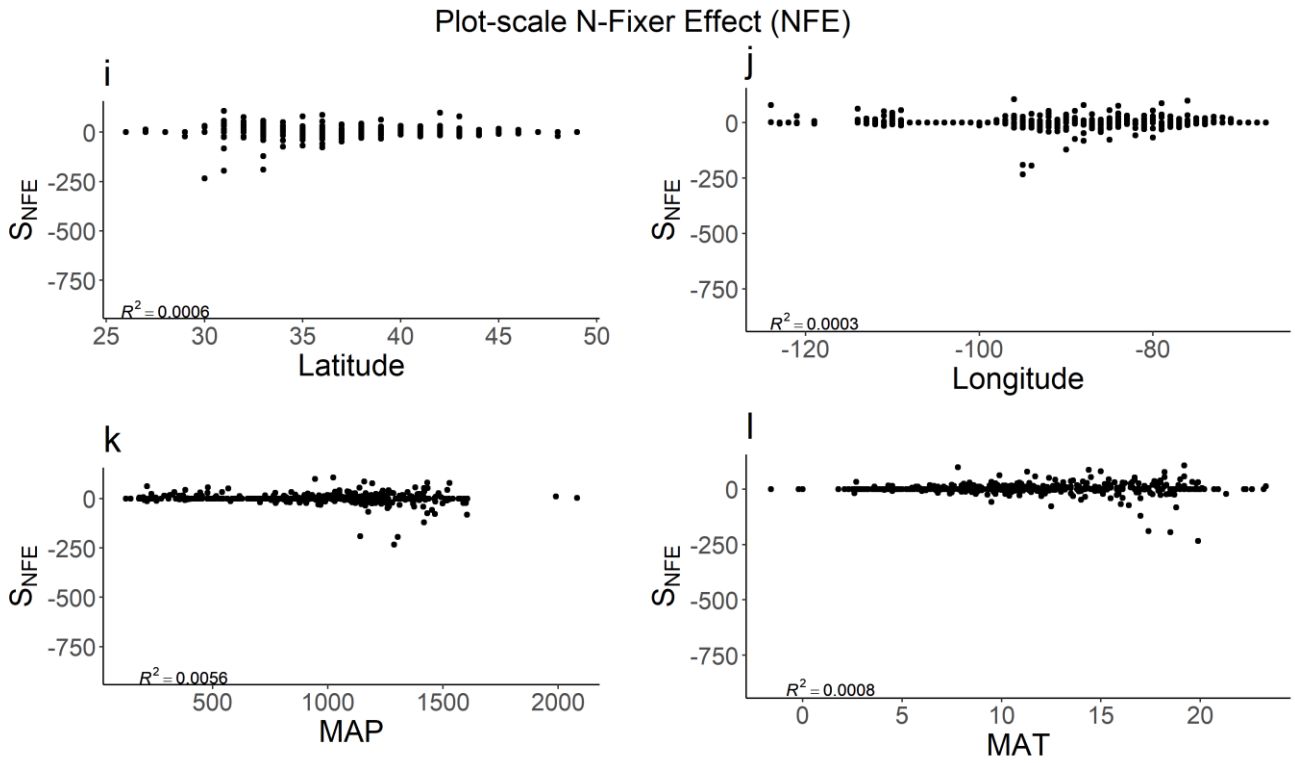

SI Figure 2. N-fixer effects (NFE) at the plot-scale in relation to geographic factors across the coterminous U.S. Each point represents a single plot from the analysis. The NFE is shown for three different demographic rates: BAINFE (a-d), RNFE (e-h), and SNFE (i-l). Latitude and longitude are in degrees, mean annual precipitation (MAP) is in mm, and mean annual temperature (MAT) is in °C.

Appendix C – Supplementary Information for Chapter 3

SI Text 1 – Methods for parameter estimates.

1.1 Diffusivity (D)

A ballpark estimate of diffusivity (*D*) was derived from a field experiment conducted at Black Rock Forest, a deciduous forest in New York dominated by oaks and maples. Though we had a low recovery rate for marked leaves in the experiment which prevented us from obtaining robust diffusivities, the field work gave us a range of possible values for leaf diffusivity. Single species leaf clusters (from *Q. rubra, Q. alba, A. rubrum, R. pseudoacacia,* or *F. grandifolia*) were constructed with 20 spray painted leaves of a single species and tracked across 4 months to observe the diffusion of leaves. When tracking leaves, we searched the area around the initial cluster position for 5 minutes and recorded the distance and angle of each painted leaf found. Diffusion was calculated by: $D = \frac{\sum_{i=1}^{n} d_i^2}{4t}$ following Turchin (1998) where *D* is diffusivity [m^2 $year^{-1}$], *d* is distance of leaf *i* [m] from its starting point, and *t* is time [years].

1.2 Advection velocity (u)

Horizontal leaf movement across the forest floor is variable and season dependent. In a study of a West Virginian hardwood forest, Orndorff & Lang (1981) found that the average downslope movement of leaf litter in December was 1.21 m day^{-1} while in April and May it was 0.65 m day^{-1}. Of the leaves they tracked 28% of leaves did not move, 69% moved 0.5 m or more downslope, and 3% of leaves moved upslope. They also observed that 90% of movement occurred in a wind storm on a single day. This suggests that most leaf movement occurs on a few

notable days so the advection velocity is driven by a small number of wind events. Hillslope is also an important driver of the advection velocity (i.e. most leaves move downhill). Boerner & Kooser (1989) also found that most redistribution occurred from January to April and that different species had different downslope redistribution rates. From Orndorff and Lang (1981), assuming that litter moved 1.21 m day^{-1} in December, 0.65 m day^{-1} in November and January through May, and 0 m day^{-1} during the other months, a rough estimate for the advection rate is 150 m $year^{-1}$.

The rank order of advection velocity for species was determined from the same field experiment described above where single species clusters of painted, senesced leaves were assembled and allowed to move for 4 months. Advection (u) was calculated as: $u = \frac{d_{mean}}{t}$. Within the range of litter advection velocities reported in the literature above, we varied the advection velocity of our target species according to rank order from the field work.

1.3 Initial leaf fall ε(x)

The normal distribution has two parameters: μ and σ. Since the average position of leaves falling from a tree on a flat surface is at the trunk of the tree we used μ = 0 m. The standard deviation of the normal distribution was determined from literature. Ferrari & Sugita (1996) found that on average in one temperate hardwood forest 90% of litter falls within 17.1 m of a tree. We used this to estimate the average standard deviation in a temperate hardwood forest is around 10.4 m. For the anisotropic wind dispersal distribution (equation 2) and the empirically derived litter distribution (equation 3), tree dbh was used to calculate the distribution. Uriarte et al. (2015)'s dispersal kernel was developed for several Puerto Rican tree species and specified the litter mass by distance from the tree as a function of dbh and several species-specific

parameters. We used a "wide", "narrow", and "typical" kernel based on three species parameterized in their study. The "wide" kernel represented windy conditions where litter falls farther from the base of the tree during the initial dispersal event or species that had wider litter fall.

Three initial conditions ($\varepsilon(x)$) were considered: (1) a normal distribution where all litter is deposited instantaneously near the base of the tree, (2) an anisotropic litter dispersal model where litter is deposited instantaneously but asymmetrically based on wind (Staelens et al. 2003), and (3) an empirically derived leaf litter dispersal kernel (Uriarte et al. 2015). These three initial conditions represented a temperate, deciduous forest where litter was dropped across a short time period relative to the time of subsequent movement.

$$\text{Normal distribution: } \varepsilon(x) = TLP * \frac{1}{\sigma\sqrt{2\pi}} e^{-\frac{(x-\mu)^2}{2\sigma^2}} \quad \textbf{(2)}$$

Here σ is the standard deviation of the distribution, μ is the mean of the distribution set at 0 m, and x the distance from the tree.

$$\text{Anisotropic dispersal: } \varepsilon(x) = \frac{a}{N} * (DBH^b \exp(-c_0 x - d * DBH)) \quad \textbf{(3)}$$

Here a, N, b, c_0, and d are species-specific parameters from Staelens *et al* (2003), *DBH* is the diameter at breast height (cm), and x is the position in linear space.

$$\text{Empirical distribution: } \varepsilon(x) = TLP * (\frac{DBH}{30})^{\alpha} \frac{1}{\eta} e^{-0.5(\frac{\ln\left(\frac{x}{X_0}\right)}{X_b})^2} \quad \textbf{(4)}$$

Here *TLP* is the total litter production (g yr^{-1}), *DBH* is the diameter at breast height (cm), α, η, X_0, and X_b are species-specific parameters obtained from Uriarte *et al* (2015), and x is the distance from the tree.

1.4 Rooting radius (β_{max})

Maximum rooting radius was estimated from a literature search. Schenk & Jackson (2002) conducted a literature review of root length in water limited environments and found that lateral tree roots ranged from 0.5 to 50 m with an arithmetic mean at 11.5 m. Hruska et al. (1999) found that a large oak had roots that extended 82 m from the base of the tree while a small oak had roots that extended 21 m from the base. This corresponded to 125% and 130% of the crown radius respectively. They also observed that the radius of the 8 largest roots was about 10 times the stem diameter of the tree. Stout (1956) excavated several large trees in Black Rock Forest and recorded the mean root area to crown area ratio. The average ratio for all oaks was 7.4 (σ = 9.3), the average for all maples was 13.0 (σ = 9.8), and for beech one tree was sampled with a ratio of 3.9.

Maximum rooting radius was tied to tree dbh using two literature derived relationships: (1) for trees less than 20 cm dbh $\beta = 5.5264 * \ln(dbh) + 8.1023$ based on logarithmic regression using data from Stout (1956), and (2) for trees greater than 20 cm $\beta = 2.8961 * dbh + 5.5059$ based on the linear regression using Stout (1956) data.

1.5 Rooting distribution $\psi(x)$

Litter nutrients that decompose in the rooting zone of a tree may not be taken up by a focal tree; active roots may not access that particular point or another tree's rooting system may overlap and steal the nutrients. The likelihood that nutrients are taken up by a tree varies through the rooting zone. To add this realism to the model we tested several rooting distributions ($\psi(x)$). Wider rooting distributions allow greater nutrient recovery while deeper rooting distributions do not. The farthest horizontal extent of the roots determines the farthest distance litter can diffuse before decomposing and still be recovered by the focal tree (model parameter β_{max}, m). The

density and distribution of absorbing root tips changes by species and forest structure (Nadelhoffer et al. 1985, Nadelhoffer and Raich 1992, Jackson et al. 1997, Hajek et al. 2013). We compare the percent of litter recovered under different rooting distributions to determine the potential effects of mycorrhizae that could dramatically extend the effective rooting zone of a tree well beyond where the roots actually stop (Simard and Durall 2004, Phillips et al. 2013, Treseder 2013, Chen et al. 2016).

Four possible rooting distributions were examined with the model: (1) uniform roots where the probability of finding roots was 1 until the root length (β_{max}) where it dropped to 0, (2) there was a high probability of finding roots which dropped off farther from the tree where $\psi(x) = b^{abs(x)}$ where b = 0.99, (3) the likelihood of finding roots dropped off rapidly some distance from the tree trunk such as the transition between coarse roots and fine roots or mycorrhizae where $\psi(x) = \frac{2}{1+e^{(x+0.5)}}$, and (4) the probability of finding roots dropped off as an exponential decay where $\psi(x) = e^{-abs(x)}$.

1.6 Immobilization rate (k)

The immobilization rate (*k*) was the rate at which nutrients stop moving. This incorporates chemical N immobilization as part of decomposition (Chapin III et al. 2011) and physical litter immobilization as leaves get trapped by objects such as fallen logs (Orndorff and Lang 1981) or aggregated into leaf mats through fungal cementing. The minimum immobilization rate for a species is defined by the decomposition rate for that species. The minimum rate assumes that N is released uniformly throughout decomposition and that leaves are not immobilized by any other processes (e.g. entrapment or aggregation). These minimum

immobilization rates (k_{min}) were derived from a literature search for species-specific decomposition rates (SI Text 2).

Immobilization rates are likely larger than k_{min} because entrapment and aggregation are frequent forest processes. In a West Virginian hardwood forest, Orndorff and Lang found that average downslope movement of litter in the surface layer was 14.3 m between December and April, however, if a particular leaf was caught under a log the average downslope movement in the same time period was only 1.4 m (Orndorff and Lang 1981). Entrapment decreased litter movement to one tenth. When conducting the field experiment, leaf litter aggregation was qualitatively important in stopping leaf litter which likely further increases *k*.

SI Table 1. Model parameters and their biological significance

Parameter	**Range**	**Interpretation**
φ	0 – 100 %	Percent of nutrients that a tree dropped in litter fall which it can recover based on where the litter decomposed and where the tree had roots
β	1 – 80 m	Lateral length of longest roots on tree
$\psi(x)$	1/exp, uniform, b^x, exp decay, modified exp decay	Root distribution – trees are more likely to have actively absorbing roots near the base of the tree but moving out the roots become less dense so fewer actively absorbing roots farther from the base (considers roots and mycorrhizae as equivalent)
$\varepsilon(x)$	Gaussian, Staelens, narrow, typical, wide	Shape of initial, instantaneous litter fall of leaves falling from tree
k	0.1 – 10 $year^{-1}$	The immobilization and decomposition rate of litter due to litter breakdown, N leaching, or immobilization from matting or leaves getting trapped under rocks and logs
D	30 – 120 m^2 $year^{-1}$	The diffusion coefficient or how quickly the litter spreads across the forest floor due to random motion (leaves circulating in air, animals shifting litter)
u	30 – 120 m $year^{-1}$	Advection velocity or how quickly the litter moves due to non-random motion (such as wind-driven movement, movement downhill, water directed movement)

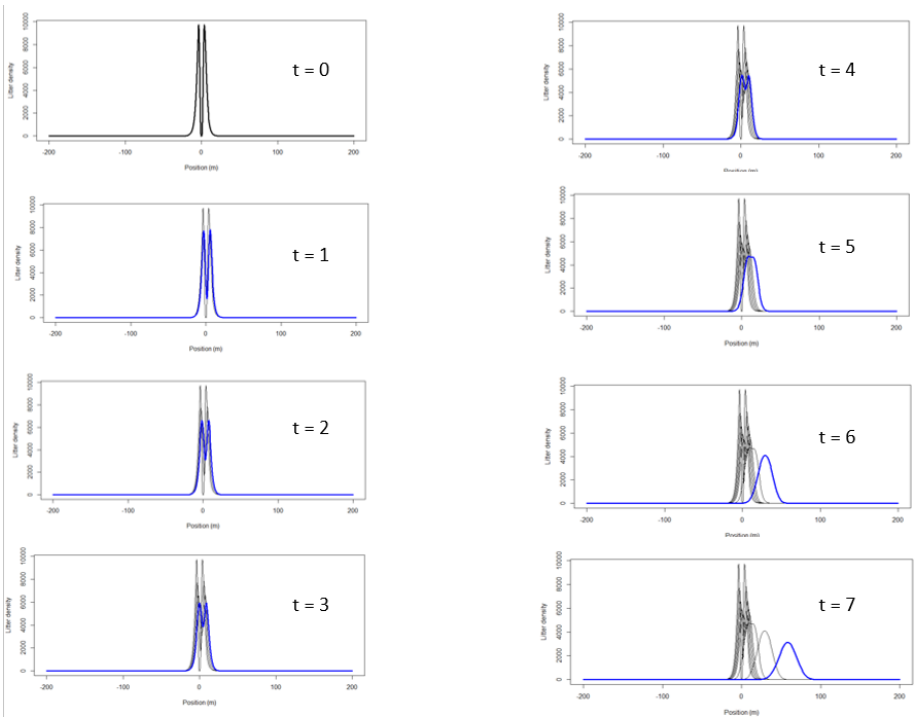

SI Figure 1. Pulse of litter density through time. t = 0 reflects the initial litter distribution ε(x). As time advances the plume spreads out due to diffusion, moves right due to advection (e.g. wind, hillslope, water transport), and gets smaller due to decomposition.

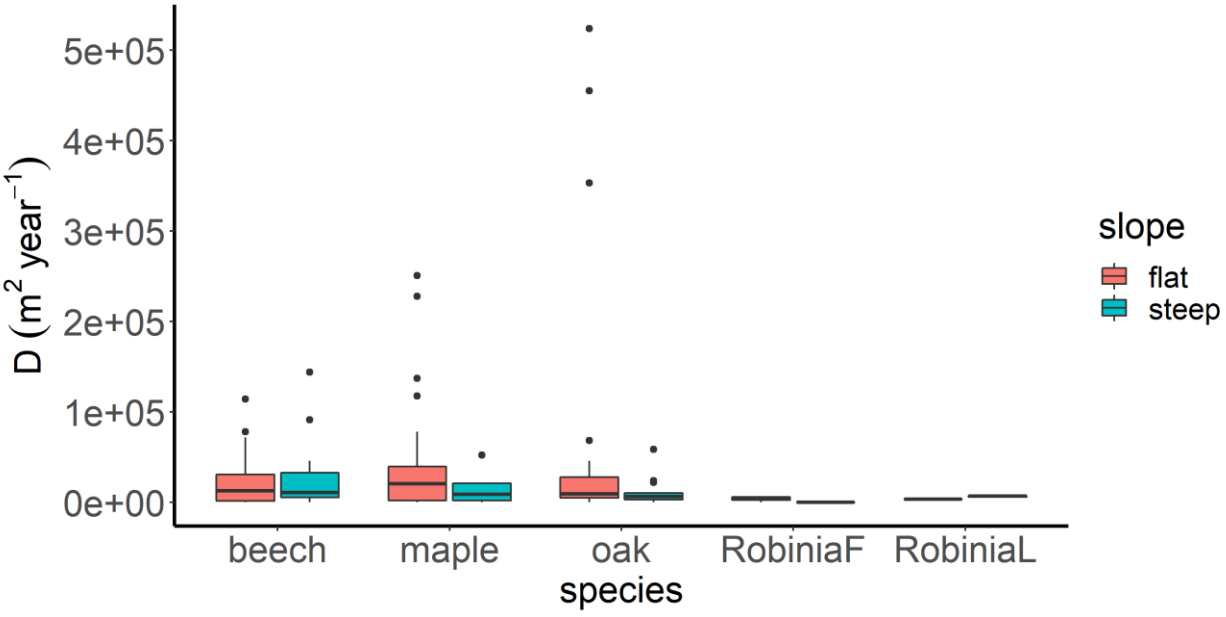

SI Figure 2. Diffusion coefficients (*D*) from field data. Note: outlier in maple with $D = 309$ m^2 year^{-1}. *Robinia* was tested in two configurations: RobiniaF was full leaves and RobiniaL was a set of leaflets

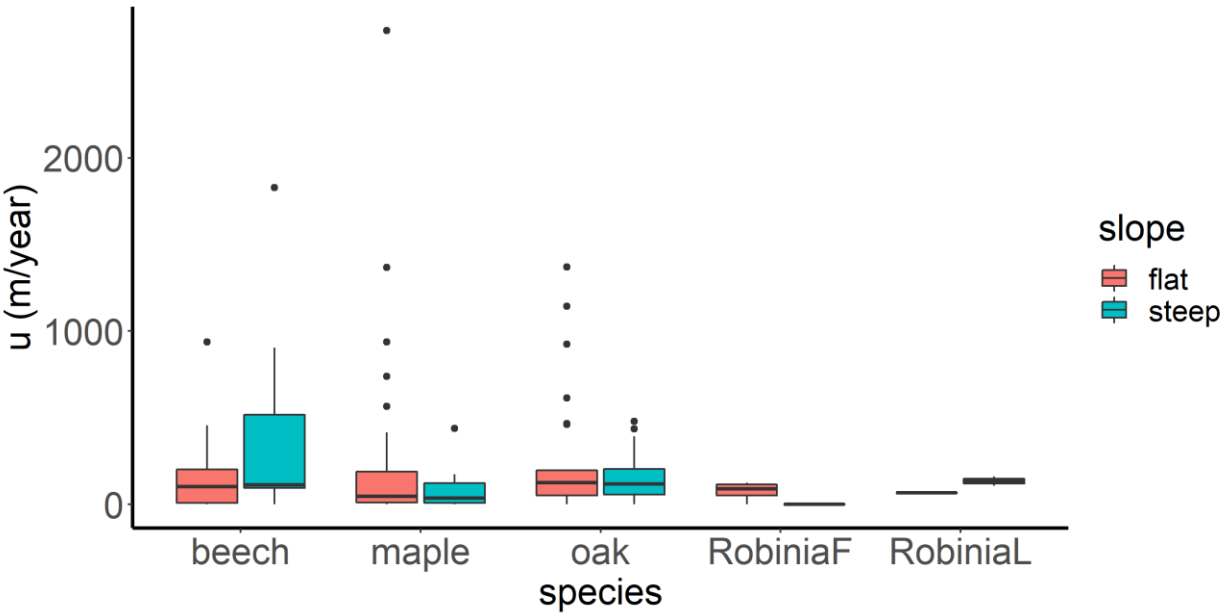

SI Figure 3. Advection coefficients (*u*) from field data. *Robinia* was tested in two configurations: RobiniaF was full leaves and RobiniaL was a set of leaflets

SI Text 2. Sources for decomposition rates.
Quercus rubra:

Lee, Y. C., Nam, J. M., & Kim, J. G. (2011). The influence of black locust (Robinia pseudoacacia) flower and leaf fall on soil phosphate. *Plant and Soil*, *341*(1–2), 269–277. doi: 10.1007/s11104-010-0642-5

Midgley, M. G., Brzostek, E., & Phillips, R. P. (2015). Decay rates of leaf litters from arbuscular mycorrhizal trees are more sensitive to soil effects than litters from ectomycorrhizal trees. *Journal of Ecology*, *103*(6), 1454–1463. doi: 10.1111/1365-2745.12467

Acer rubra:

Alexander, H. D., & Arthur, M. A. (2014). Increasing Red Maple Leaf Litter Alters Decomposition Rates and Nitrogen Cycling in Historically Oak-Dominated Forests of the Eastern U.S. *Ecosystems*, *17*(8), 1371–1383. doi: 10.1007/s10021-014-9802-4

Midgley, M. G., Brzostek, E., & Phillips, R. P. (2015). Decay rates of leaf litters from arbuscular mycorrhizal trees are more sensitive to soil effects than litters from ectomycorrhizal trees. *Journal of Ecology*, *103*(6), 1454–1463. doi: 10.1111/1365-2745.12467

Fagus grandifolia:

Jacob, M., Viedenz, K., Polle, A., & Thomas, F. M. (2010). Leaf litter decomposition in temperate deciduous forest stands with a decreasing fraction of beech (Fagus sylvatica). *Oecologia*, *164*(4), 1083–1094. doi: 10.1007/s00442-010-1699-9

Robinia pseudoacacia:

Hirschfeld, J. R., Finn, J. T., & Patterson III, W. A. (1984). Effects of Robinia pseudoacacia on leaf litter decomposition and nitrogen mineralization in a northern hardwood stand. *Canadian Journal of Forest Research*, *14,* 201–205.

Lee, Y. C., Nam, J. M., & Kim, J. G. (2011). The influence of black locust (Robinia pseudoacacia) flower and leaf fall on soil phosphate. *Plant and Soil*, *341*(1–2), 269–277. doi: 10.1007/s11104-010-0642-5

SI Text 3. Methods for stand level analysis

A forest stand was simulated using 5 trees along a line. We examined several scenarios, including even sized stands and uneven sizes stands as well as a range of root overlaps: 0% overlap, 25% overlap, and 75% overlap. Root overlap is an indicated forest density where more

dense forests have more root overlap and less dense forests have less root overlap. The tree spacings in meters are shown below with tree dbh in cm in parentheses for each tree:

Scenario	**Tree 1** position (m), dbh (cm)	**Tree 2** position (m), dbh (cm)	**Tree 3** position (m), dbh (cm)	**Tree 4** position (m), dbh (cm)	**Tree 5** position (m), dbh (cm)
Even, 0%	-160 (40)	-80 (40)	0 (40)	80 (40)	160 (40)
Even, 25%	-140 (40)	-70 (40)	0 (40)	70 (40)	140 (40)
Even, 75%	-100 (40)	-50 (40)	0 (40)	50 (40)	100 (40)
Uneven, 0%	-180 (20)	-100 (60)	0 (40)	50 (10)	90 (30)
Uneven, 25%	-150 (20)	-90 (60)	0 (40)	47.5 (10)	77.5 (30)
Uneven, 75%	-90 (20)	-70 (60)	0 (40)	42.5 (10)	52.5 (30)

To calculate stand-level φ we divided the amount of litter from a given species that decomposed within the rooting radius of any other individual of the same species. For stand-level φ we used the even size, 25% root overlap scenario with u of 50 m year^{-1}. The decomposition rate, k, and diffusion coefficient, D, were species-specific and match values in Table 1. For the mixed-species stand-level φ we assumed trees 1, 3, and 5 were the focal species while trees 2 and 4 were a non-focal species.

SI Table 2. Diffusion coefficient data. Mean values are shown for D with standard deviation in parentheses. We assumed that missing leaves went to 1000 cm at a random angle (drawn from a uniform distribution).

Species	**Slope**	**D (m^2 year^{-1})**
Beech	Flat	256 (322)
Beech	Steep	314 (445)
Maple	Flat	404 (595)
Maple	Steep	154 (187)
Oak	Flat	575 (1357)
Oak	Steep	101 (138)
Robinia (full)	Flat	37.9 (28.1)
Robinia (full)	Steep	0.30 (NA)
Robinia (leaflets)	Flat	33.6 (NA)
Robinia (leaflets)	Steep	67.6 (19.7)

This analysis likely overestimates *D* since missing leaves were not spread uniformly around the radius. For species-level analysis half the average experimental *D* value was used. Instead slope or wind likely pushed them in one direction which would have decreased the diffusion coefficient data. For species-specific simulations we used half the species average value for *D*.

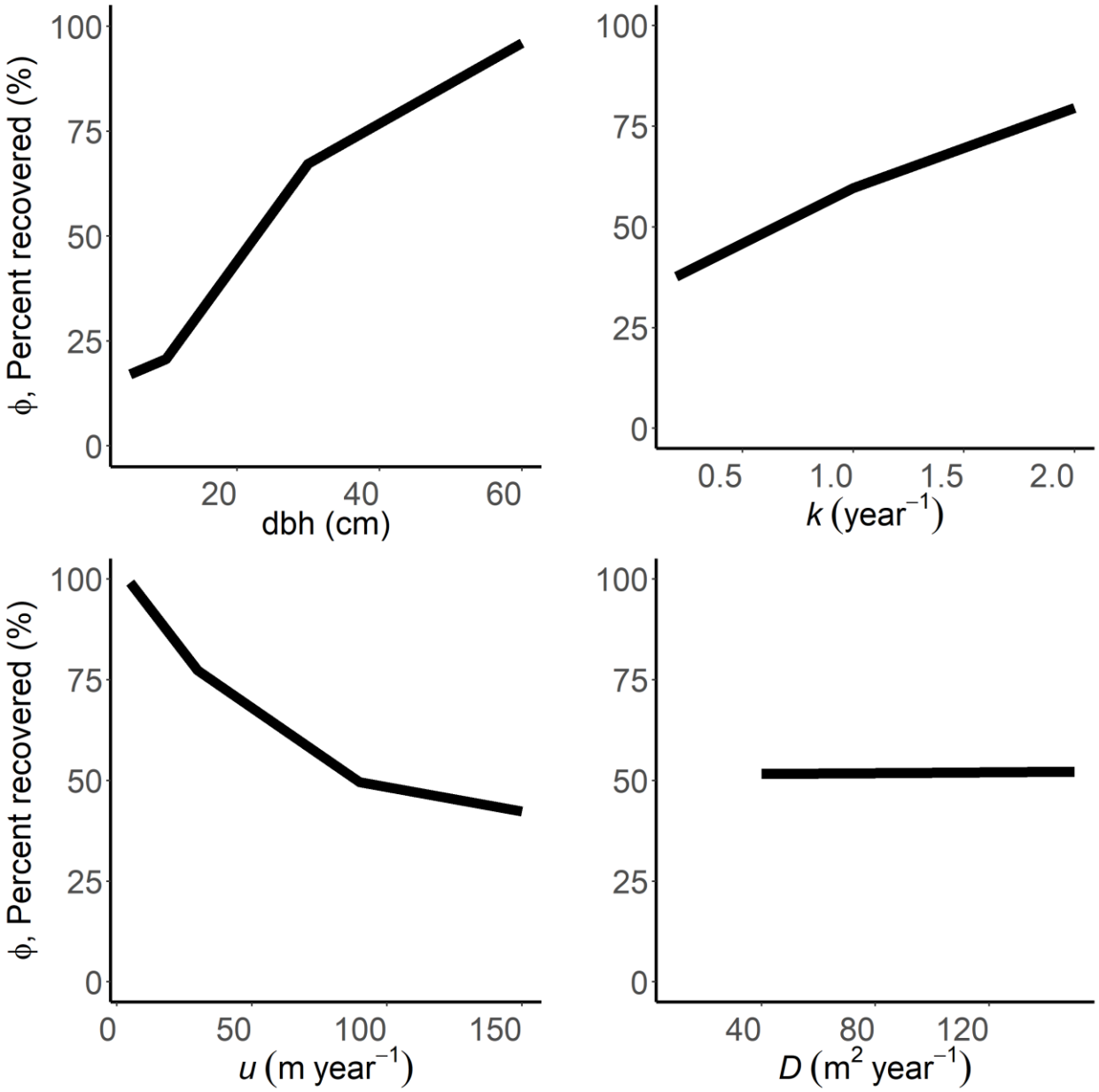

SI Figure 4. The percent of litter recovered as an effect of parameters: (a) *dbh* in cm, (b) *k* in year^{-1}, (c) *u* in m year^{-1}, and (d) *D* m^2 year^{-1}. For all parameters that are not the parameter on the x-axis values used were: *dbh* = 20 cm, *k* = 0.7 year^{-1}, *u* = 80 m year^{-1}, and *D* = 70 m^2 year^{-1}.

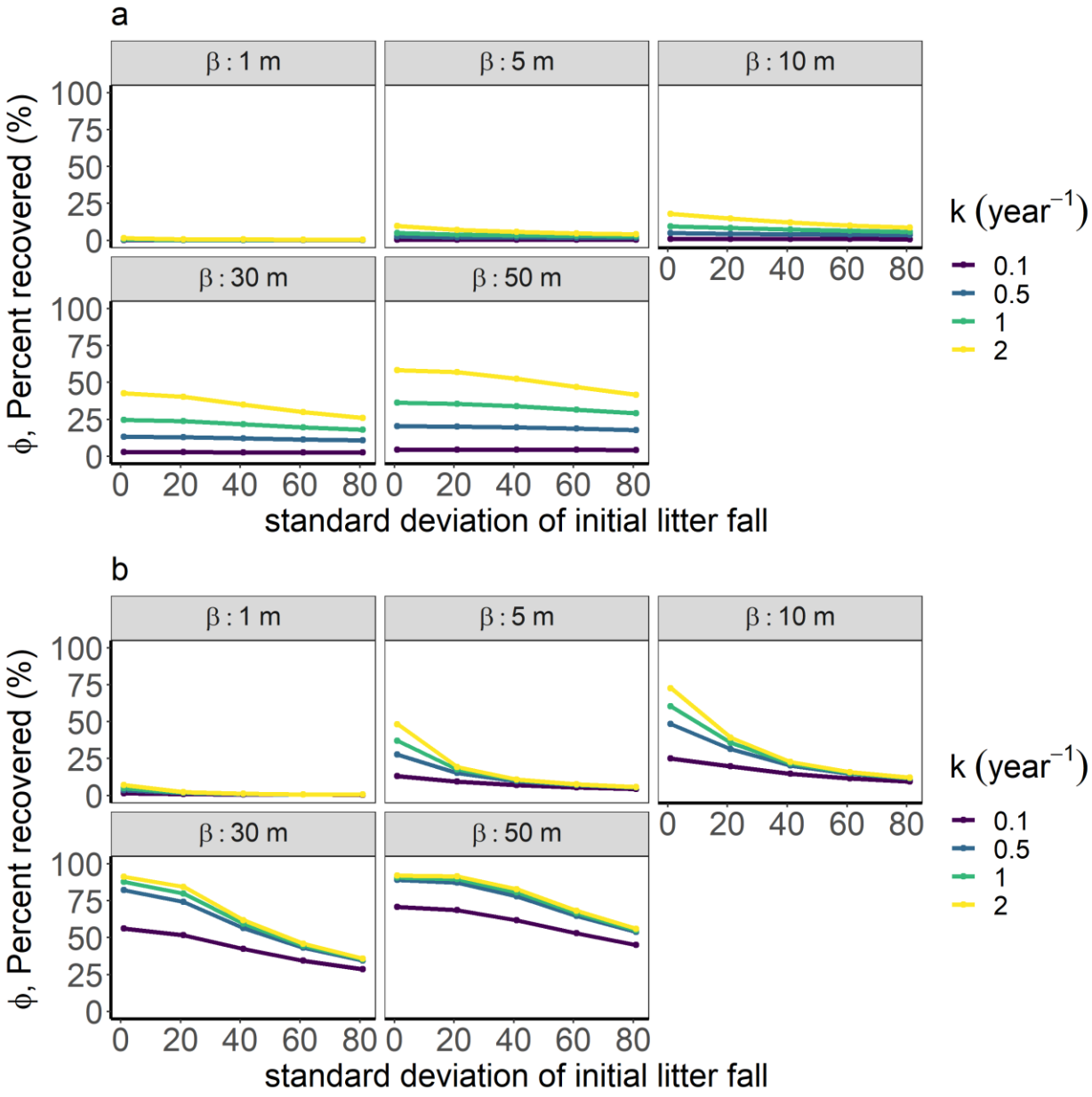

SI Figure 5. The effect of tree properties on the percent of leaf litter recovered (ϕ) by a focal tree. The facets show different rooting radii. Here the initial litter fall distribution was a normal distribution with a varying standard deviation (higher standard deviation indicated that leaf litter distributed farther). The diffusion coefficient (*D*) was 100 m^2 yr^{-1} and the advection velocity (*u*)

was 100 m yr^{-1}. In (a) facets show different rooting radii, u = 100 m $year^{-1}$, and D = 77 m^2 $year^{-1}$. In (b) facets also show different rooting radii, u = 1 m $year^{-1}$ and D = 77 m^2 $year^{-1}$.

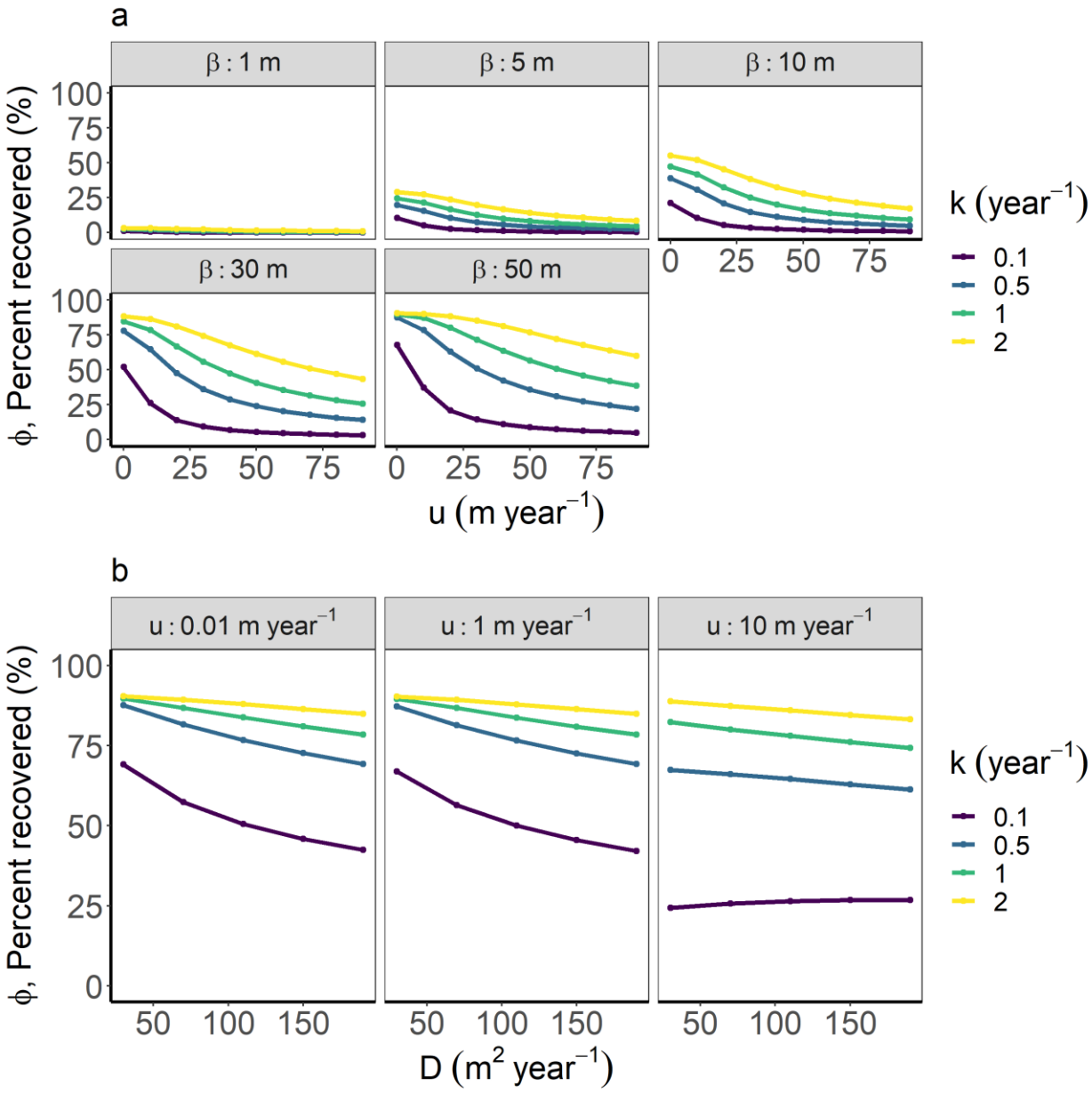

SI Figure 6. The effect of (a) advection velocity (u), and (b) diffusion coefficient (D) on the percent of nutrients recovered. For small trees (β = 1 m) the percent of litter recovered remains low regardless of advection. However, for large trees (β = 50 m) the percent of litter recovered varies by advection velocity. (a) Facets show different rooting radii, D = 100 m^2 $year^{-1}$, and the initial litter fall is a normal distribution with standard deviation 10 m. (b) Facets show different advection velocities (u), the initial litter fall is a normal distribution with a standard deviation of 10 m and the tree has a rooting radius (β) of 30 m.

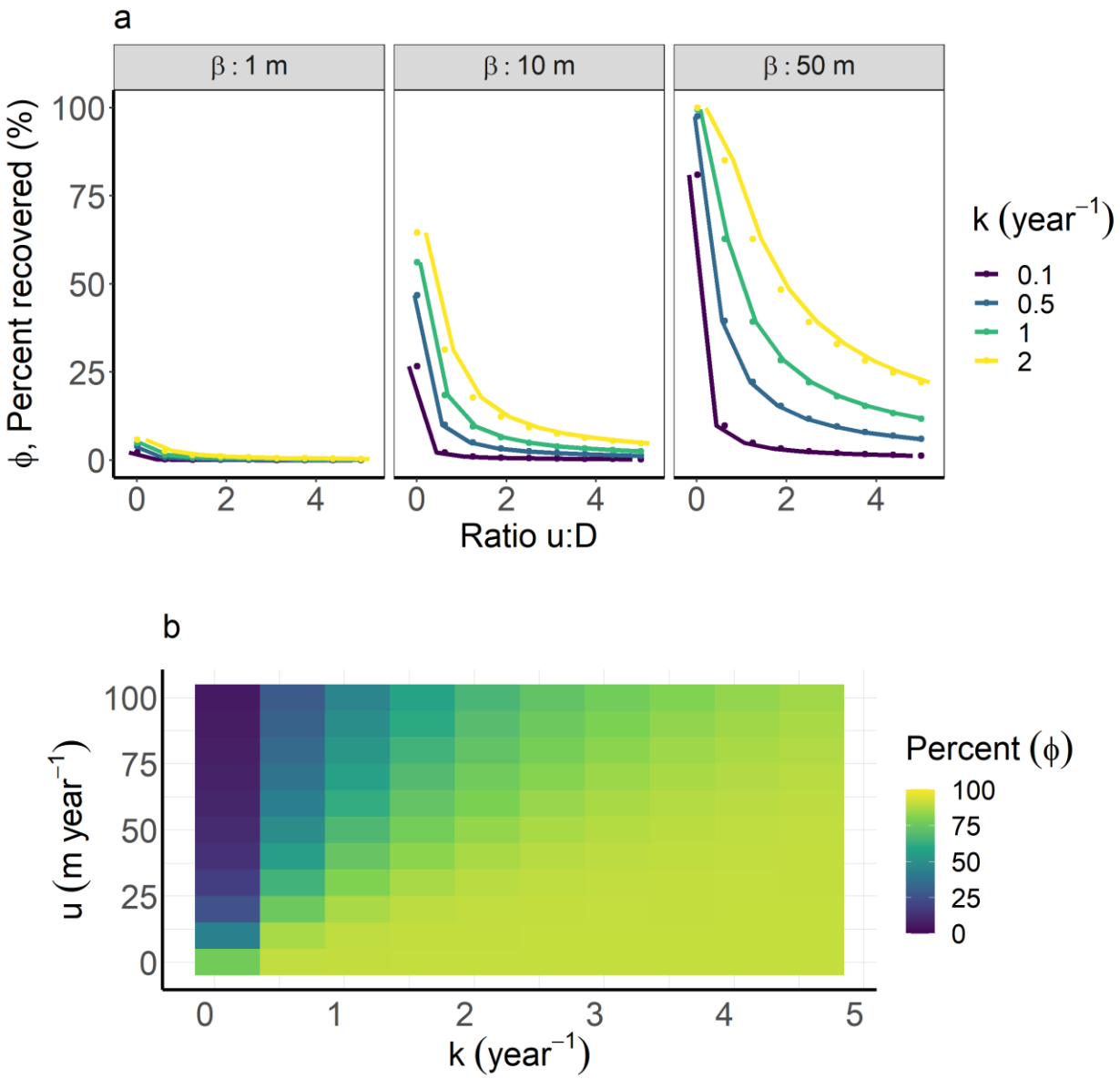

SI Figure 7. a) The effect of the relative strength of *u* (advection) and *D* (diffusion) on the percent of litter recovered (φ). Colors represent different decomposition (*k*) values. Facets show different *B* (root radius). Trees with faster decomposing litter recover a greater percent of litter regardless of other model parameters. However, nutrient recovery increases with both longer tree roots and a lower ratio of *u* to *D*. b) Interaction between advection (*u*) and decomposition (*k*) for a tree of DBH 20.6 cm and *D* 70 m^2 $year^{-1}$. Color represents the fraction of nutrients recovered (φ) on a scale of 0 to 100%. A tree can recover the vast majority of its nutrients if it has a sufficiently large *k* or sufficiently low *u*.

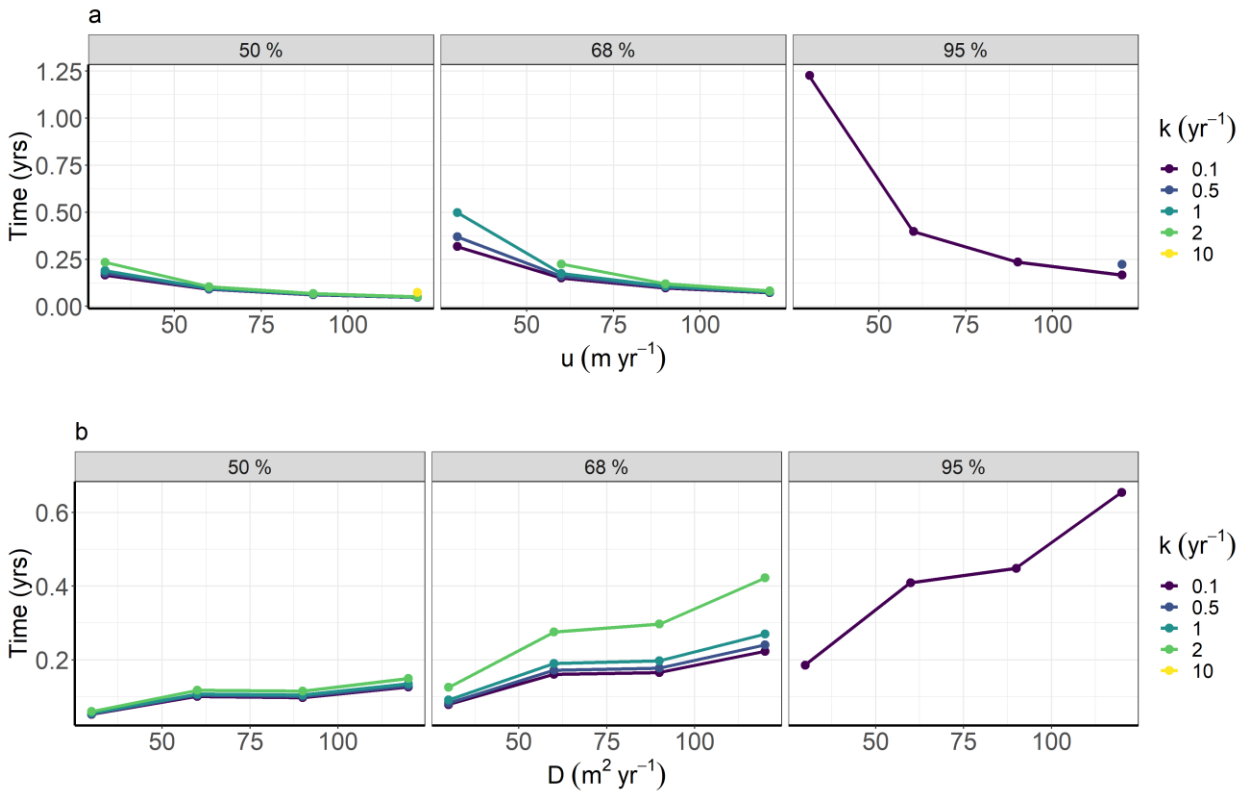

SI Figure 8. Time for 50%, 68% or 95% of litter to get 10 m away from tree trunk. a) Advection velocity (*u*) varies across the x-axis, time for percent of litter to reach 10 m is reported on the y-axis, and facets show different percentages. Litter that reached 10 m could have decomposed or reached that position as mobile litter. Missing points represent conditions under which the specified percent of litter never reached 10 m. D = 100 m^2 year^{-1}. Faster decomposing litter (larger k) was less likely to reach 10 m and when it did reach 10 m it took longer for the specified percent to reach that distance. As u increased the time for a specified percent of litter to reach 10 m decreased. b) Diffusion coefficient (D) varies across the x-axis, time for percent of litter to reach 10 m is reported on the y-axis, and facets show different percentages. u = 50 m year^{-1}. As D increased, the time for a specified percent of litter to reach 10 m increased.

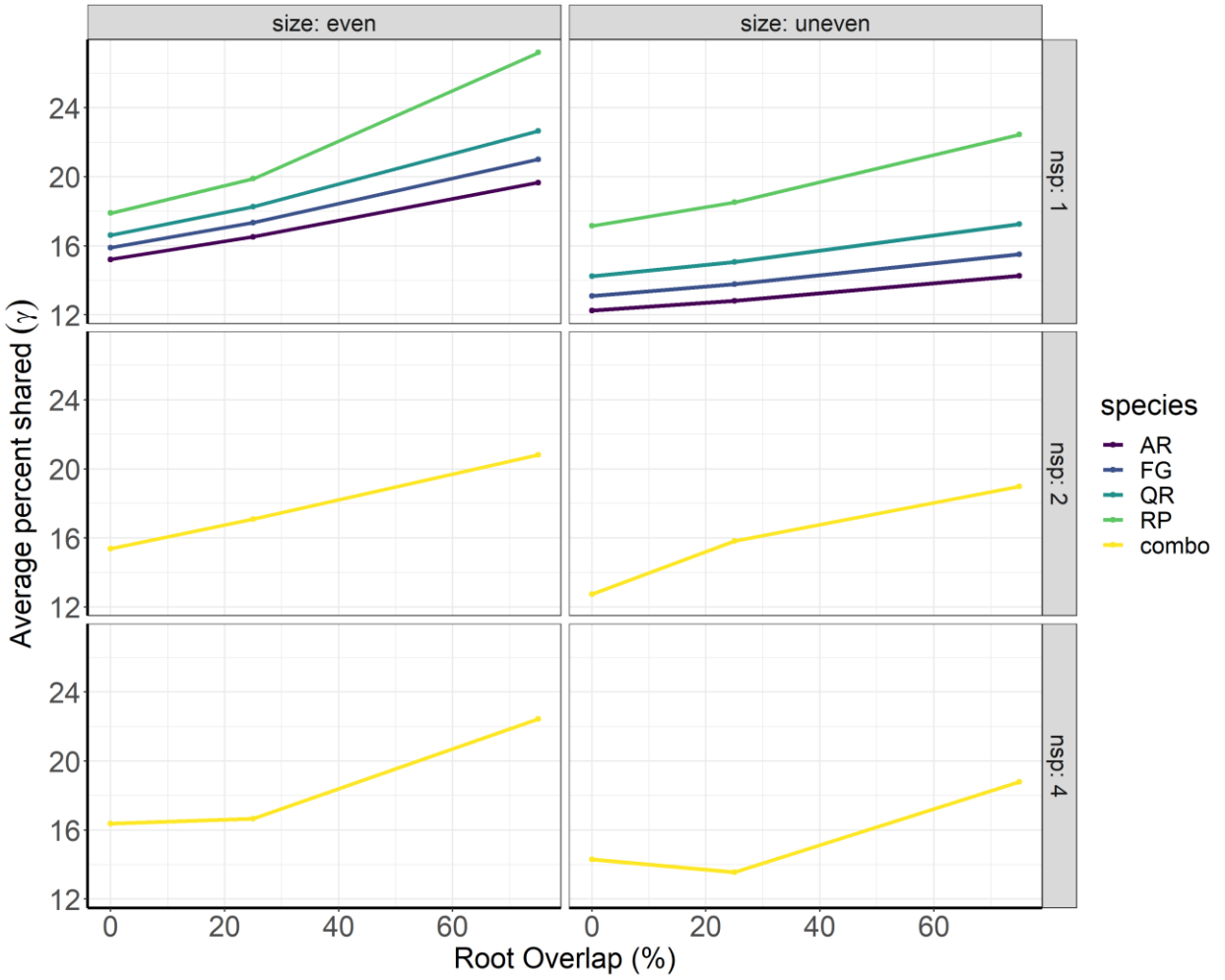

SI Figure 9. Stand level model average percent of litter shared with neighbors. Columns show stands of even size (dbh = 40 cm) and uneven stands (variety of dbh). Rows show the diversity of the stand where nsp = 1 is a single species stand, nsp = 2 is a 2 species stand, and nsp = 4 is a stand with all species present. AR: *Alnus rubra*, FG: *Fagus grandifolia*, QR: *Quercus rubra*, RP: *Robinia pseudoacacia*. *Robinia* litter decomposes fastest and diffuses the slowest which resulted in the greatest percent being shared with neighbors. Even aged stands share more litter with neighbors because the spacing of trees tends to be less.

SI Table 3. Stand level model calculation of species-level φ. Tree positions are as described for stand-level analyses in SI Text 3. Values for k (year^{-1}) and D (m^2 year^{-1}) for each species are as follows: *AR*: 0.48, 180.5, *FG*: 0.55, 139.5, *QR*: 0.67, 196, *RP*: 1.32, 21.6. We used the base value for u of 50 m year^{-1}.

Species	**Species-level φ (%)** Single–species stand	**Species-level φ (%)** Mixed–species stand
Acer rubra	74.0	47.9
Fagus grandifolia	77.6	50.1
Quercus rubrum	81.8	53.7

Robinia pseudoacacia	89.6	63.4

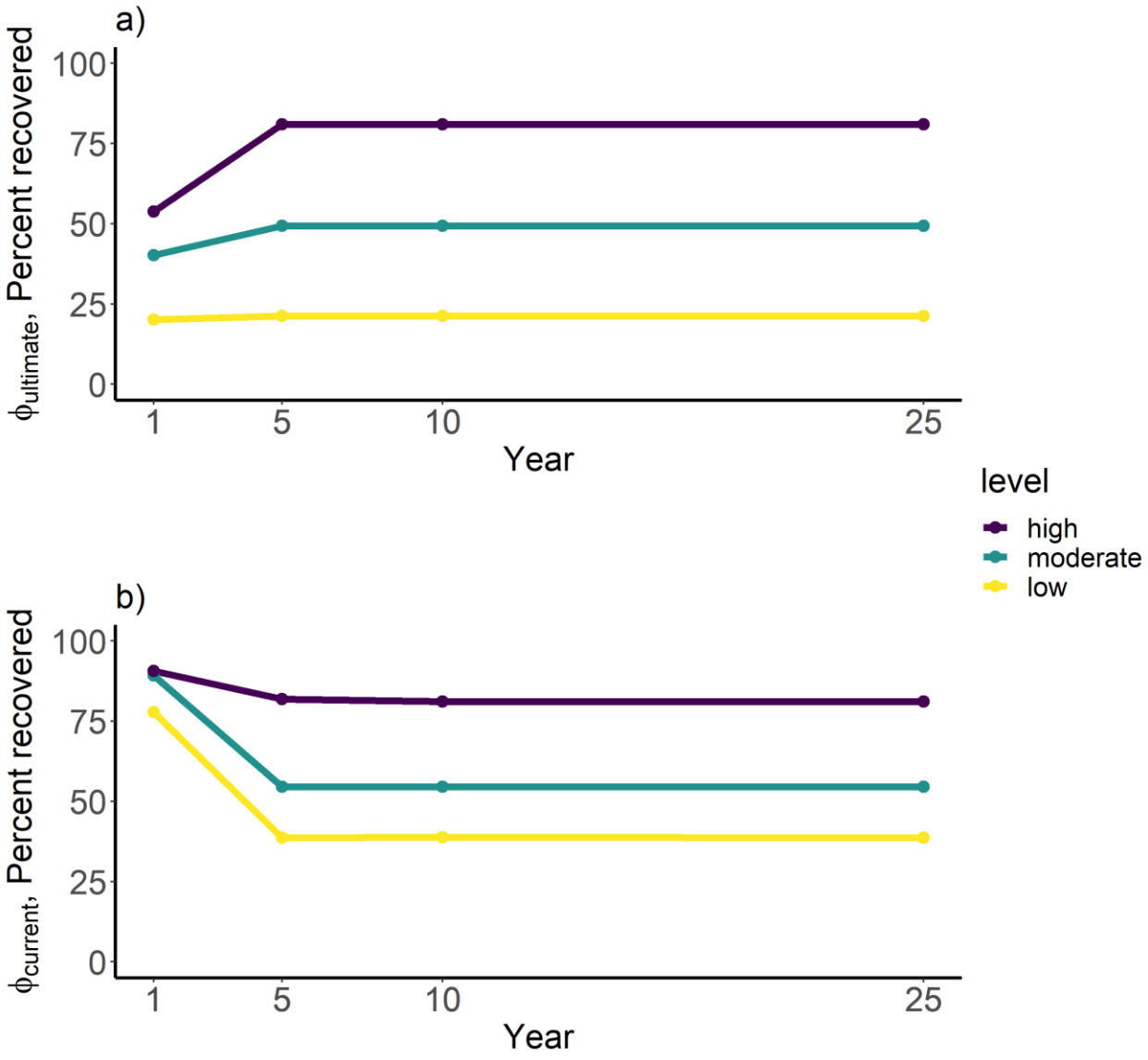

SI Figure 10. Percent litter nutrients recovered by time elapsed since litterfall. Panel a) shows $\varphi_{ultimate}$ or the percent of nutrients a tree recovers in a given period of time out of all nutrients dropped in litterfall. Panel b) shows $\varphi_{current}$ or the percent of nutrients a tree recovers in a given period of time out of the nutrients decomposed from litter at that time. The "high" level corresponds to k=0.9 y^{-1}, u=25 m y^{-1}, D=50 m^2 y^{-1}, "moderate" level corresponds to k=0.6 y^{-1}, u=50 m y^{-1}, D=100 m^2 y^{-1}, and "low" level corresponds to k=0.3 y^{-1}, u=75 m y^{-1}, D=150 m^2 y^{-1}.

SI Text 4 – Methods for forest stand model

Using this model with a single tree probed the extent to which a tree can access its own litter nutrients, a central assumption in many ecosystem and plant-soil feedback models (questions 1 and 2). To explore the extent to which a tree "share" litter with neighbors (question 3), we extend our model to a stand of several trees. This model was a one dimensional stand where we adjusted the spacing between trees and tree properties. We assumed that all trees experienced similar environmental conditions (e.g. wind speed, precipitation) so there was some similarity in u, D, and k. Litter that decomposed within the rooting radius of a neighbor could be accessed by that neighbor. We also investigated stand configurations where tree roots overlapped and separately considered the litter that immobilized in the zone of root overlap and the litter that immobilized in an area where the neighbor had exclusive root overlap.

SI Text 5 – Stand-scale dynamics results

The percent of litter that decomposed within a neighbors roots after 25 years (γ) informed theory on plant-soil feedbacks and facilitation theory. Our model showed that trees can share virtually no litter with a neighbor (< 0.0001%) or the majority of their litter (67%) depending on the spacing between neighbors, root overlap, and whether the neighbor was downwind of the focal tree. For a neighbor with 20 m-long roots situated 50 m downwind of a focal tree with 82 m roots in a high wind environment (u = 130 m y^{-1}, D = 100 m^2 y^{-1}) with a moderate decomposition rate (k = 0.8 y^{-1}), the neighbor captures 25% of the focal tree's litter. However, a similar neighbor upwind of the focal tree captures < 0.0001% of the focal tree's litter. In some cases, a focal tree will share more of its litter with neighbors that it can recapture itself. For example, a tree with 50 m-long roots situated 100 m upstream of a large tree (β = 82 m) with the

same parameters above will share 67% of its litter with the downwind neighbor while only capturing 31% of litter itself.

In an even sized stand, as the root overlap of trees increases, γ also increases (Figure SI 11). In both even and uneven sized stands as root overlap increased, the percent of litter shared with an average neighbor increased (Figure 5). When decomposition rate was faster, the percent shared with a neighbor increased more as root overlap increased. The amount of litter that trees shared with neighbors also depended on tree traits and environmental parameters. The effect of *k* was mediated by the root overlap. In low *u* stands a greater fraction of litter was shared with neighbors when *k* was slower. Since less litter immobilized in the focal tree's rooting zone, a greater fraction moved into the rooting zones of neighbors (Figure SI 11 across grid).

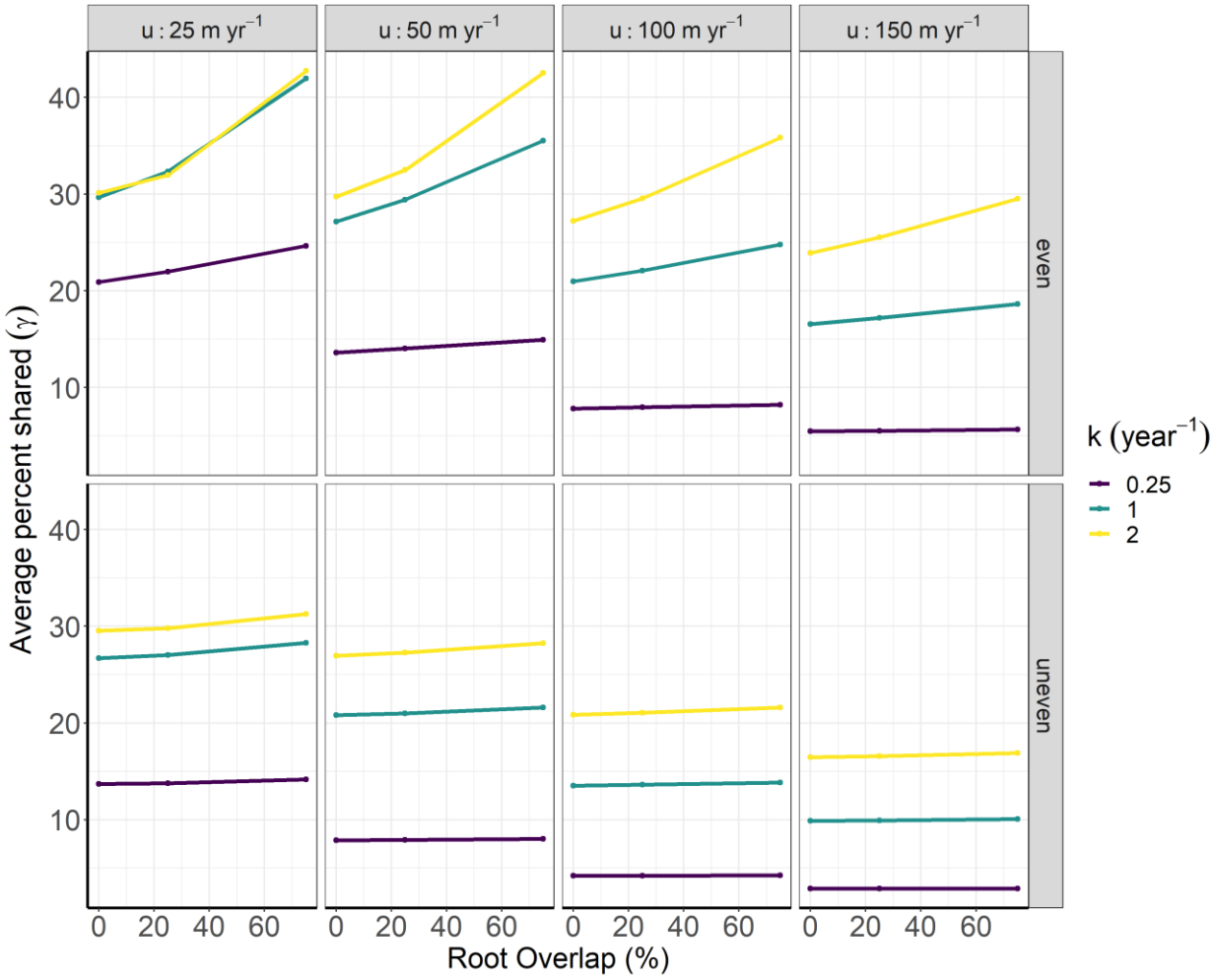

SI Figure 11. Average percent of litter shared with neighboring trees in even and uneven stands. Colors indicate different decomposition rates. Even stands were composed of three trees with 40 m rooting radii and trunks 70 m apart. Uneven stands were composed of three trees: β = 60 m, β = 10 m, and β = 40 m. Different degrees of root overlap are shown on the x-axis (0%, 25%, and 75%). For uneven stands the root overlap was defined based on the smaller tree.

SI Text 6 – Discussion of temporal dynamics

The percent of total litter that a tree could recover increased slightly over time, though after the first few years most of the litter had already decomposed or moved out of the rooting zone and so additional time had little effect on $\varphi_{ultimate}$ (Figure 10a). The percent of litter decomposed at that point in time that the tree could capture ($\varphi_{current}$) decreased over time (Figure 10b). As more time

passes there is also more opportunity for other organisms to take up mineralized N and prevent nutrient return to the focal tree.

SI Text 7 – Discussion of leaf traits

Other leaf traits were important determinants of nutrient recovery including specific leaf area (SLA) and shape irregularity. Leaves with higher SLA tended to have lower *D* (Pearson correlation -0.09) and *u* (Pearson correlation -0.17). So individuals with higher SLA would recover an even greater percent of litter nutrients than would be predicted from a correlation with foliar N alone. Irregularly shaped leaves may immobilize more because they easily mat together, effectively increasing *k*.

SI Text 8 – Discussion of stand level implications

The effect of traits on PSF depends on an individual's immediate neighbors. If trees grow in monodominant stands, such as *R. psuedoacacia* then it could still be advantageous at the species-level to have a low individual φ and make good conditions for conspecifics. The species-level φ for a pure *R. pseudoacacia* stand was 90% (SI Table 3). By contrast, when *R. pseudoacacia* grew in a mixed-species stand the species-level φ was only 63% (SI Table 3). Plants whose offspring recruited close to the parent tree could benefit from high nutrient retention near the parent plant. The effects for offspring could further the advantages of dropping nutrient rich litter which does not spread out and might favor a nutrient recovery strategy over reducing nutrients dropped in leaf litter to begin with (Clark et al. 2005).

Tree density also impacted nutrient return. In tightly packed stands, trees would benefit from their neighbors more with fast decomposition. Given that the early successional forests studied in Batterman et al (2013) were densely packed with small trees it is plausible that N-

fixers could provide 50% of N demand through leaflitter nutrient transfer. However, in low density forests, the decomposition rate did not impact neighbor litter sharing as strongly (Figure SI 11). Though litter sharing could be substantial (up to 25% even for small trees with β = 40 m) it largely depended on environmental conditions and may not be enough to drive the competitive interaction between N-fixers and their neighbors.